

Dental Pulp Stem Cells: an Alternative Source of Mesenchymal Stem Cells with Potential Osteogenic Regenerative Capacities

Arkaitz Mucientes

IdISSC

Eva Herranz

IdISSC

Enrique Moro

Hospital Clinico San Carlos

Aranzazu González-Corchón

Hospital Clinico San Carlos

María Jesús Peña-Soria

Hospital Clínico Universitario San Carlos Instituto Cardiovascular: Hospital Clinico Universitario San Carlos Instituto Cardiovascular

Pilar Pena

Instituto de Cerámica y Vidrio: Instituto de Ceramica y Vidrio

Carmen Baudín

Instituto de Cerámica y Vidrio: Instituto de Ceramica y Vidrio

Lydia Abasolo

IdISSC

Luis Rodriguez-Rodriguez

IdISSC

José Ramón Lamas

IdISSC

Benjamin Fernandez-Gutierrez (✉ benjamin.fernandez@salud.madrid.org)

Hospital Clinico San Carlos <https://orcid.org/0000-0002-6126-8786>

Research

Keywords: Mesenchymal stem cell, osteogenesis, osteogenic differentiation, dental pulp

Posted Date: November 12th, 2020

DOI: <https://doi.org/10.21203/rs.3.rs-102952/v1>

License: © ⓘ This work is licensed under a Creative Commons Attribution 4.0 International License.

[Read Full License](#)

Abstract

Background: Bone innate ability to repair without scarring is surpassed by major bone damage. Current gold-standard strategies do not achieve a full recovery of the bone biomechanical properties. To bypass these limitations, tissue engineering techniques based on hybrid materials made up of osteoprogenitor cells, like mesenchymal stem cells (MSCs), and bioactive ceramic scaffolds, like calcium phosphate-based (CaPs), are promising. Biological properties of the MSCs, including osteogenic potential, are influenced by the tissue source. The aim of this study is to define the MSC source and construct (MSC and scaffold combination) most interesting for its clinical application in the context of bone regeneration.

Methods: MSCs of 9 healthy donors were isolated from adipose tissue, bone marrow and dental pulp. MSCs were cultured both on plastic surface and on CaPs (hydroxyapatite and β -tricalcium phosphate) to compare their biological features: proliferation rate, osteogenic potential, cell viability and activity, ability to colonize the CaPs and ALP activity.

Results: iTRAQ results generated the hypothesis that anatomical proximity to bone has a direct effect on MSC phenotype. On plastic, MSCs isolated from dental pulp (DPSCs) were the MSCs with the highest proliferation capacity and the greatest osteogenic potential. On both CaPs, DPSCs are the MSCs with the greatest capacity to colonize bioceramics. Furthermore, results show a trend for DPSCs are the MSCs with the most robust increase in the ALP activity.

Conclusion: Based in our results, we propose DPSCs as a suitable MSCs for bone/dental regeneration cell-based strategies.

Background

Bone regeneration and bone remodelling can be considered as two sides of the same coin. While bone remodelling is a life-long process, bone regeneration occurs mainly during bone healing. [1] It is known that for small fractures or injuries, the bone has an innate ability to repair without scarring. [2] These regenerative processes are largely surpassed by major bone damage such as skeletal reconstruction surgeries, bone defects of varied origins (traumatic, infectious and tumoral) or congenital skeletal dysplasias. Current orthopaedic surgery strategies are mostly bone grafting (both autologous and allogenic) and osteodistraction. [3] They can be combined with the use of growth factors or osteoinductive scaffolds. However, the successful recovery of the bone biomechanical properties is limited. To bypass these limitations, novel strategies have been developed. Among those, hybrid materials consisting of osteoprogenitor cells, like mesenchymal stem cells (MSCs), and bioactive ceramic scaffolds have been proposed as promising tools. [4]

Calcium phosphate-based (CaPs) bioceramics have been used both in maxillo-facial surgeries and dentistry for over 30 years. CaPs are biocompatible, osteoconductive, osteoinductive and, in some cases, bioactive. Due to these properties, CaPs are widely used as scaffolds for bone regeneration and tissue engineering. Among the different CaPs bioceramics, hydroxyapatite (HA) and β -tricalcium phosphate (β -

TCP) have been widely used. [5] The Ca:P ratio determines properties such as the solubility and tendency for resorption in the body. [6] HA is considered relatively non-biodegradable while β -TCP degrades readily and can be completely replaced by newly formed bone.

Adult MSCs can be isolated from almost every tissue. [7] They have multipotential capacities and can differentiate into cells of several mesenchymal lineages (cartilage, bone, tendons, muscles, and adipocytes) among other cell type. [8] Besides, MSCs have migratory and homing abilities which enhances their immunomodulatory and immunological tolerance induction potential. [9] Although MSCs derived from different sources present similar phenotypic characteristics, the intensity of these vary depending on the tissue source. [10]

Bone Marrow MSCs (BM-MSCs) were the first described MSCs and are often considered as the gold-standard in MSCs. [11] They have been widely used and studied in trials looking for potential regenerative therapies in the last years. Adipose-derived MSCs (ASCs) present several advantages compared to MSCs obtained from other sources: adipose depots are ubiquitous in the body, easily accessible with minimum invasion and contain a large number of stem cells. [12] Furthermore, their capacity to promote osteogenesis in animal models has been described. [13] MSCs isolated from dental pulp (DPSCs) are usually isolated after surgical removal of wisdom teeth, so they are considered as a non-invasive source of MSCs. DPSCs present a high proliferative capacity and easily differentiate into odontoblasts, osteoblasts and chondrocytes. [14] DPSCs have been recently proposed to be used in regenerative therapies for bone diseases, among other condition. [15]

Considering the osteogenic potential as a property influenced by the tissue, several comparative studies of MSCs derived from various sources on different surfaces have been published. [16–21] Despite these, a clarification is still needed regarding the influence of the cell source and surface in the osteogenic potential. Osteogenic potential maximization in a context of the bone-regeneration process would be an important step. The aim of this study is to define the MSC source and construct (MSC and scaffold combination) with the highest osteogenic potential.

Methods

Proteomic analysis by iTRAQ labelling

Data obtained in a previous proteomic analysis where MSCs from subchondral bone and cartilage were compared (not published). Specifically, results obtained after comparing these locations in healthy individuals were analysed.

Briefly, MSCs were obtained surgically from subchondral bone and cartilage of a donor without osteoporotic or osteoarthritis signs. Total protein content was isolated, dried in air and then re-suspended in 25 μ l of iTRAQ dissolution buffer (ABSciex, Foster City, CA, USA). Protein concentrations were determined by Bradford assay (Sigma-Aldrich, St. Louis, MO, USA). iTRAQ labelling (ABSciex, Foster City, CA, USA) was performed with SB(116) and C(117) mass tags and desalted with home-made C-18 Stage-

tips. Fractions separated in a nanoLC system (Tempo, Eksigent) were automatically deposited on a MALDI plate and analysed by MSMS (4800 MALDI-TOF/TOF system, ABSciex). Relative quantitative analysis was done using ProteinPilot software (ABSciex) using the Paragon™ Algorithm for protein identification and quantification. Only proteins identified with at least 95% confidence, a Prot Score of at least 1.3, a p -value ≤ 0.05 and ratio ($\neq 1$) were considered as modulated.

Samples

MSCs from 3 different localizations (bone marrow, dental pulp, and adipose tissue), obtained from healthy donors (Table 1), were used for *in vitro* biological studies. Written informed consent was obtained from all donors before sample collection. The study was approved following the guidelines of the institutional ethics committee (Comité Ético de Investigación Clínica Hospital Clínico San Carlos) and the principles expressed in the Declaration of Helsinki.

Table 1

Main characteristics of healthy donors

Donor	Cell type	Sex	Age
Donor 1	BM-MSC	F	57
Donor 2	BM-MSC	M	56
Donor 3	BM-MSC	M	55
Donor 4	ASC	F	53
Donor 5	ASC	F	56
Donor 6	ASC	M	50
Donor 7	DPSC	F	44
Donor 8	DPSC	M	58
Donor 9	DPSC	M	59

Discs of CaPs bioceramics used in this study were synthesised, sintered, and polished if needed. They were kindly supplied by Instituto de Cerámica y Vidrio (ICV-CSIC). Discs had a diameter of 18mm and 4mm thickness. Sintering temperature employed for β -TCP was 1130 °C and for HA was 1250 °C.

Cell isolation and culture

ASCs were obtained from adipose tissue after surgical biopsies, according to Yang *et al.* [22] DPSCs were isolated after dental pulp mechanical extraction from wisdom exodontias, as described by Huang *et al.*

[23] Finally, BM-MSCs were obtained from femoral channel aspirates of bone marrow, taken during joint replacement surgery, in a Ficoll density gradient and cultured directly as described by Gudlevicine *et al.* [24]

Once isolated, cells were expanded in growth medium: DMEM supplemented with 10% FBS and antibiotics; DPSCs required 20% FBS instead of the 10% usually established as described by Alkhalil *et al.* [25] Cell cultures were expanded at 37°C in a 5% CO₂ atmosphere. The medium was changed every 3 days until cell confluence at passage 3.

Cell characterization

In order to confirm that cells satisfied the minimal criteria for the definition of MSC proposed by the International Society for Cellular Therapy, [26] flow cytometry and histochemistry assays were carried out as we previously described. [27]

Biological features on plastic surface

MSC proliferation rate

During cell expansion, cell proliferation was evaluated by calculating the population doubling time (Dt), which is defined by:

$$Dt = T \ln 2 / \ln(N_f / N_i)$$

Where “T” represents the time elapsed between determinations of the final number of cells (N_f) obtained from an initial cell number (N_i).

Osteogenic commitment of each MSC

Alizarin Red staining was carried out along culture on plastic. The coloured area of cell cultures after alizarin red staining was quantified, in terms of percentage, with ImageJ 1.43v software (National Institutes of Health, free available: <https://imagej.nih.gov/ij/index.html>).

Cell behaviour on CaPs

Cell activity/viability

Prior to cell seeding, the scaffolds were previously submerged in growth medium for 24 hours and then seeded with 1ml of a cellular suspension containing 50 000 cells.

Monitorization of cell viability was performed using the colourimetric indicator AlamarBlue™ (Cat#Y00-100. Thermo Fisher Scientific, Waltham, MA USA). The variation of absorbance at 570nm was measured at 24 hours, 4 and 7 days using Heales MB-580 microplate reader (Shenzhen Heales Technology

Development Co. Ltd. Guangdong. China). The amount of absorbance corresponds to cell metabolic activity.

Scanning Electronic Microscopy (SEM)

The cellular organization, adhesion and colonization of the scaffolds were assessed at 24 hours and 7 days. Each sample was subjected to fixation with a phosphate buffer solution containing 4% paraformaldehyde and 2.5% glutaraldehyde for 30 minutes. After fixation, samples were washed 3 times with phosphate-buffered saline (PBS) for 20 minutes followed by incubation for 45 minutes with a solution of 1% osmium tetroxide and, finally, washed again with PBS 3 times for 10 minutes. The next step was the dehydration of the samples by immersing them in increasing ethanol concentrations: 30%, 50%, 70%, 96% and 100%. The final step was to introduce the samples into the critical-point device and cover them with vaporized gold. Samples were observed and analysed by scanning electron microscopy (SEM JEM 6400, JEOL, Japan).

ALP activity

Early osteoblast differentiation was evaluated by measuring the alkaline phosphatase (ALP) activity, which is expressed just before the matrix mineralization occurs and its role as osteogenic activity marker is established [28]. The evaluation was made using 24-well plates and 3 conditions for each sample were evaluated: cell in plastic with growth medium as an internal control; cells seeded on HA with osteogenic medium and β -TCP with osteogenic medium. Duplicates for each experimental condition were made.

Osteogenesis progression was measured between 24h and 7 days, at this time points media was discarded and ceramic discs recovered, washed with PBS and stored at -20°C soaked in lysis buffer (0.1 wt%, Triton-X 100, 1 mM MgCl₂, 0.1 mM ZnCl₂). The ALP activity was determined by a colourimetric method using a commercial kit (Thermo Fisher Scientific, Cat#37629), following the manufacturer instructions, and measuring the absorbance at 405nm.

Statistical analysis

Statistical analysis was performed using GraphPad Prism version 7.00 for Windows, (GraphPad Software, La Jolla California USA, www.graphpad.com). We have used two-tailed paired/unpaired Student's t-test for comparison of normal variables. Normal variables were presented as mean \pm SD (standard deviation). The level of significance $p < 0.05$ was considered statistically significant. Each experiment was done with replicates.

Results

iTRAQ results analysis

The different protein components between MSCs from subchondral bone and cartilage were analysed using an iTRAQ-based comparative analysis. We have previously performed this iTRAQ in the context of

osteoarthritis vs control patients and in this case we have analysed quantitative differences between subchondral bone and cartilage only from healthy control individuals.

Results obtained revealed the identification of 1012 unique proteins in samples. Fifty of those proteins display statistically significant differences (Table 2). Among those, 5 proteins have been previously associated with the osteoblast differentiation process: PALLD, HSPA5/GRP78, FLNA, IGFBP3 and DSTN.

Table 2 - Differentially expressed proteins identified in MSC isolated from subchondral bone compared to MSC from cartilage

Uniprot ID	Gene	Protein	Coverage	Peptides	Fold change	p-value
AMPN_HUMAN	ANPEP	Aminopeptidase N	38,1	27	11,272	0,0001
PALLD_HUMAN	PALLD	Palladin	13,4	4	4,6989	0,0145
K2C1_HUMAN	KRT1	Keratin, type II cytoskeletal 1	30,6	11	4,3652	0,0164
TPM1_HUMAN	TPM1	Tropomyosin alpha-1 chain	41,6	13	4,3652	0,0173
TAGL_HUMAN	TAGLN	Transgelin	68,2	13	4,2855	0,0001
K1C10_HUMAN	KRT10	Keratin, type I cytoskeletal 10	26,5	8	3,5645	0,0085
FRIH_HUMAN	FTH1	Ferritin heavy chain	45,9	3	3,4356	0,034
DHB4_HUMAN	HSD17B4	Peroxisomal multifunctional enzyme type 2	19,2	5	3,4041	0,0078
VIME_HUMAN	VIM	Vimentin	91,6	235	3,342	0,0291
SQRD_HUMAN	SQRDL	Sulfide:quinone oxidoreductase, mitochondrial	29,3	10	2,9923	0,003
PDIA1_HUMAN	P4HB	Protein disulfide-isomerase	71,3	48	2,729	0,0028
KPYM_HUMAN	PKM2	Pyruvate kinase isozymes M1/M2	76,5	69	2,6062	0,0123
ATPB_HUMAN	ATP5B	ATP synthase subunit beta, mitochondrial	65,6	21	2,5351	0,0118
GRP78_HUMAN	HSPA5	78 kDa glucose-regulated protein	69	53	2,5119	0,0001
GLCM_HUMAN	GBA	Glucosylceramidase	16	4	2,421	0,0472
DPYL3_HUMAN	DPYSL3	Dihydropyrimidinase-related protein 3	47	14	2,3768	0,0232
SPTB2_HUMAN	SPTBN1	Spectrin beta chain, brain 1	28,2	31	2,0512	0,0251
GDIR1_HUMAN	ARHGDI1	Rho GDP-dissociation inhibitor 1	59,8	8	2,0137	0,0105

Table 2 - Differentially expressed proteins identified in MSC isolated from subchondral bone compared to MSC from cartilage

ACADV_HUMAN	ACADVL	Very long-chain specific acyl-CoA dehydrogenase, mitochondrial	28,7	7	1,8707	0,0486
ATPA_HUMAN	ATP5A1	ATP synthase subunit alpha, mitochondrial	57,7	24	1,8535	0,007
MYL6_HUMAN	MYL6	Myosin light polypeptide 6	86,8	16	1,7865	0,0487
LMO7_HUMAN	LMO7	LIM domain only protein 7	28,4	11	1,6144	0,0436
5NTD_HUMAN	FLNA	5'-nucleotidase	53,5	22	1,5704	0,044
FLNA_HUMAN	FLNA	Filamin-A	61,4	126	1,5276	0,0036
HS90A_HUMAN	HSP90AA1	Heat shock protein HSP 90-alpha	56,4	29	1,5276	0,0351
H32_HUMAN	HIST2H3A	Histone H3.2	36	7	0,8872	0,0298
H2AJ_HUMAN	H2AFJ	Histone H2A.J	41,1	7	0,7798	0,0365
PDLI7_HUMAN	PDLIM7	PDZ and LIM domain protein 7	12,9	1	0,7311	0,0042
ALDR_HUMAN	AKR1B1	Aldose reductase	37	5	0,6918	0,0237
FLNC_HUMAN	FLNC	Filamin-C	14,8	14	0,631	0,0145
MVP_HUMAN	MVP	Major vault protein	49,7	23	0,5649	0,0078
VINC_HUMAN	VCL	Vinculin	41,5	23	0,5546	0,0245
RS15A_HUMAN	RPS15A	40S ribosomal protein S15a	47,7	4	0,5248	0,0221
SFPQ_HUMAN	SFPQ	Splicing factor, proline- and glutamine-rich	21,1	3	0,4966	0,0205
PLIN3_HUMAN	PLIN3	Perilipin-3	55,8	14	0,4875	0,0418
NNMT_HUMAN	NNMT	Nicotinamide N-methyltransferase	31,8	6	0,4742	0,04
1433Z_HUMAN	YWHAZ	14-3-3 protein zeta/delta	71,8	14	0,4699	0,0217
PRDX1_HUMAN	PRDX1	Peroxisredoxin-1	70,9	21	0,4169	0,0199

Table 2 - Differentially expressed proteins identified in MSC isolated from subchondral bone compared to MSC from cartilage						
ANX11_HUMAN	ANXA11	Annexin A11	36,4	9	0,3733	0,0014
G6PD_HUMAN	G6PD	Glucose-6-phosphate 1-dehydrogenase	43,5	15	0,3664	0,0006
HYEP_HUMAN	EPHX1	Epoxide hydrolase 1	19,6	7	0,3467	0,0069
6PGD_HUMAN	PGD	6-phosphogluconate dehydrogenase, decarboxylating	38,3	10	0,2911	0,004
CALU_HUMAN	CALU	Calumenin	53,3	14	0,2655	0,0057
NQO1_HUMAN	NQO1	NAD(P)H dehydrogenase [quinone] 1	46	11	0,2512	0,0153
TKT_HUMAN	TKT	Transketolase	56	21	0,1486	0,0051
ANXA5_HUMAN	ANXA5	Annexin A5	78,4	38	0,1294	0,0002
ENOA_HUMAN	ENO1	Alpha-enolase	84,3	54	0,1	0,0419
ANXA2_HUMAN	ANXA2	Annexin A2	87,6	74	0,0871	0,0019
IBP3_HUMAN	IGFBP3	Insulin-like growth factor-binding protein 3	39,9	5	0,0802	0,0424
DEST_HUMAN	DSTN	Destrin	65,5	8	0,0614	0,0245
Note: Proteins are listed according to Fold-Change, in decreasing order. In bold, proteins previously related to osteogenic process.						

Scanning Electronic Microscopy

Cell morphology and behaviour when growing on β -TCP and HA scaffolds were studied by SEM at both 24 hours and 7 days after culture. In all cases, cells do not show visual signs of cytotoxicity. Cells can be visualized in its normal shape and size.

Regarding β -TCP, cell adhesion seems to be faster in BM-MSCs (Fig. 5C) than in ASCs and DPSCs (Figs. 5A and 5E). After 7 days, cell overlays were observed in β -TCP discs independently of the MSC seeded (Figs. 5B-D-F). When culturing on HA, the adhesion process was similar for all MSCs (Figs. 6A-C-E). On day 7, BM-MSCs and ASCs (Figs. 6B-D) exhibited similar appearance, and the number of cells increased without forming layers. In contrast, DPSCs (Fig. 6F) formed a multilayer covering the entire surface. Finally, all MSCs colonized the existing internal pores in both CaPs (Fig. 7).

Osteogenic Potential

Figure 8 shows a significant differential ALP activity at both 24 hours and 7 days, being higher on HA (t = 24 hours, β -TCP = 0.4249, HA = 0.6213, $p = 0.0014$; t = 7 days, β -TCP = 0.6201, HA = 0.9517, $p = 0.0002$).

According to cell localization (Fig. 9), each localization shows a significant increase in ALP activity (ASCs, $t_1 = 0.515$, $t_2 = 0.9060$, $p = 0.0007$; BM-MSCs, $t_1 = 0.6293$, $t_2 = 0.8686$, $p = 0.0358$; DPSCs, $t_1 = 0.417$, $t_2 = 0.7147$, $p = 0.0002$). The initial differences between locations disappeared at final time point (t = 24 hours, ASCs = 0.5150, BM-MSCs = 0.6293, DPSCs = 0.4170, $p = 0.0306$; t = 7 days, ASCs = 0.9016, BM-MSCs = 0.8636, DPSCs = 0.7147, $p = 0.2394$).

Finally, the increase in ALP activity, in percentage, was calculated. DPSCs presented a bigger although not significant increase in the ALP activity than the other sources (ASCs = 62.58%, BM-MSCs = 40.15%, DPSCs = 72.51%, $p = 0.4202$). Regarding biomaterial-cells combinations, DPSC + HA increased the most, although not significant different were obtained (ASCs + HA = 98.60%, BM-MSCs + HA = 43.46%, DPSCs + HA = 132.20%, ASCs + β -TCP = 78.38%, BM-MSCs + β -TCP = 112.20%, DPSCs + β -TCP = 56.44%, $p = 0.1479$) (Figs. 10 and 11).

Discussion

In bone regeneration context, therapies based on using osteoprogenitor cells are promising. However, the full therapeutic potential of these techniques has not been achieved. A full understanding of how different biological aspects influence the osteogenic potential is required. Anatomical localization of the cells used is among those characteristics. To our knowledge, this is the first comparative work that analyses a possible osteogenic commitment depending on the anatomic localization of non-commercial human MSCs from bone marrow, adipose tissue and dental pulp, seeded both on plastic surface and CaPs (β -TCP and HA).

The starting point of this work was the analysis of the results obtained in a previous iTRAQ where MSCs from subchondral bone and cartilage were compared in an osteoarthritis (OA) study. OA is a condition characterized by excessive bone growth, and the main affected tissues are subchondral bone and cartilage. Specifically, results obtained after comparing these locations in healthy individuals were analysed in a free-hypothesis context. Fifty proteins were identified (Table 2). Five out of those 50 proteins have been communicated as related to osteogenic process. FLNA, HSPA5/GRP78 and PALLD were up-regulated in subchondral bone and its expression correlated with osteoblast differentiation as they contribute to the stabilization of cytoskeleton, which is necessary for the osteogenesis, and regulate protein folding and calcium flux. [29–32] In contrast, DSTN and IBP3, inhibitors of the osteoblast differentiation, [33,34] were down-regulated in MSCs isolated from subchondral bone. Considering this background, MSCs from subchondral bone display a more established commitment to osteogenesis compared to MSCs from cartilage. This supports the hypothesis that an anatomical proximity to bone has a direct effect on MSC phenotype in terms of increased osteogenic commitment.

To confirm this hypothesis, we analysed the biological behaviour of MSCs isolated from locations with different proximity to bone (adipose tissue, bone marrow and dental pulp) on different surfaces. All cells used in this work met the minimal criteria to be defined as MSCs (see Additional file 1). [26]

When cultured on plastic surfaces, two biological characteristics of MSCs were evaluated: proliferative ability and osteogenic potential. Evaluating the cell proliferation is important for cell-based therapies since it has been communicated that failures on stem cell therapies is likely to be due to a massive cell death occurring after cell transplantation. [35] Our *in vitro* results established that DPSCs have the highest proliferation rate (Fig. 1), in line with previous studies. [36] Besides, it was observed that DPSCs present a smaller size. Since DPSCs have a higher proliferation rate, it is likely this smaller size is a consequence of this due to the indirect relationship between proliferation and cell size. [37,38] Alizarin Red staining is commonly used as an osteogenic differentiation indicator as mineralized nodules are red-coloured. Microscopy images show that DPSCs exhibit the most intense staining, and its quantification evidence significant differences (Fig. 2). These results indicate that DPSCs present the most *in vitro* osteogenic capacity, followed by BM-MSCs and ASCs as the least osteogenic. This staining pattern confirms and extends results obtained by Tamaki *et al.* [16] Furthermore, it has been described that DPSCs likely have an advantage for osteogenic differentiation over other MSCs, [19] and DPSCs only differentiate into osteoblasts at high passages. [39]

Once MSCs were seeded on the scaffolds and constructs generated, it was studied their cell viability, colonization ability, and osteogenic capacity. Viability test showed that β -TCP is more cell-friendly than HA (Fig. 3). Both β -TCP and HA are biomaterials commonly used in bone tissue engineering and dentistry to treat bone defects. Implant surface quality is a major factor in biocompatibility. When the surface of the implanted biomaterial is exposed to tissue fluids, an initial interaction occurs between the living bone and tissue and the implant surface. In this sense, the use of materials filled with tricalcium phosphate appears promising following the observation that more living cells are in this material. [40] Regarding MSCs, viability test is favourable for DPSCs at 24hs and 4 days comparing to ASCs or BM-MSCs. These differences are not significant at 7 days (Fig. 4).

SEM images (Figs. 5 and 6) are coherent since only DPSCs developed cell layer on HA whereas on β -TCP the three source-derived MSCs did it. CaPs are porous, so it is required pore colonization by the cells for an optimal colonization of the CaP. Specific images of the pores existing in both CaPs proof a pore successfully colonization by all MSCs after 24 hours (Fig. 7). Besides, cytotoxicity was not appreciated in the studied samples. It is remarkable that DPSCs have shown to be the MSCs with the greatest proliferation ability on both plastic surface and bioceramics. This feature is an advantage for bone regeneration as a high MSCs density enhances the osteogenic differentiation. [41] These results indicate, together with other studies, that DPSCs could be the optimal stem cells for dental and bone regeneration. [18,42]

The interplay of the tissue engineering triad (cells, signaling molecules, and scaffolds) is essential for recapitulation of the biological events of tissue regeneration. These elements have been used either

separately or in combination for the reconstitution of the pulp-dentin complex and bone defects. Recent data imply that β -TCP is a bioactive and biocompatible material capable of enhancing DPSCs proliferation, migration, and adhesion. Moreover, recent data are conclusive about DPSCs higher levels of osteogenic and odontogenic differentiation markers such as COL1, DSPP, OC, RUNX2, and DMP-1. Our results suggest, in accordance with the literature, that DPSCs may be a valuable tool in the context of dental and bone regeneration. [43]

Regarding osteogenic potential, ALP activity test results (Fig. 8) mismatch viability results (Fig. 3): while β -TCP appears to be the best in terms of viability, HA obtained the highest values in ALP activity. These results indicate that a combination of materials would be more effective. Referring to cell sources, ASCs and BM-MSCs present similar absolute values, that are slightly superior to DPSCs values but no significant. Interestingly, this pattern in ALP activity also appears in recent studies that compare multi-sources derived MSCs seeded on plastic surfaces, [20,21] although these studies obtained significant differences. The absence of significance in our results could be due to the osteoinductive properties that both CaPs present, [44,45] which the plastic surface lacks. Since DPSCs present the highest metabolic activity during osteogenesis on both CaPs (see Additional file 2), we consider conceivable that CaPs enhance the osteogenesis preferentially on DPSCs over other MSCs. In relation to biomaterial-cells combinations, the highest increase in ALP activity, although not significant, was obtained by DPSCs + HA combination.

Conclusions

In summary, our results point to DPSCs as ideal cell in bone regeneration scenario. Within bone regeneration, DPSCs might be especially beneficial in periodontal regeneration. Supporting this, a Phase 3 clinical study using DPSCs for alveolar cleft lip and palate repair has recently been initiated (ClinicalTrials.gov Identifier: NCT03766217), and promising results of the using DPSCs for periodontal regeneration has been published. [46] Moreover, a combination of the best viability of β -TCP and the enhanced osteogenic capacity of HA would be appropriate. Other studies will be necessary to obtain the best combination of cells and biomaterials together with other signaling enhancers or inhibitors as different proteins have really demonstrated in the field of dentistry and bone regeneration. [47,48]

Abbreviations

MSC

Mesenchymal Stem Cell

CaP

Calcium phosphate-based ceramic

BM-MSCS

Bone Marrow MSC

ASC

Adipose-derived MSC

DPSC
Dental Pulp MSC
SEM
Scanning Electron Microscopy
ALP
Alakine Phosphatase
OA
Osteoarthritis
 β -TCP
Beta-Tricalcium Phosphate
HA
Hydroxyapatite

Declarations

Ethics approval and consent to participate

Written informed consent was obtained from all donors before sample collection. The study was approved following the guidelines of the institutional ethics committee (Comité Ético de Investigación Clínica Hospital Clínico San Carlos) and the principles expressed in the Declaration of Helsinki.

Consent for publication

Not applicable.

Availability of data and materials

The datasets used and/or analysed during the current study are available from the corresponding author on reasonable request.

Competing interests

The authors declare that they have no competing interests

Funding

This work was supported by grants RIER (Instituto de Salud Carlos III) and FIS PI13/01863 (Instituto de Salud Carlos III).

Authors' contributions

AM and EV performed the experiments and collected and assembled data. EM, AG-C, MJP-S, PP and CB provided study materials or patients. AM, LA and LR-R performed the data analysis and interpreted the

results. AM wrote the manuscript. JRL and BF-G planned the study and reviewed and edited the paper. All authors read and approved the final manuscript.

Acknowledgements

We thank the Hospital Clínico San Carlos surgeons for providing the samples used in the study.

References

1. Dimitriou R, Jones E, McGonagle D, Giannoudis P V. Bone regeneration: current concepts and future directions. *BMC Med* [Internet]. 2011;9:66. Available from: <http://bmcmmedicine.biomedcentral.com/articles/10.1186/1741-7015-9-66>
2. Einhorn TA. The Cell and Molecular Biology of Fracture Healing. *Clin Orthop Relat Res* [Internet]. 1998;355S:S7–21. Available from: <http://journals.lww.com/00003086-199810001-00003>
3. Giannoudis P V, Calori GM, Begue T, Schmidmaier G. Bone regeneration strategies: Current trends but what the future holds? *Injury* [Internet]. 2013;44:S1–2. Available from: <https://linkinghub.elsevier.com/retrieve/pii/S0020138313700020>
4. Wang P, Zhao L, Chen W, Liu X, Weir M, Xu H. Stem Cells and Calcium Phosphate Cement Scaffolds for Bone Regeneration. *J Dent Res* [Internet]. 2014;93:618–25. Available from: <http://journals.sagepub.com/doi/10.1177/0022034514534689>
5. Wagoner Johnson AJ, Herschler BA. A review of the mechanical behavior of CaP and CaP/polymer composites for applications in bone replacement and repair. *Acta Biomater* [Internet]. 2011;7:16–30. Available from: <https://linkinghub.elsevier.com/retrieve/pii/S1742706110003296>
6. Descamps M, Boilet L, Moreau G, Tricoteaux A, Lu J, Leriche A, et al. Processing and properties of biphasic calcium phosphates bioceramics obtained by pressureless sintering and hot isostatic pressing. *J Eur Ceram Soc* [Internet]. 2013;33:1263–70. Available from: <https://linkinghub.elsevier.com/retrieve/pii/S0955221913000265>
7. da Silva Meirelles L, Chagastelles PC, Nardi NB. Mesenchymal stem cells reside in virtually all post-natal organs and tissues. *J Cell Sci* [Internet]. 2006;119:2204–13. Available from: <http://www.ncbi.nlm.nih.gov/pubmed/16684817>
8. Pittenger MF, Mackay AM, Beck SC, Jaiswal RK, Douglas R, Mosca JD, et al. Multilineage potential of adult human mesenchymal stem cells. *Science* [Internet]. 1999;284:143–7. Available from: <http://www.ncbi.nlm.nih.gov/pubmed/10102814>
9. Castro-Manrreza ME, Montesinos JJ. Immunoregulation by mesenchymal stem cells: biological aspects and clinical applications. *J Immunol Res* [Internet]. 2015;2015:394917. Available from: <http://www.ncbi.nlm.nih.gov/pubmed/25961059>

10. Escacena N, Quesada-Hernández E, Capilla-Gonzalez V, Soria B, Hmadcha A. Bottlenecks in the Efficient Use of Advanced Therapy Medicinal Products Based on Mesenchymal Stromal Cells. *Stem Cells Int* [Internet]. 2015;2015:1–12. Available from: <http://www.hindawi.com/journals/sci/2015/895714/>
11. Hass R, Kasper C, Böhm S, Jacobs R. Different populations and sources of human mesenchymal stem cells (MSC): A comparison of adult and neonatal tissue-derived MSC. *Cell Commun Signal* [Internet]. 2011;9:12. Available from: <https://biosignaling.biomedcentral.com/articles/10.1186/1478-811X-9-12>
12. Baer PC, Geiger H. Adipose-Derived Mesenchymal Stromal/Stem Cells: Tissue Localization, Characterization, and Heterogeneity. *Stem Cells Int*. 2012;
13. Xia L, Lin K, Jiang X, Fang B, Xu Y, Liu J, et al. Effect of nano-structured bioceramic surface on osteogenic differentiation of adipose derived stem cells. *Biomaterials*. 2014;
14. Potdar PD, Jethmalani YD. Human dental pulp stem cells: Applications in future regenerative medicine. *World J Stem Cells* [Internet]. 2015;7:839–51. Available from: <http://www.wjgnet.com/1948-0210/full/v7/i5/839.htm>
15. Kichenbrand C, Velot E, Menu P, Moby V. Dental Pulp Stem Cell-Derived Conditioned Medium: An Attractive Alternative for Regenerative Therapy. *Tissue Eng Part B Rev* [Internet]. 2019;25:78–88. Available from: <http://www.ncbi.nlm.nih.gov/pubmed/30156475>
16. Tamaki Y, Nakahara T, Ishikawa H, Sato S. In vitro analysis of mesenchymal stem cells derived from human teeth and bone marrow. *Odontology*. 2013;
17. Li C, Wu X, Tong J, Yang X, Zhao J, Zheng Q, et al. Comparative analysis of human mesenchymal stem cells from bone marrow and adipose tissue under xeno-free conditions for cell therapy. *Stem Cell Res Ther* [Internet]. 2015;6:55. Available from: <http://www.ncbi.nlm.nih.gov/pubmed/25884704>
18. Lobo SE, Glickman R, da Silva WN, Arinzeh TL, Kerkis I. Response of stem cells from different origins to biphasic calcium phosphate bioceramics. *Cell Tissue Res*. 2015;
19. Ren H, Sang Y, Zhang F, Liu Z, Qi N, Chen Y. Comparative Analysis of Human Mesenchymal Stem Cells from Umbilical Cord, Dental Pulp, and Menstrual Blood as Sources for Cell Therapy. *Stem Cells Int* [Internet]. 2016;2016:1–13. Available from: <http://www.hindawi.com/journals/sci/2016/3516574/>
20. D’Alimonte I, Mastrangelo F, Giuliani P, Pierdomenico L, Marchisio M, Zuccarini M, et al. Osteogenic Differentiation of Mesenchymal Stromal Cells: A Comparative Analysis Between Human Subcutaneous Adipose Tissue and Dental Pulp. *Stem Cells Dev* [Internet]. 2017;26:843–55. Available from: <https://www.liebertpub.com/doi/10.1089/scd.2016.0190>
21. Zhang Y, Xing Y, Jia L, Ji Y, Zhao B, Wen Y, et al. An In Vitro Comparative Study of Multisource Derived Human Mesenchymal Stem Cells for Bone Tissue Engineering. *Stem Cells Dev* [Internet]. 2018 [cited 2019 Jun 11];27:1634–45. Available from: <https://www.liebertpub.com/doi/10.1089/scd.2018.0119>

22. Yang X-F, He X, He J, Zhang L-H, Su X-J, Dong Z-Y, et al. High efficient isolation and systematic identification of human adipose-derived mesenchymal stem cells. *J Biomed Sci* [Internet]. 2011;18:59. Available from: <http://www.ncbi.nlm.nih.gov/pubmed/21854621>
23. Huang GTJ, Sonoyama W, Chen J, Park SH. In vitro characterization of human dental pulp cells: various isolation methods and culturing environments. *Cell Tissue Res* [Internet]. 2006;324:225–36. Available from: <http://www.ncbi.nlm.nih.gov/pubmed/16440193>
24. Gudleviciene Z, Kundrotas G, Liudkeviciene R, Rascon J, Jurga M. Quick and effective method of bone marrow mesenchymal stem cell extraction. *Open Med (Warsaw, Poland)* [Internet]. 2015;10:44–9. Available from: <http://www.ncbi.nlm.nih.gov/pubmed/28352676>
25. Alkhalil M, Smajilagić A, Redžić A. Human dental pulp mesenchymal stem cells isolation and osteoblast differentiation. *Med Glas*. 2015;12:27–32.
26. Dominici M, Le Blanc K, Mueller I, Slaper-Cortenbach I, Marini F, Krause DS, et al. Minimal criteria for defining multipotent mesenchymal stromal cells. The International Society for Cellular Therapy position statement. *Cytotherapy* [Internet]. 2006 [cited 2019 Jun 11];8:315–7. Available from: <http://www.ncbi.nlm.nih.gov/pubmed/16923606>
27. Tornero-Esteban P, Peralta-Sastre A, Herranz E, Rodríguez-Rodríguez L, Mucientes A, Abásolo L, et al. Altered Expression of Wnt Signaling Pathway Components in Osteogenesis of Mesenchymal Stem Cells in Osteoarthritis Patients. *PLoS One* [Internet]. 2015;10:e0137170. Available from: <http://www.ncbi.nlm.nih.gov/pubmed/26352263>
28. Golub EE, Boesze-Battaglia K. The role of alkaline phosphatase in mineralization. *Curr Opin Orthop* [Internet]. 2007;18:444–8. Available from: <https://rupress.org/jem/article/93/5/415/10511/THE-ROLE-OF-ALKALINE-PHOSPHATASE-IN-OSTEOGENESIS>
29. Wall ME, Rachlin A, Otey CA, Loba EG. Human adipose-derived adult stem cells upregulate palladin during osteogenesis and in response to cyclic tensile strain. *Am J Physiol Cell Physiol* [Internet]. 2007 [cited 2019 Jun 11];293:C1532-8. Available from: <http://www.physiology.org/doi/10.1152/ajpcell.00065.2007>
30. Yu H, Tay CY, Leong WS, Tan SCW, Liao K, Tan LP. Mechanical behavior of human mesenchymal stem cells during adipogenic and osteogenic differentiation. *Biochem Biophys Res Commun* [Internet]. 2010 [cited 2019 Jun 11];393:150–5. Available from: <https://linkinghub.elsevier.com/retrieve/pii/S0006291X10001701>
31. Tan J, Zhou L, Xue P, An Y, Luo L, Zhang R, et al. Tumor Necrosis Factor- α Attenuates the Osteogenic Differentiation Capacity of Periodontal Ligament Stem Cells by Activating PERK Signaling. *J Periodontol* [Internet]. 2016 [cited 2019 Jun 11];87:e159-71. Available from: <http://doi.wiley.com/10.1902/jop.2016.150718>

32. Corsetti G, Romano C, Stacchiotti A, Pasini E, Dioguardi FS. Endoplasmic Reticulum Stress and Apoptosis Triggered by Sub-Chronic Lead Exposure in Mice Spleen: a Histopathological Study. *Biol Trace Elem Res* [Internet]. 2017;178:86–97. Available from: <http://link.springer.com/10.1007/s12011-016-0912-z>
33. Chen L, Shi K, Frary CE, Ditzel N, Hu H, Qiu W, et al. Inhibiting actin depolymerization enhances osteoblast differentiation and bone formation in human stromal stem cells. *Stem Cell Res* [Internet]. 2015 [cited 2019 Jun 11];15:281–9. Available from: <https://linkinghub.elsevier.com/retrieve/pii/S1873506115000823>
34. Eguchi K, Akiba Y, Akiba N, Nagasawa M, Cooper LF, Uoshima K. Insulin-like growth factor binding Protein-3 suppresses osteoblast differentiation via bone morphogenetic protein-2. *Biochem Biophys Res Commun* [Internet]. 2018 [cited 2019 Jun 11];507:465–70. Available from: <https://linkinghub.elsevier.com/retrieve/pii/S0006291X18324793>
35. Chacko SM, Ahmed S, Selvendiran K, Kuppusamy ML, Khan M, Kuppusamy P. Hypoxic preconditioning induces the expression of prosurvival and proangiogenic markers in mesenchymal stem cells. *Am J Physiol Physiol* [Internet]. 2010;299:C1562–70. Available from: <https://www.physiology.org/doi/10.1152/ajpcell.00221.2010>
36. Tsutsui T. Dental Pulp Stem Cells: Advances to Applications. *Stem Cells Cloning Adv Appl* [Internet]. 2020;Volume 13:33–42. Available from: <https://www.dovepress.com/dental-pulp-stem-cells-advances-to-applications-peer-reviewed-article-SCCAA>
37. Björklund M. Cell size homeostasis: Metabolic control of growth and cell division. *Biochim Biophys Acta - Mol Cell Res* [Internet]. 2019;1866:409–17. Available from: <https://linkinghub.elsevier.com/retrieve/pii/S0167488918302544>
38. Lloyd AC. The Regulation of Cell Size. *Cell* [Internet]. 2013;154:1194–205. Available from: <https://linkinghub.elsevier.com/retrieve/pii/S0092867413010842>
39. Yu J, He H, Tang C, Zhang G, Li Y, Wang R, et al. Differentiation potential of STRO-1 + dental pulp stem cells changes during cell passaging. *BMC Cell Biol* [Internet]. 2010;11:32. Available from: <http://www.ncbi.nlm.nih.gov/pubmed/20459680>
40. Kozakiewicz M, Wach T. New Oral Surgery Materials for Bone Reconstruction—A Comparison of Five Bone Substitute Materials for Dentoalveolar Augmentation. *Materials (Basel)* [Internet]. 2020;13:2935. Available from: <https://www.mdpi.com/1996-1944/13/13/2935>
41. Wang X, Song W, Kawazoe N, Chen G. The osteogenic differentiation of mesenchymal stem cells by controlled cell-cell interaction on micropatterned surfaces. *J Biomed Mater Res Part A* [Internet]. 2013;101:3388–95. Available from: <http://doi.wiley.com/10.1002/jbm.a.34645>

42. Wongsupa N, Nuntanaranont T, Kamolmattayakul S, Thuaksuban N. Biological characteristic effects of human dental pulp stem cells on poly-ε-caprolactone-biphasic calcium phosphate fabricated scaffolds using modified melt stretching and multilayer deposition. *J Mater Sci Mater Med* [Internet]. 2017;28:25. Available from: <http://link.springer.com/10.1007/s10856-016-5833-z>
43. Sabbagh J, Ghassibe-Sabbagh M, Fayyad-Kazan M, Al-Nemer F, Fahed JC, Berberi A, et al. Differences in osteogenic and odontogenic differentiation potential of DPSCs and SHED. *J Dent*. 2020;101:103413.
44. Thorpe AA, Creasey S, Sammon C, Le Maitre CL. Hydroxyapatite nanoparticle injectable hydrogel scaffold to support osteogenic differentiation of human mesenchymal stem cells. *Eur Cell Mater* [Internet]. 2016;32:1–23. Available from: <http://www.ncbi.nlm.nih.gov/pubmed/27377664>
45. Tsukanaka M, Fujibayashi S, Otsuki B, Takemoto M, Matsuda S. Osteoinductive potential of highly purified porous β-TCP in mice. *J Mater Sci Mater Med* [Internet]. 2015;26:132. Available from: <http://www.ncbi.nlm.nih.gov/pubmed/25698341>
46. Ferrarotti F, Romano F, Gamba MN, Quirico A, Giraudi M, Audagna M, et al. Human intrabony defect regeneration with micrografts containing dental pulp stem cells: A randomized controlled clinical trial. *J Clin Periodontol* [Internet]. 2018;45:841–50. Available from: <http://www.ncbi.nlm.nih.gov/pubmed/29779220>
47. Fischer NG, Münchow EA, Tamerler C, Bottino MC, Aparicio C. Harnessing biomolecules for bioinspired dental biomaterials. *J Mater Chem B*. 2020;8:8713–47.
48. Deb S, Chana S. Biomaterials in Relation to Dentistry. *Front Oral Biol* [Internet]. 2015;17:1–12. Available from: <https://www.karger.com/Article/FullText/381686>

Figures

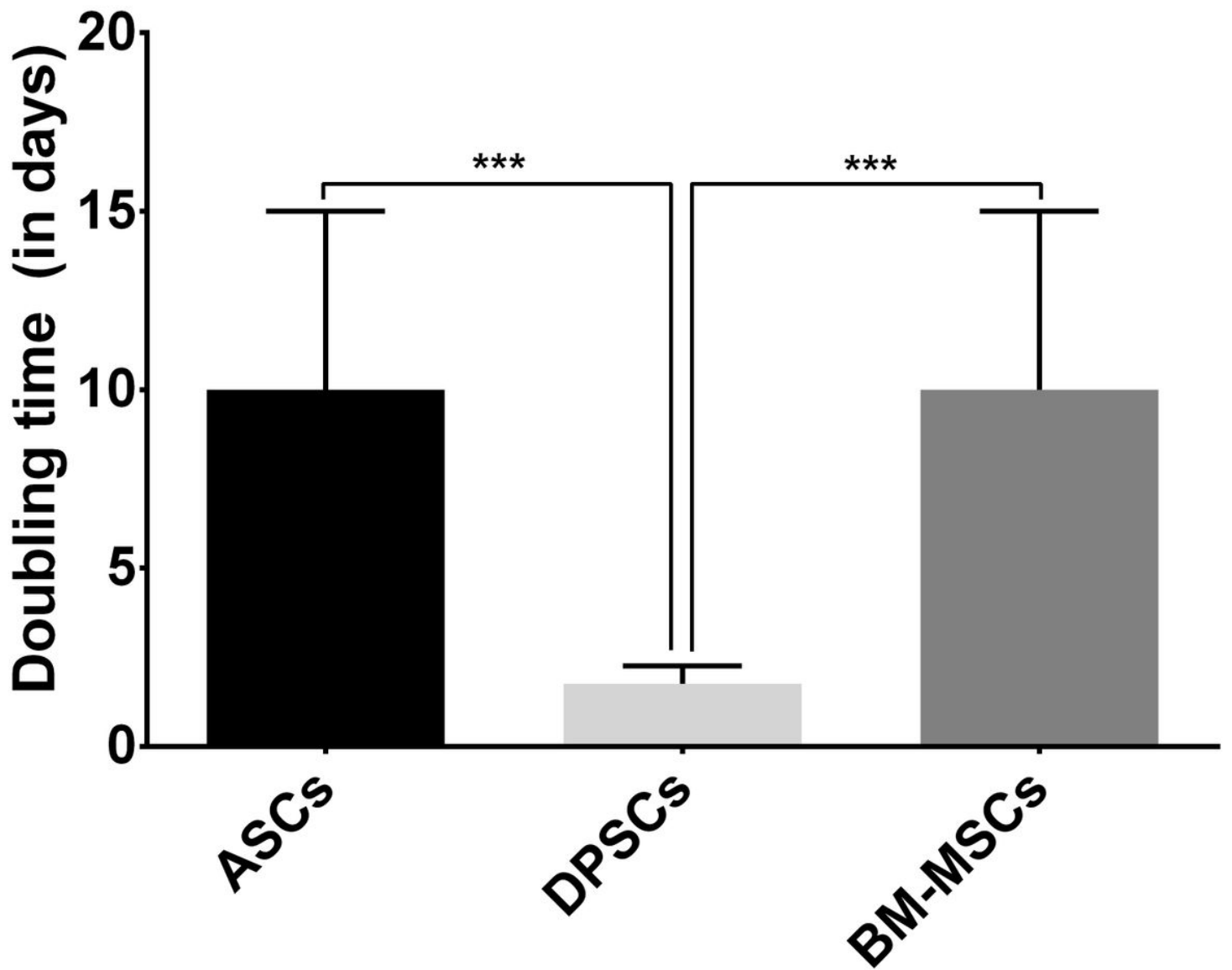


Figure 1

MSCs proliferation. Doubling time (in days) when cultured in plastic presented by MSC isolated from adipose tissue (ASCs), dental pulp (DPSCs) and bone marrow (BM-MSCs).

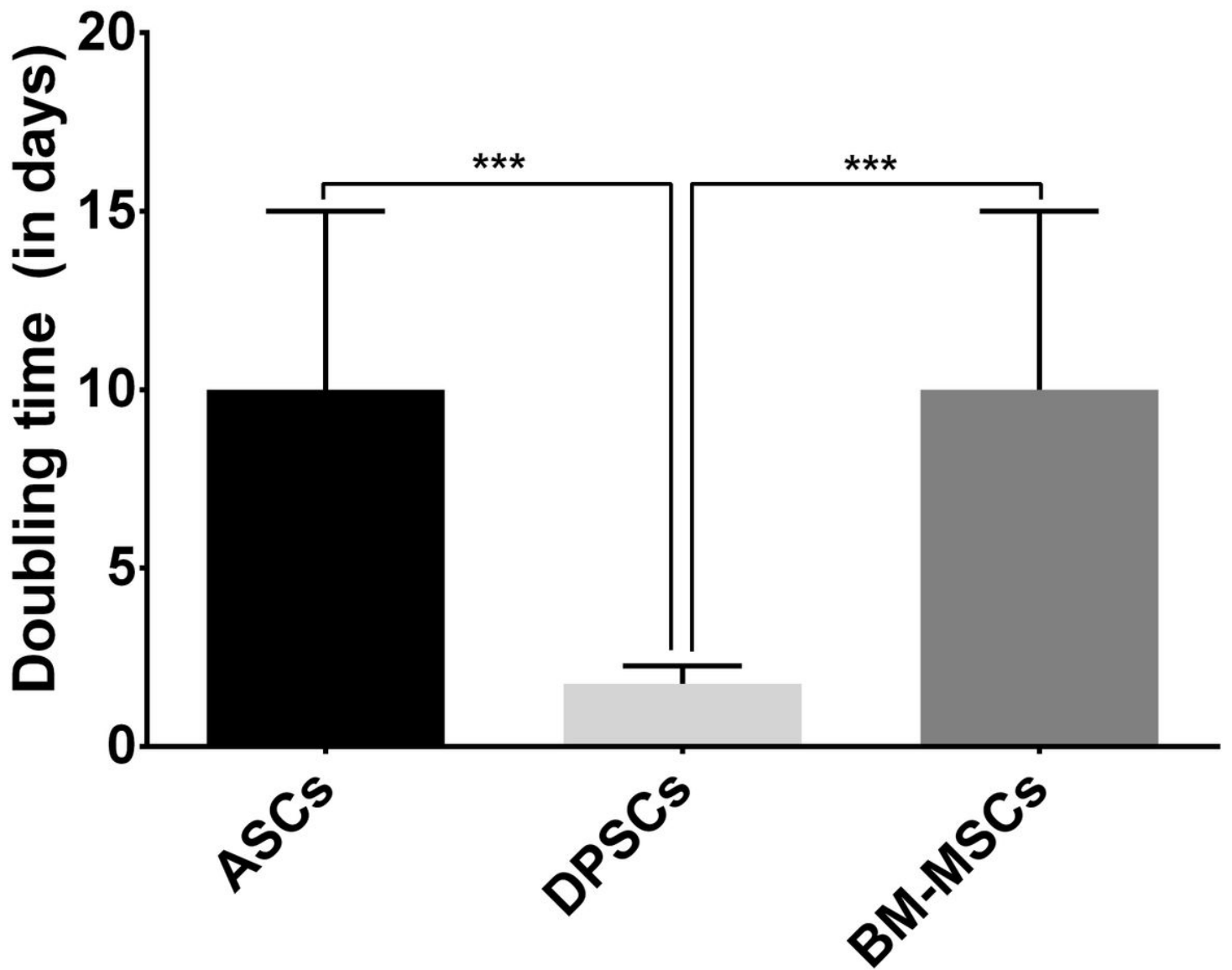


Figure 1

MSCs proliferation. Doubling time (in days) when cultured in plastic presented by MSC isolated from adipose tissue (ASCs), dental pulp (DPSCs) and bone marrow (BM-MSCs).

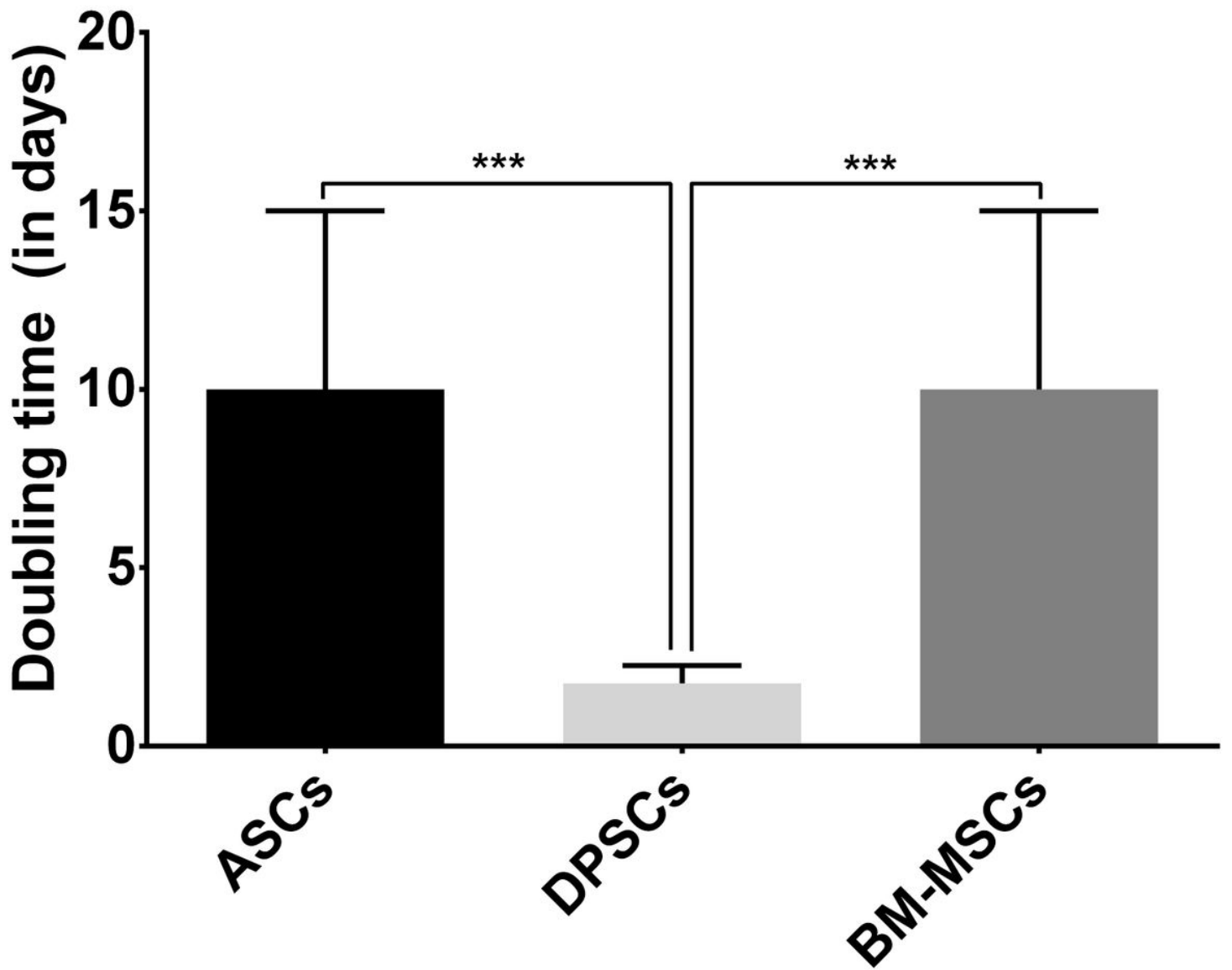


Figure 1

MSCs proliferation. Doubling time (in days) when cultured in plastic presented by MSC isolated from adipose tissue (ASCs), dental pulp (DPSCs) and bone marrow (BM-MSCs).

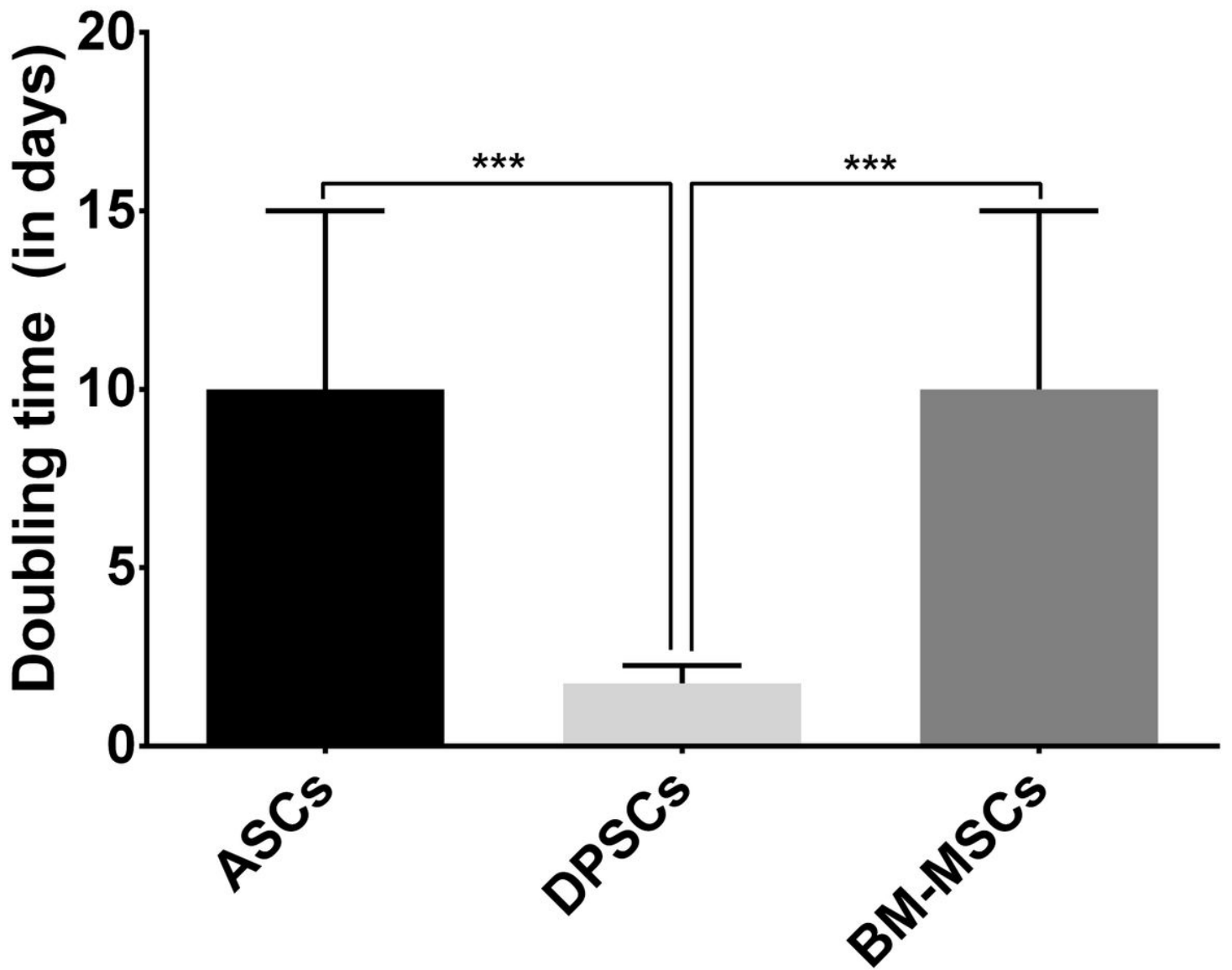


Figure 1

MSCs proliferation. Doubling time (in days) when cultured in plastic presented by MSC isolated from adipose tissue (ASCs), dental pulp (DPSCs) and bone marrow (BM-MSCs).

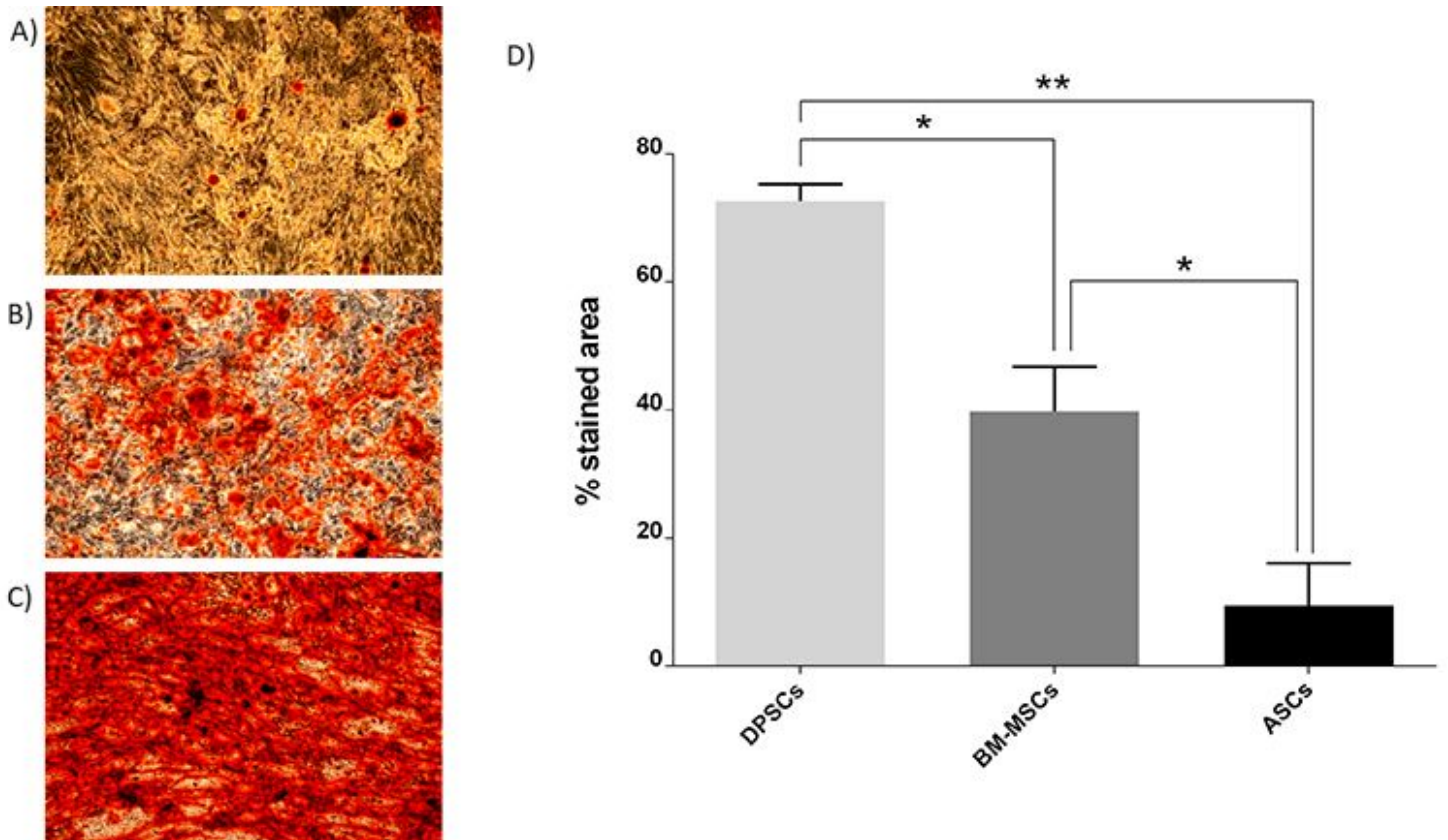


Figure 2

Alizarin Red staining and its quantification of different source-derived mesenchymal stem cells. A) Alizarin Red staining of ASCs after 21 days of culture in osteogenic medium (x10). B) Alizarin Red staining of BM-MSCs after 21 days of culture in osteogenic medium (x10). C) Alizarin Red staining of DPSCs after 21 days of culture in osteogenic medium (x10). D) Alizarin Red staining quantification of MSC according to the cell source: adipose tissue (ASCs), dental pulp (DPSCs) and bone marrow (BM-MSCs).

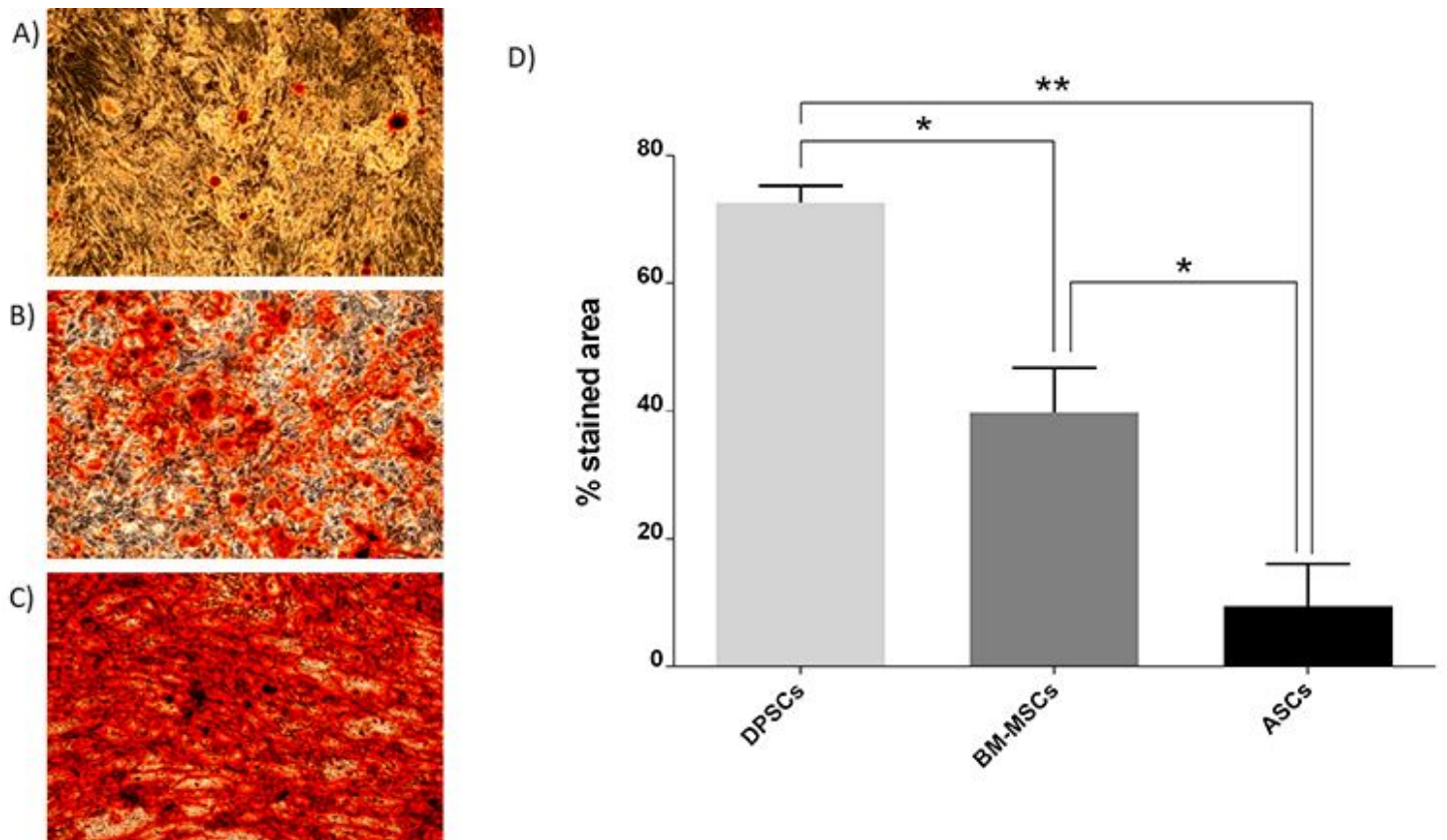


Figure 2

Alizarin Red staining and its quantification of different source-derived mesenchymal stem cells. A) Alizarin Red staining of ASCs after 21 days of culture in osteogenic medium (x10). B) Alizarin Red staining of BM-MSCs after 21 days of culture in osteogenic medium (x10). C) Alizarin Red staining of DPSCs after 21 days of culture in osteogenic medium (x10). D) Alizarin Red staining quantification of MSC according to the cell source: adipose tissue (ASCs), dental pulp (DPSCs) and bone marrow (BM-MSCs).

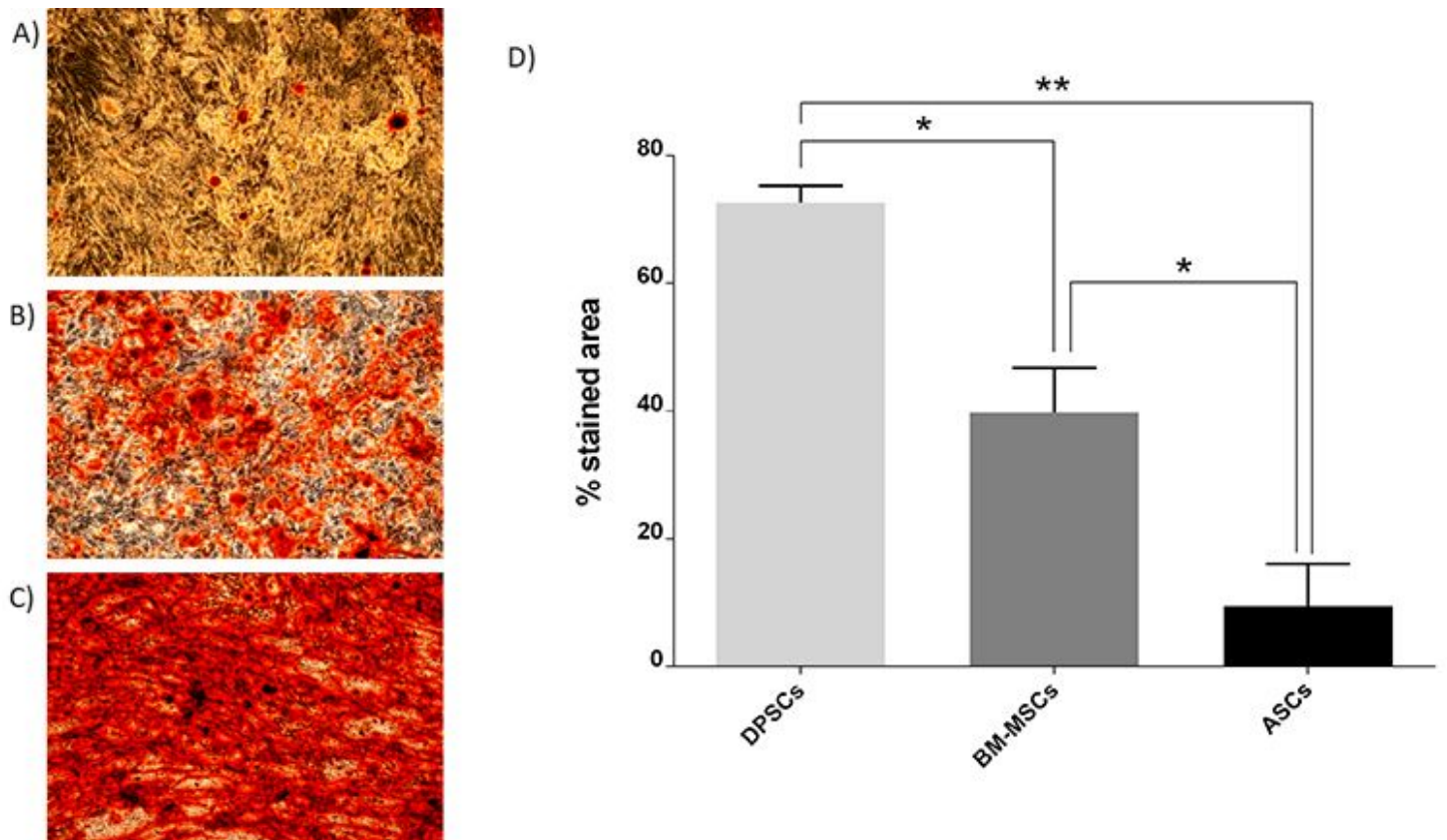


Figure 2

Alizarin Red staining and its quantification of different source-derived mesenchymal stem cells. A) Alizarin Red staining of ASCs after 21 days of culture in osteogenic medium (x10). B) Alizarin Red staining of BM-MSCs after 21 days of culture in osteogenic medium (x10). C) Alizarin Red staining of DPSCs after 21 days of culture in osteogenic medium (x10). D) Alizarin Red staining quantification of MSC according to the cell source: adipose tissue (ASCs), dental pulp (DPSCs) and bone marrow (BM-MSCs).

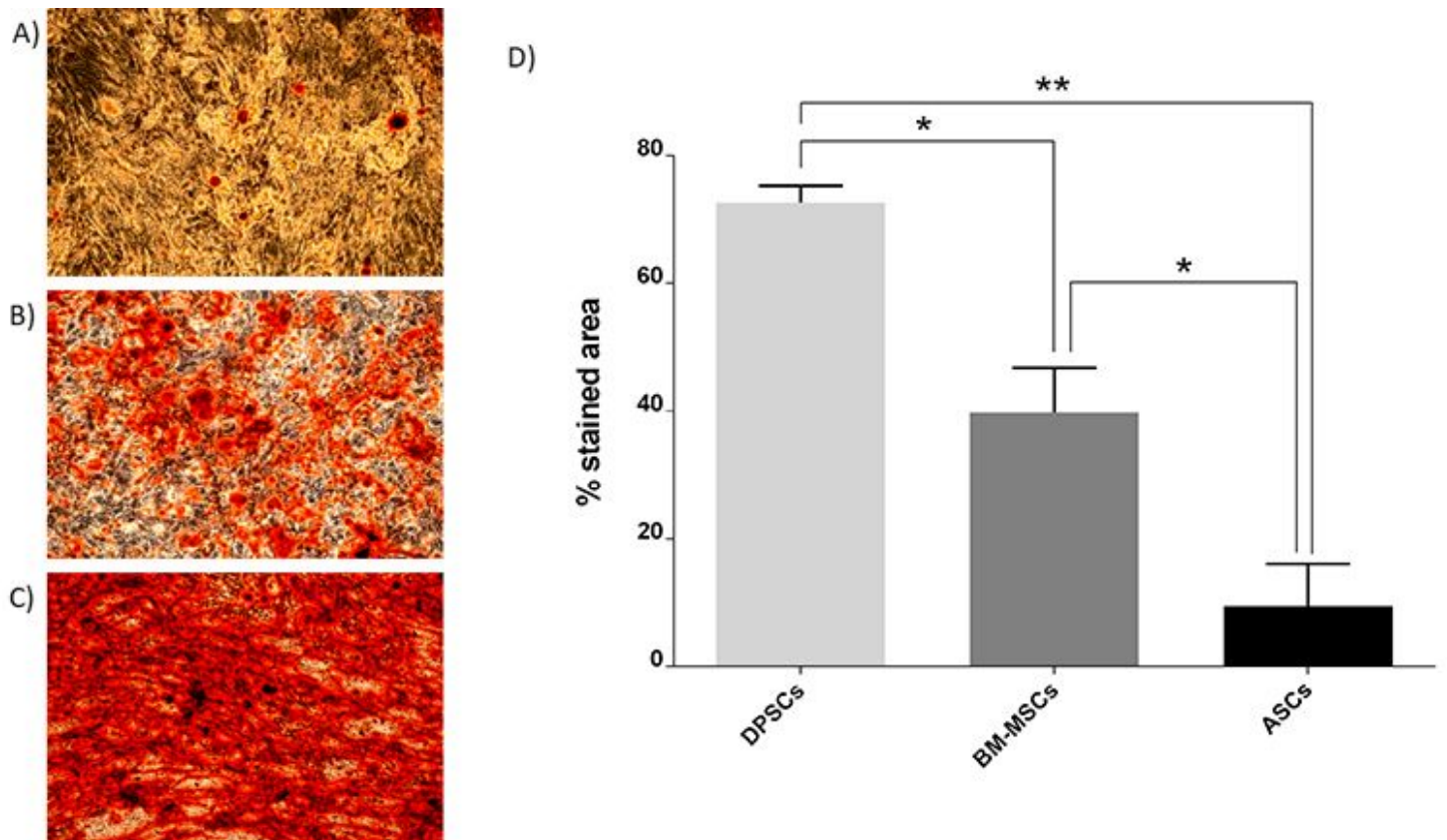


Figure 2

Alizarin Red staining and its quantification of different source-derived mesenchymal stem cells. A) Alizarin Red staining of ASCs after 21 days of culture in osteogenic medium (x10). B) Alizarin Red staining of BM-MSCs after 21 days of culture in osteogenic medium (x10). C) Alizarin Red staining of DPSCs after 21 days of culture in osteogenic medium (x10). D) Alizarin Red staining quantification of MSC according to the cell source: adipose tissue (ASCs), dental pulp (DPSCs) and bone marrow (BM-MSCs).

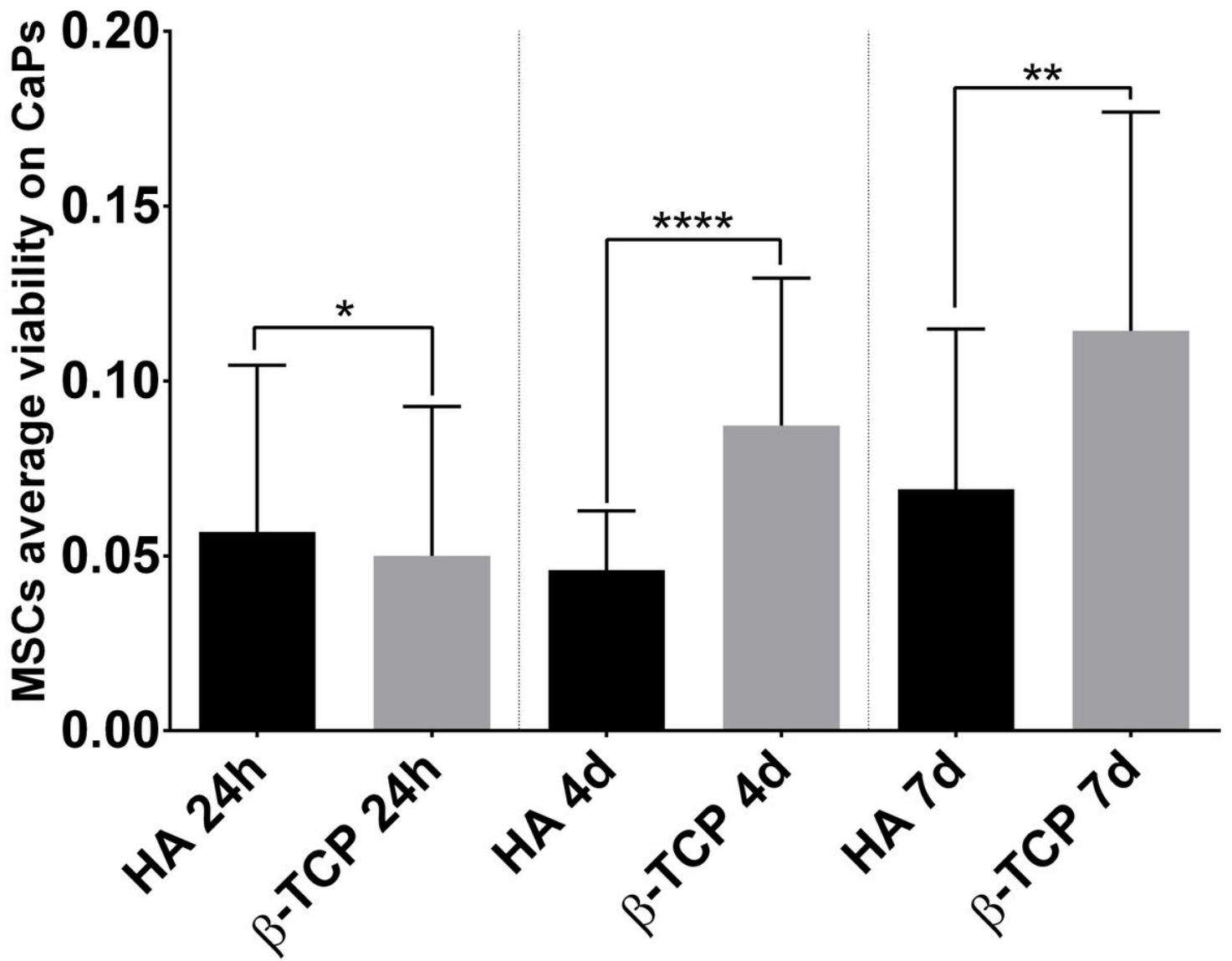


Figure 3

Average viability showed by all MSCs on each CaP. Hydroxyapatite (HA) and β -tricalcium phosphate (β -TCP). All data are shown as mean \pm standard deviation. Significance level: * ≤ 0.05 ** ≤ 0.01 *** ≤ 0.001 **** ≤ 0.0001 .

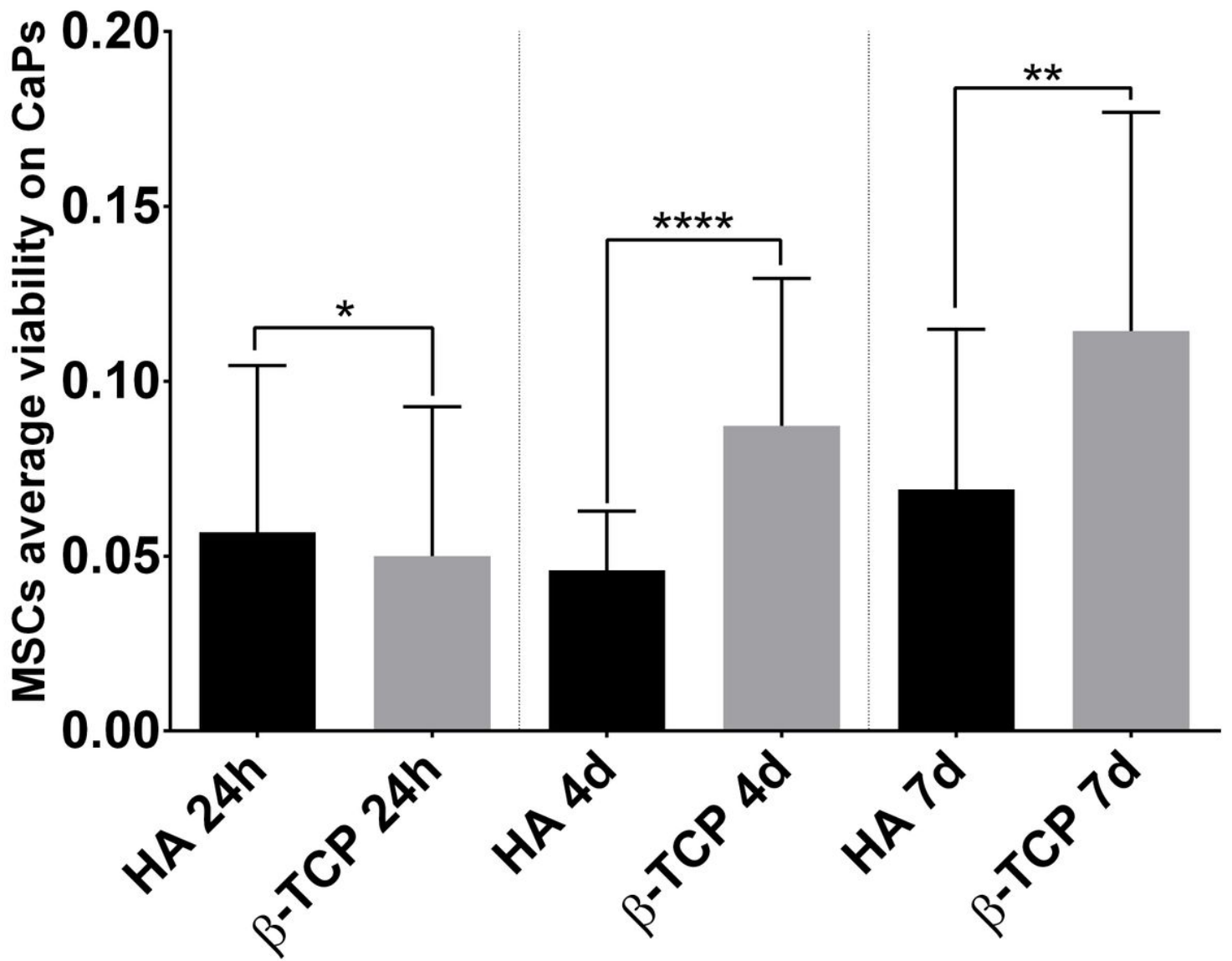


Figure 3

Average viability showed by all MSCs on each CaP. Hydroxyapatite (HA) and β -tricalcium phosphate (β -TCP). All data are shown as mean \pm standard deviation. Significance level: * ≤ 0.05 ** ≤ 0.01 *** ≤ 0.001 **** ≤ 0.0001 .

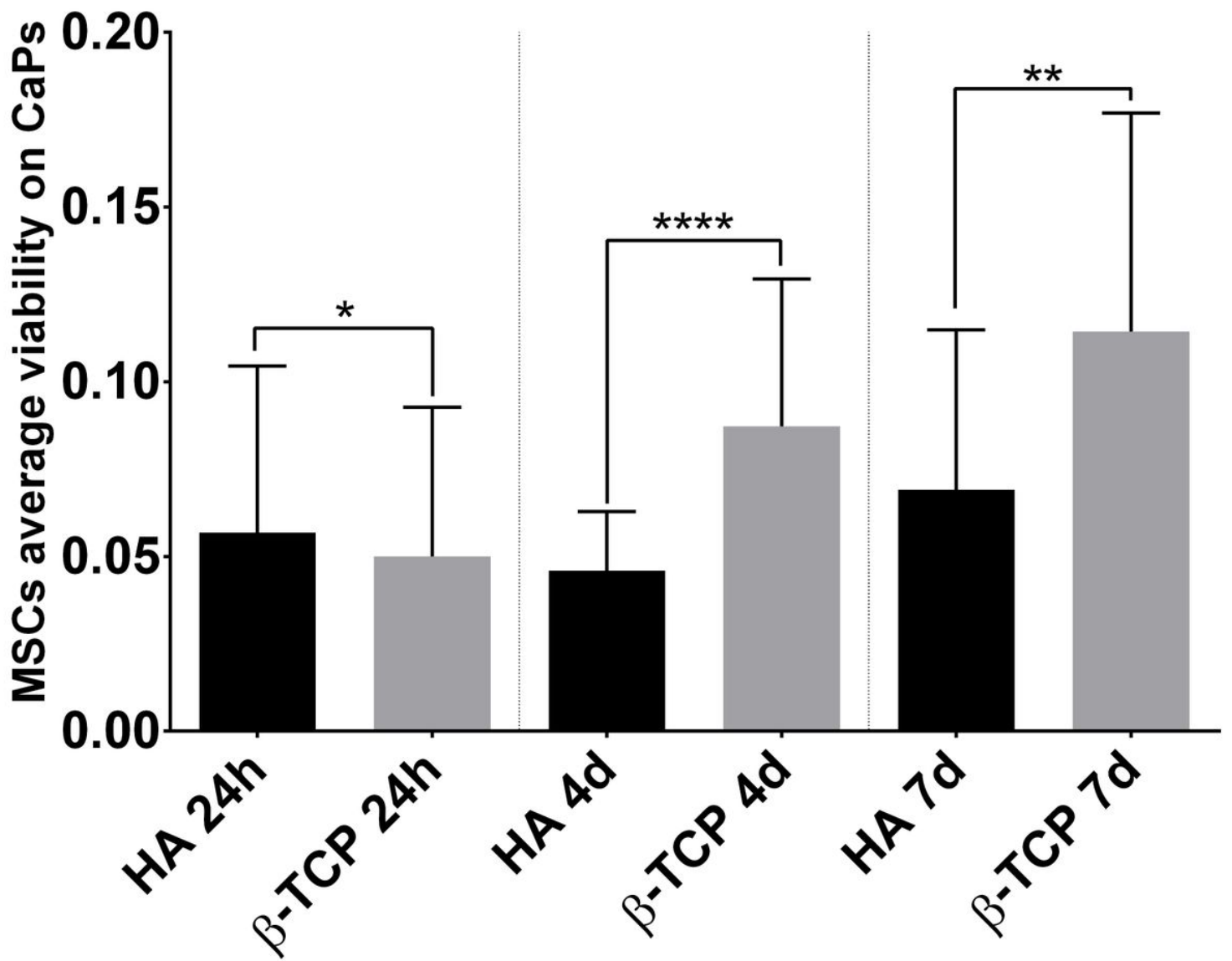


Figure 3

Average viability showed by all MSCs on each CaP. Hydroxyapatite (HA) and β -tricalcium phosphate (β -TCP). All data are shown as mean \pm standard deviation. Significance level: * ≤ 0.05 ** ≤ 0.01 *** ≤ 0.001 **** ≤ 0.0001 .

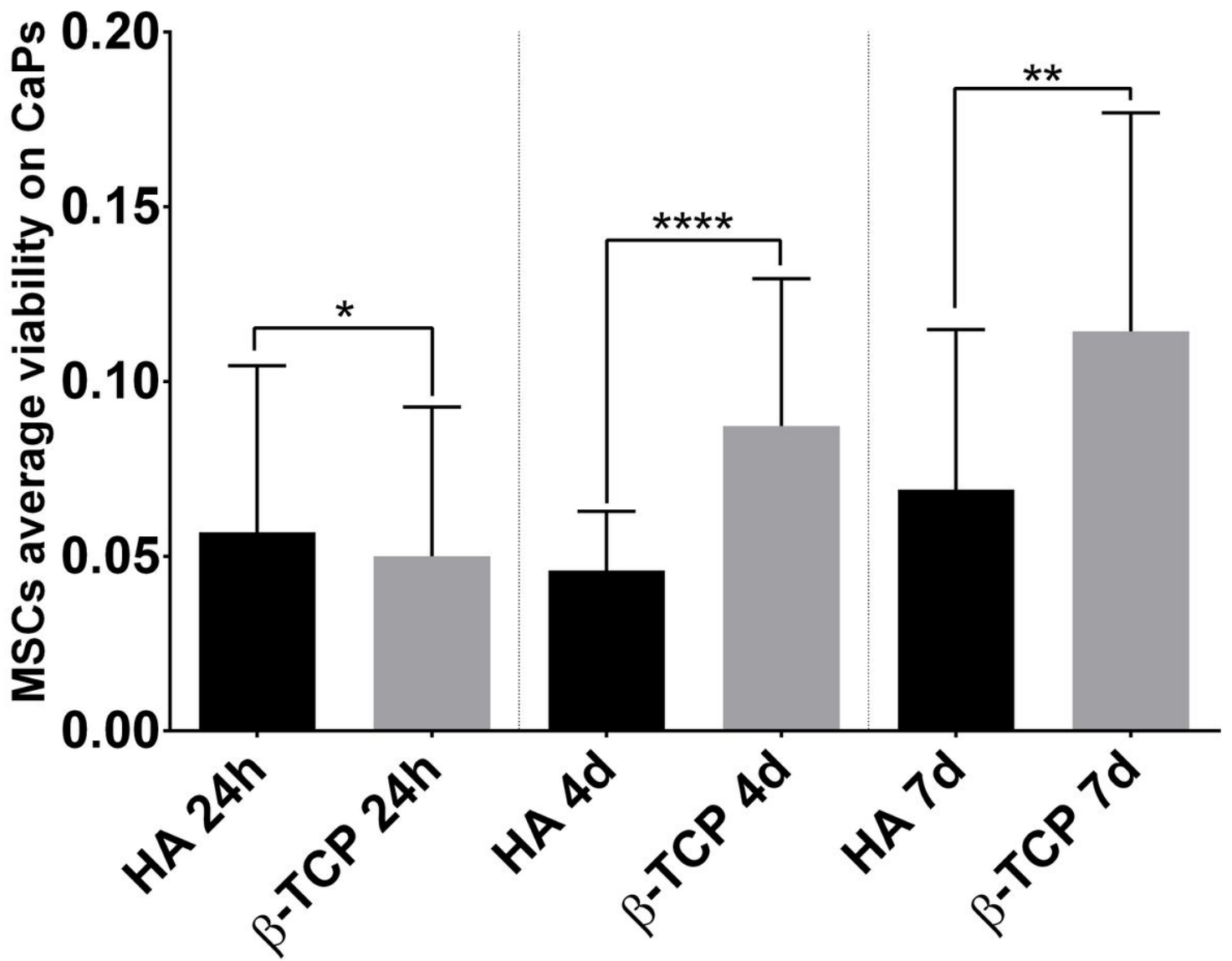


Figure 3

Average viability showed by all MSCs on each CaP. Hydroxyapatite (HA) and β -tricalcium phosphate (β -TCP). All data are shown as mean \pm standard deviation. Significance level: * ≤ 0.05 ** ≤ 0.01 *** ≤ 0.001 **** ≤ 0.0001 .

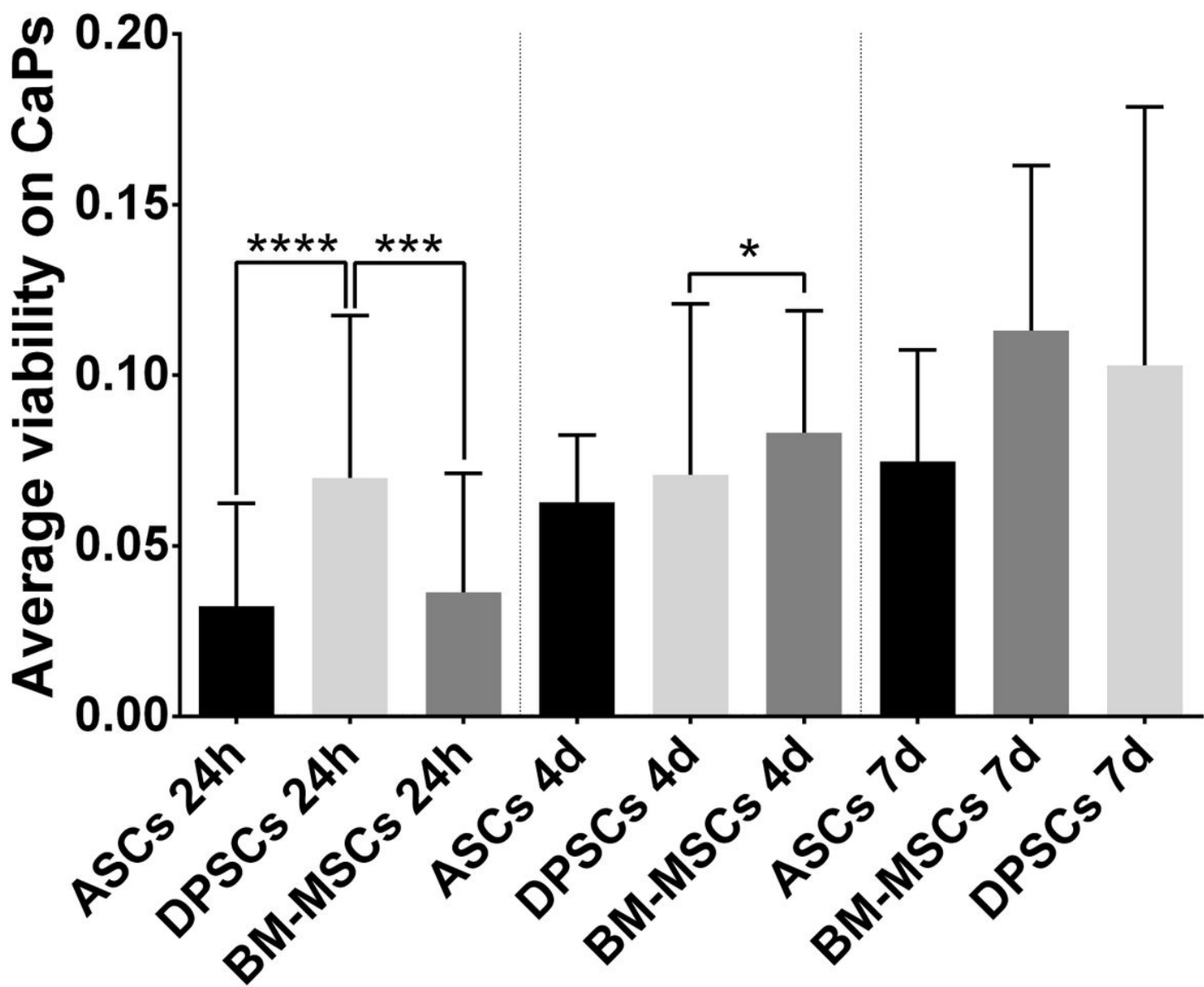


Figure 4

Average viability showed by each MSC on both CaPs. Adipose tissue (ASCs), dental pulp (DPSCs) and bone marrow (BM-MSCs). All data are shown as mean \pm standard deviation. Significance level: * ≤ 0.05 ** ≤ 0.01 *** ≤ 0.001 **** ≤ 0.0001 .

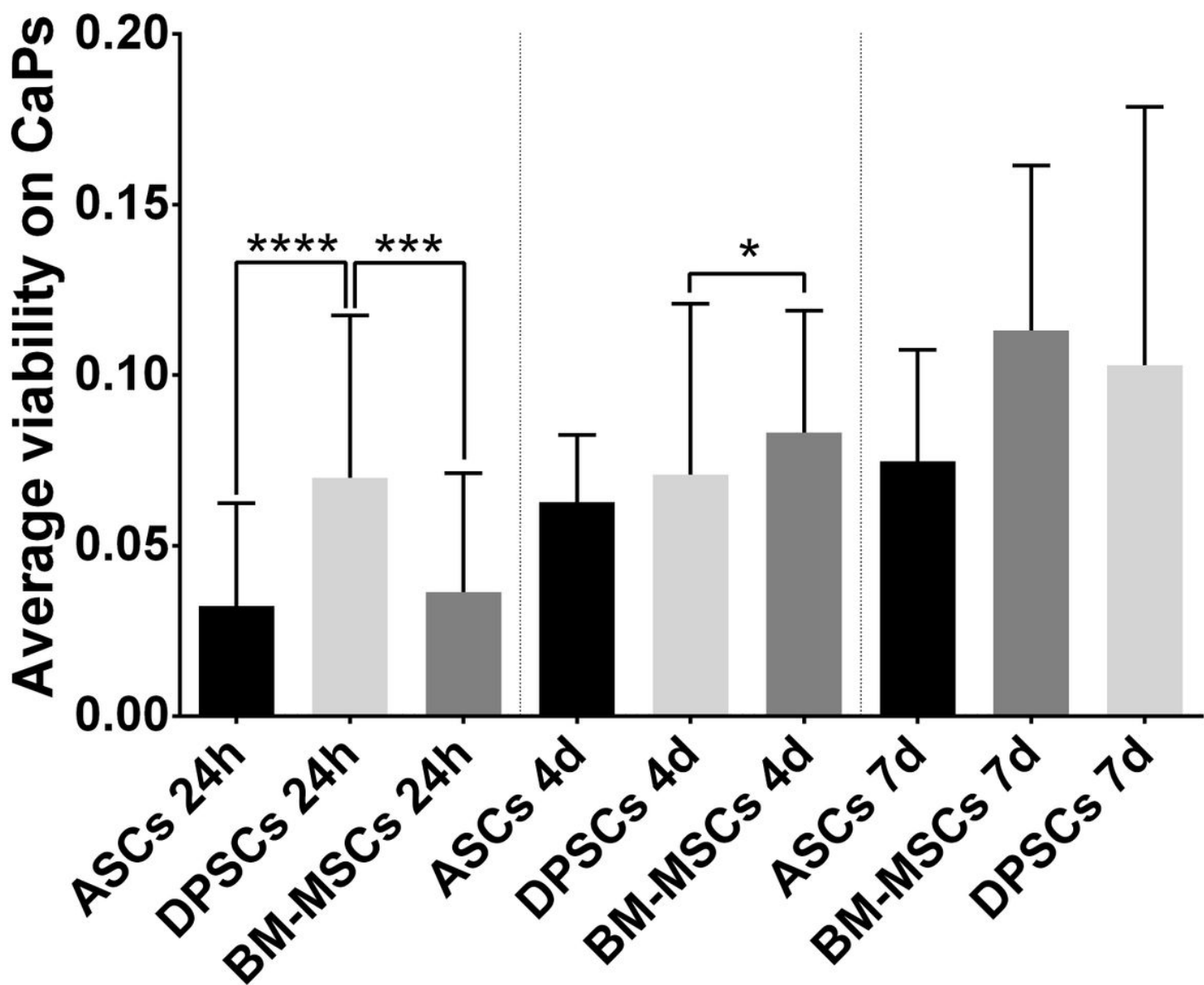


Figure 4

Average viability showed by each MSC on both CaPs. Adipose tissue (ASCs), dental pulp (DPSCs) and bone marrow (BM-MSCs). All data are shown as mean \pm standard deviation. Significance level: * ≤ 0.05 ** ≤ 0.01 *** ≤ 0.001 **** ≤ 0.0001 .

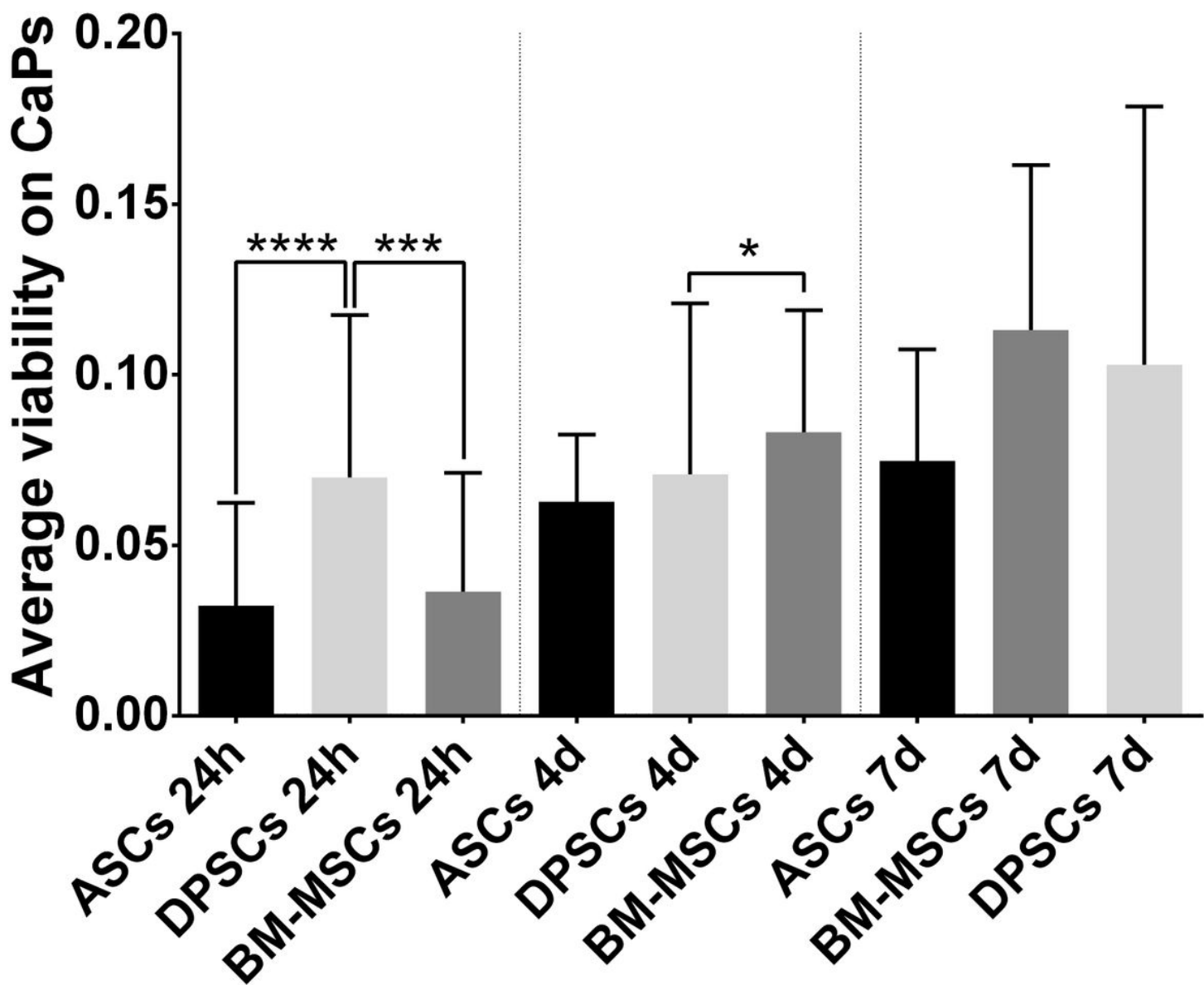


Figure 4

Average viability showed by each MSC on both CaPs. Adipose tissue (ASCs), dental pulp (DPSCs) and bone marrow (BM-MSCs). All data are shown as mean \pm standard deviation. Significance level: * ≤ 0.05 ** ≤ 0.01 *** ≤ 0.001 **** ≤ 0.0001 .

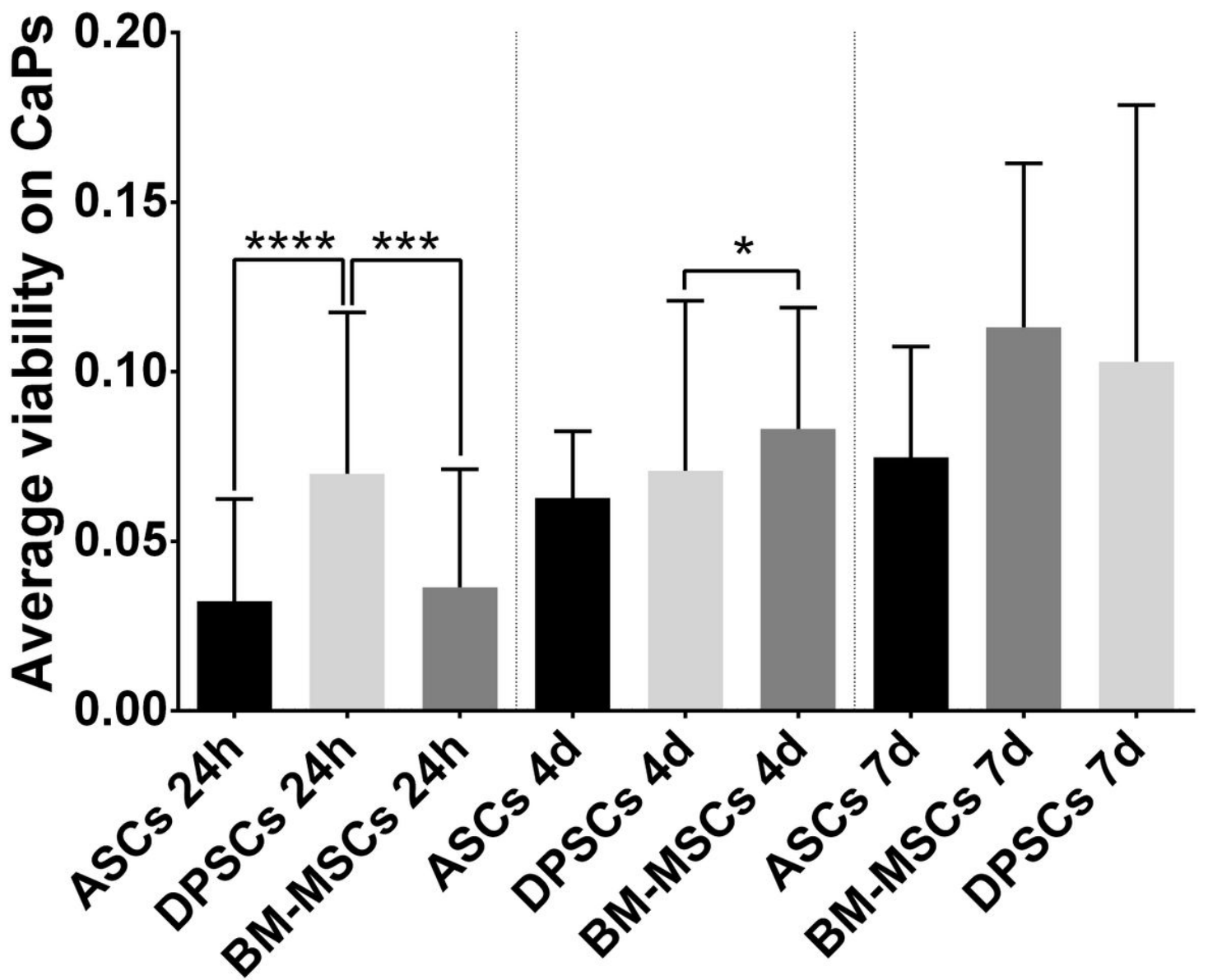


Figure 4

Average viability showed by each MSC on both CaPs. Adipose tissue (ASCs), dental pulp (DPSCs) and bone marrow (BM-MSCs). All data are shown as mean \pm standard deviation. Significance level: * ≤ 0.05 ** ≤ 0.01 *** ≤ 0.001 **** ≤ 0.0001 .

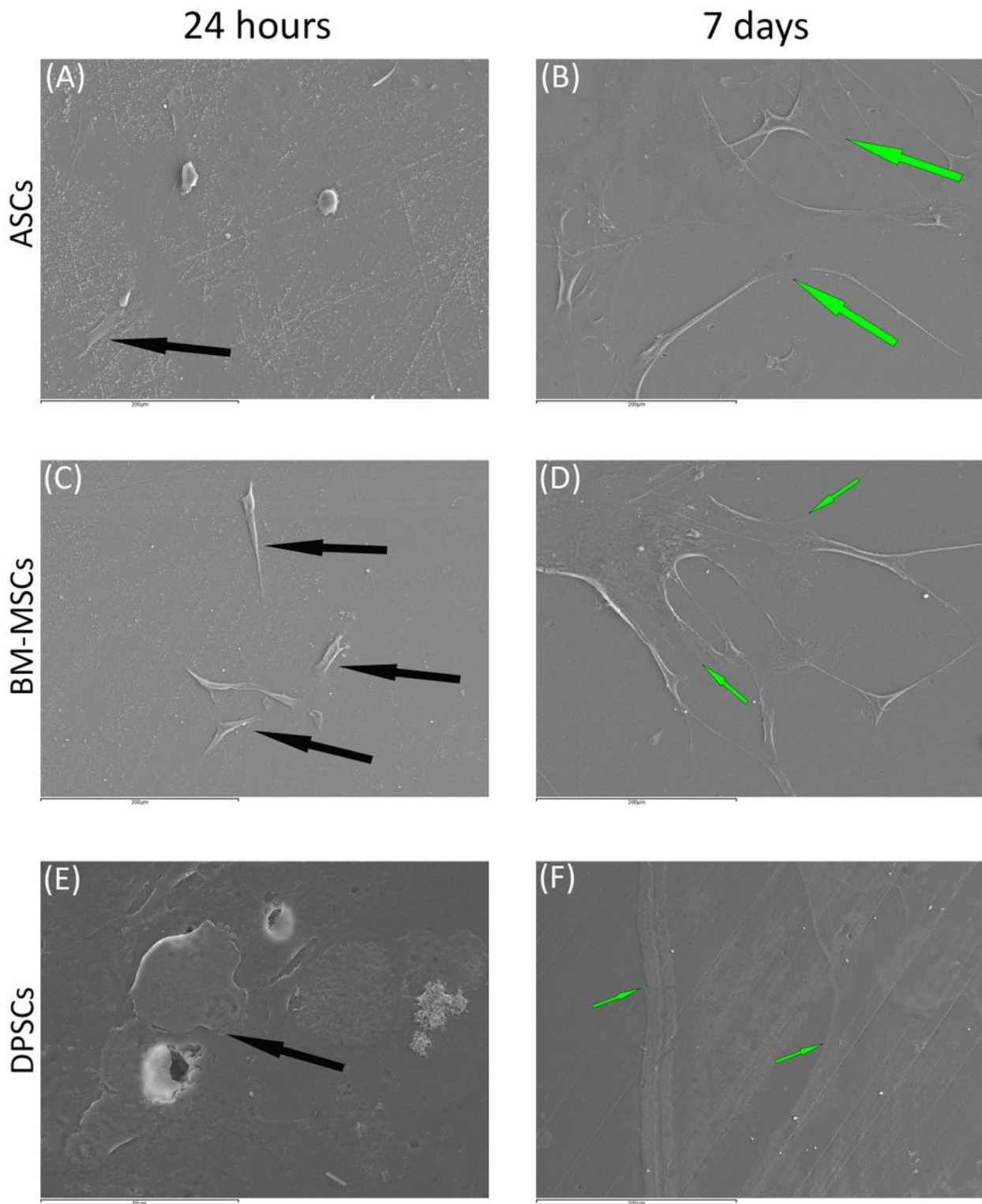


Figure 5

Behaviour of MSC seeded on β -TCP scaffold at different time points. A) ASCs on β -TCP scaffold after 24 hours (scale bar:200 μ m). B) ASCs forming cell layer on β -TCP scaffold after 7 days (scale bar:200 μ m). C) BM-MSCs on β -TCP scaffold after 24 hours (scale bar:200 μ m). D) BM-MSCs forming cell layer on β -TCP scaffold after 7 days scale bar:200 μ m). E) DPSCs on β -TCP scaffold at 24 hours (scale bar:50 μ m). F)

DPSCs forming cell layer on β -TCP scaffold after 7 days (scale bar:200 μ m). Black arrows point to unique cells. Green arrows point to cell layers.

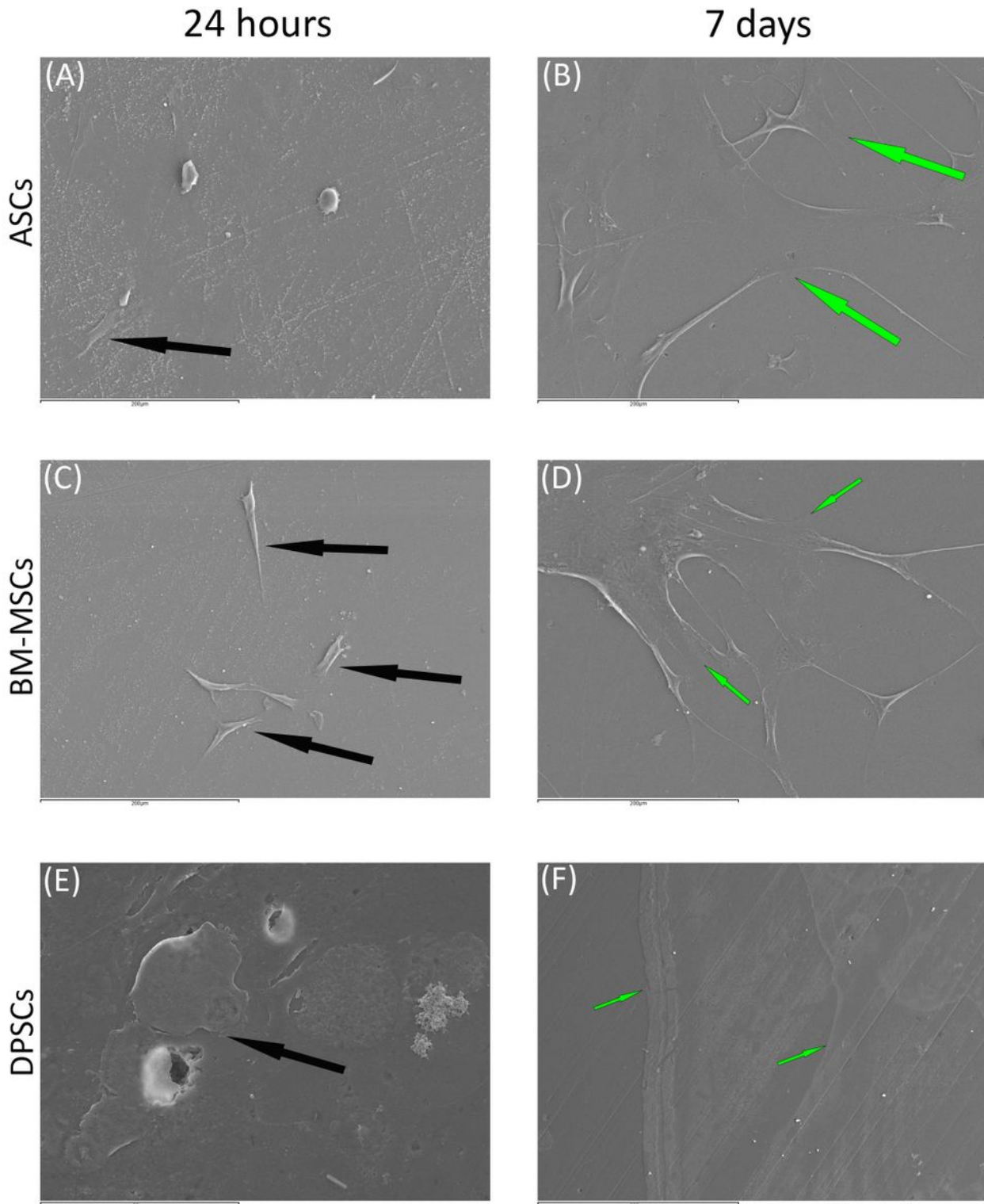


Figure 5

Behaviour of MSC seeded on β -TCP scaffold at different time points. A) ASCs on β -TCP scaffold after 24 hours (scale bar:200 μ m). B) ASCs forming cell layer on β -TCP scaffold after 7 days (scale bar:200 μ m). C) BM-MSCs on β -TCP scaffold after 24 hours (scale bar:200 μ m). D) BM-MSCs forming cell layer on β -TCP

scaffold after 7 days scale bar:200µm). E) DPSCs on β-TCP scaffold at 24 hours (scale bar:50µm). F) DPSCs forming cell layer on β-TCP scaffold after 7 days (scale bar:200µm). Black arrows point to unique cells. Green arrows point to cell layers.

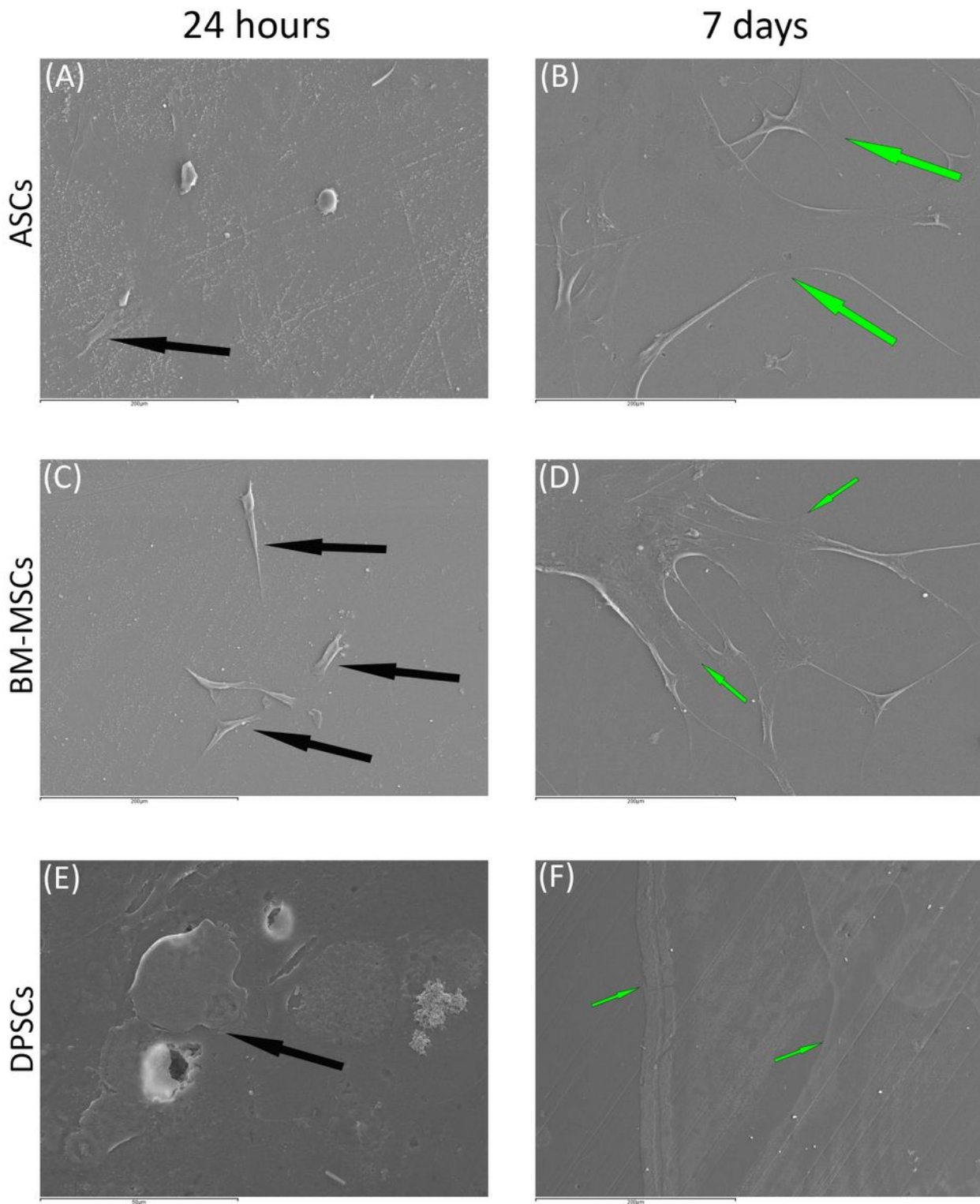


Figure 5

Behaviour of MSC seeded on β-TCP scaffold at different time points. A) ASCs on β-TCP scaffold after 24 hours (scale bar:200µm). B) ASCs forming cell layer on β-TCP scaffold after 7 days (scale bar:200µm). C)

BM-MSCs on β -TCP scaffold after 24 hours (scale bar:200 μ m). D) BM-MSCs forming cell layer on β -TCP scaffold after 7 days scale bar:200 μ m). E) DPSCs on β -TCP scaffold at 24 hours (scale bar:50 μ m). F) DPSCs forming cell layer on β -TCP scaffold after 7 days (scale bar:200 μ m). Black arrows point to unique cells. Green arrows point to cell layers.

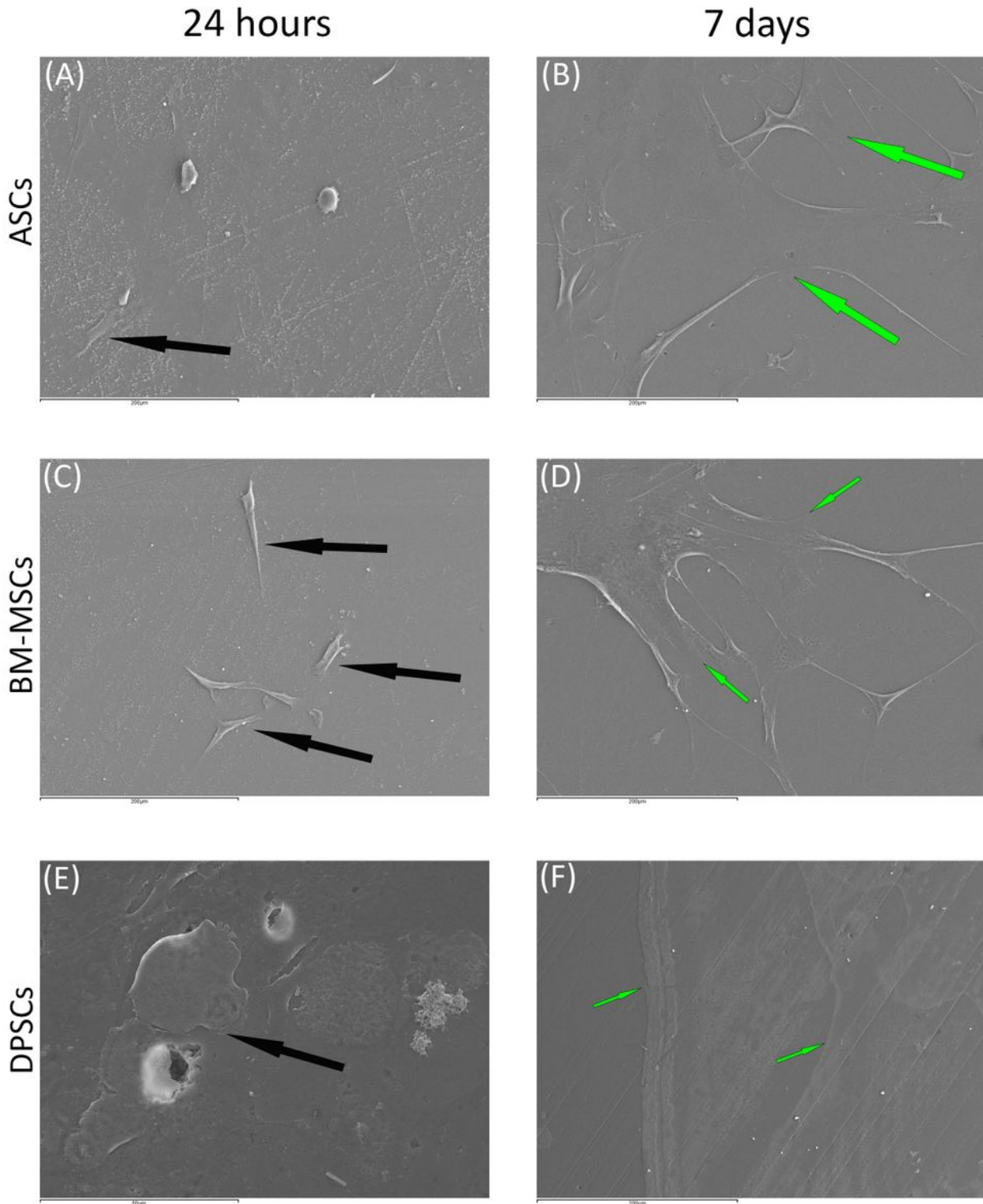


Figure 5

Behaviour of MSC seeded on β -TCP scaffold at different time points. A) ASCs on β -TCP scaffold after 24 hours (scale bar:200 μ m). B) ASCs forming cell layer on β -TCP scaffold after 7 days (scale bar:200 μ m). C) BM-MSCs on β -TCP scaffold after 24 hours (scale bar:200 μ m). D) BM-MSCs forming cell layer on β -TCP scaffold after 7 days scale bar:200 μ m). E) DPSCs on β -TCP scaffold at 24 hours (scale bar:50 μ m). F) DPSCs forming cell layer on β -TCP scaffold after 7 days (scale bar:200 μ m). Black arrows point to unique cells. Green arrows point to cell layers.

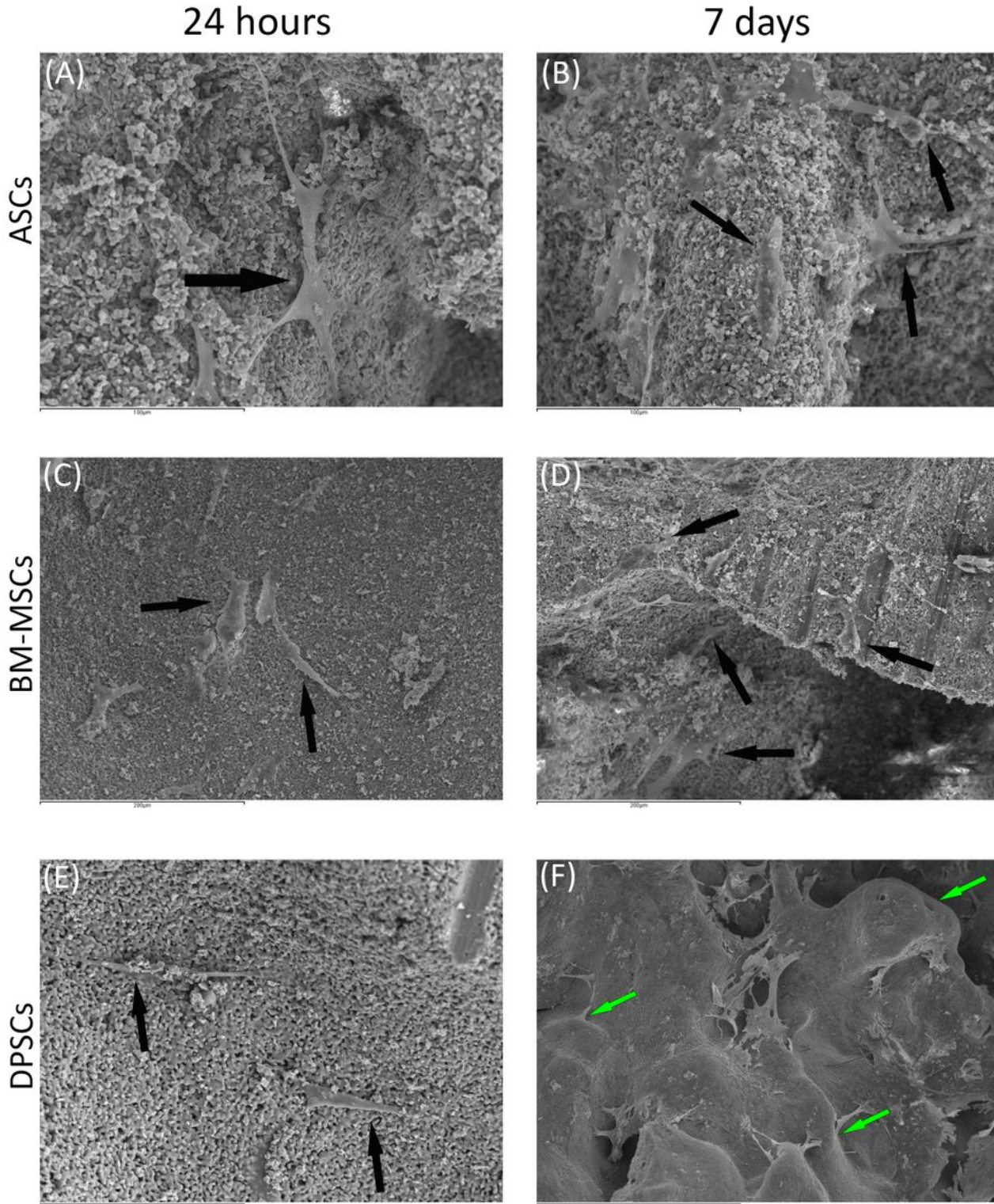


Figure 6

Behaviour of MSC seeded on HA scaffold at different time points. A) ASCs on HA scaffold after 24 hours (scale bar:100µm). B) ASCs forming cell layer on HA scaffold after 7 days (scale bar:100µm). C) BM-MSCs on HA scaffold after 24 hours (scale bar:200µm). D) BM-MSCs forming cell layer on HA scaffold after 7 days scale bar:200µm). E) DPSCs on HA scaffold at 24 hours (scale bar:100µm). F) DPSCs forming cell layer on HA scaffold after 7 days (scale bar:1mm). Black arrows point to unique cells. Green arrows point to cell layers.

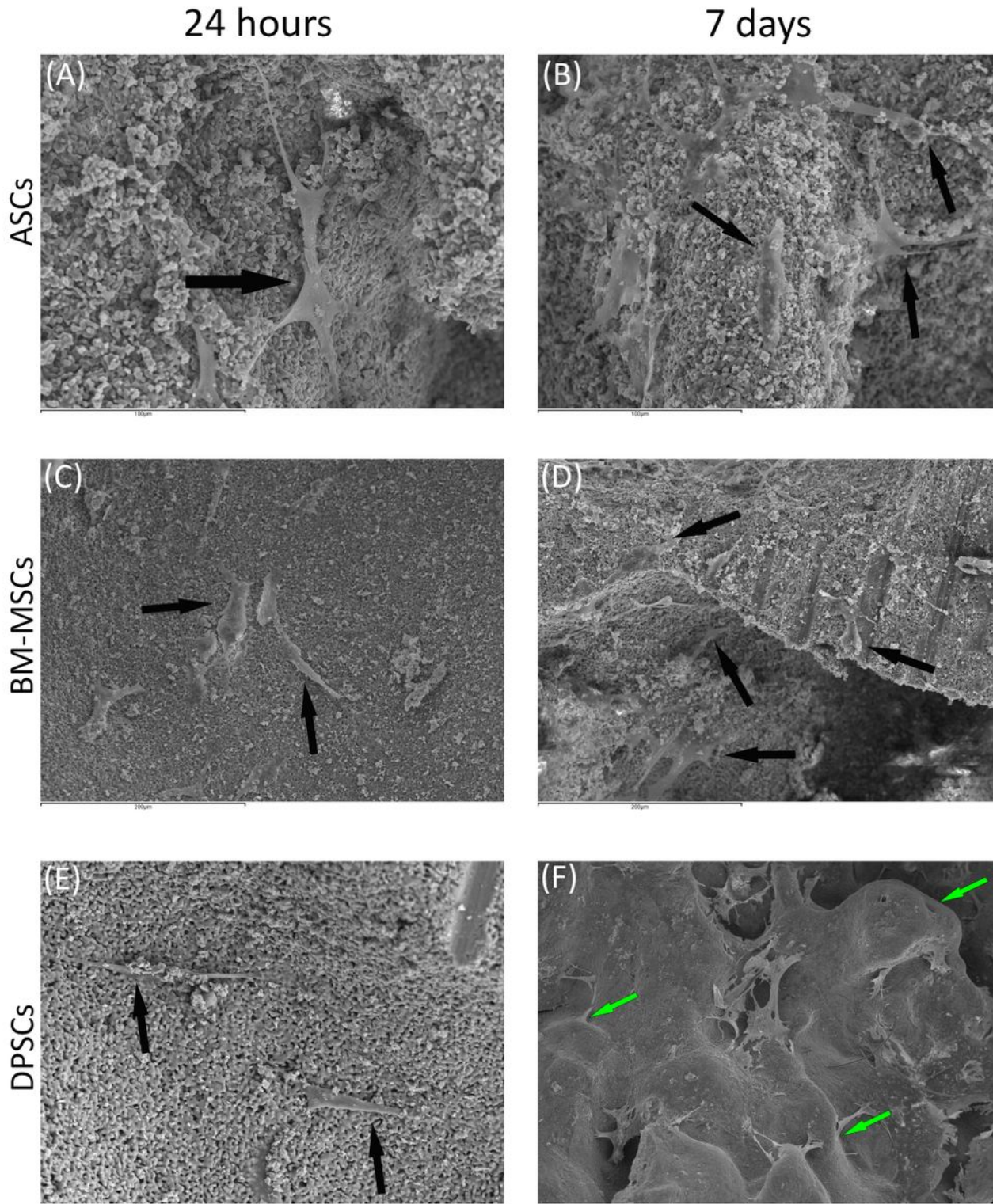


Figure 6

Behaviour of MSC seeded on HA scaffold at different time points. A) ASCs on HA scaffold after 24 hours (scale bar:100µm). B) ASCs forming cell layer on HA scaffold after 7 days (scale bar:100µm). C) BM-MSCs on HA scaffold after 24 hours (scale bar:200µm). D) BM-MSCs forming cell layer on HA scaffold after 7 days scale bar:200µm). E) DPSCs on HA scaffold at 24 hours (scale bar:100µm). F) DPSCs forming cell layer on HA scaffold after 7 days (scale bar:1mm). Black arrows point to unique cells. Green arrows point to cell layers.

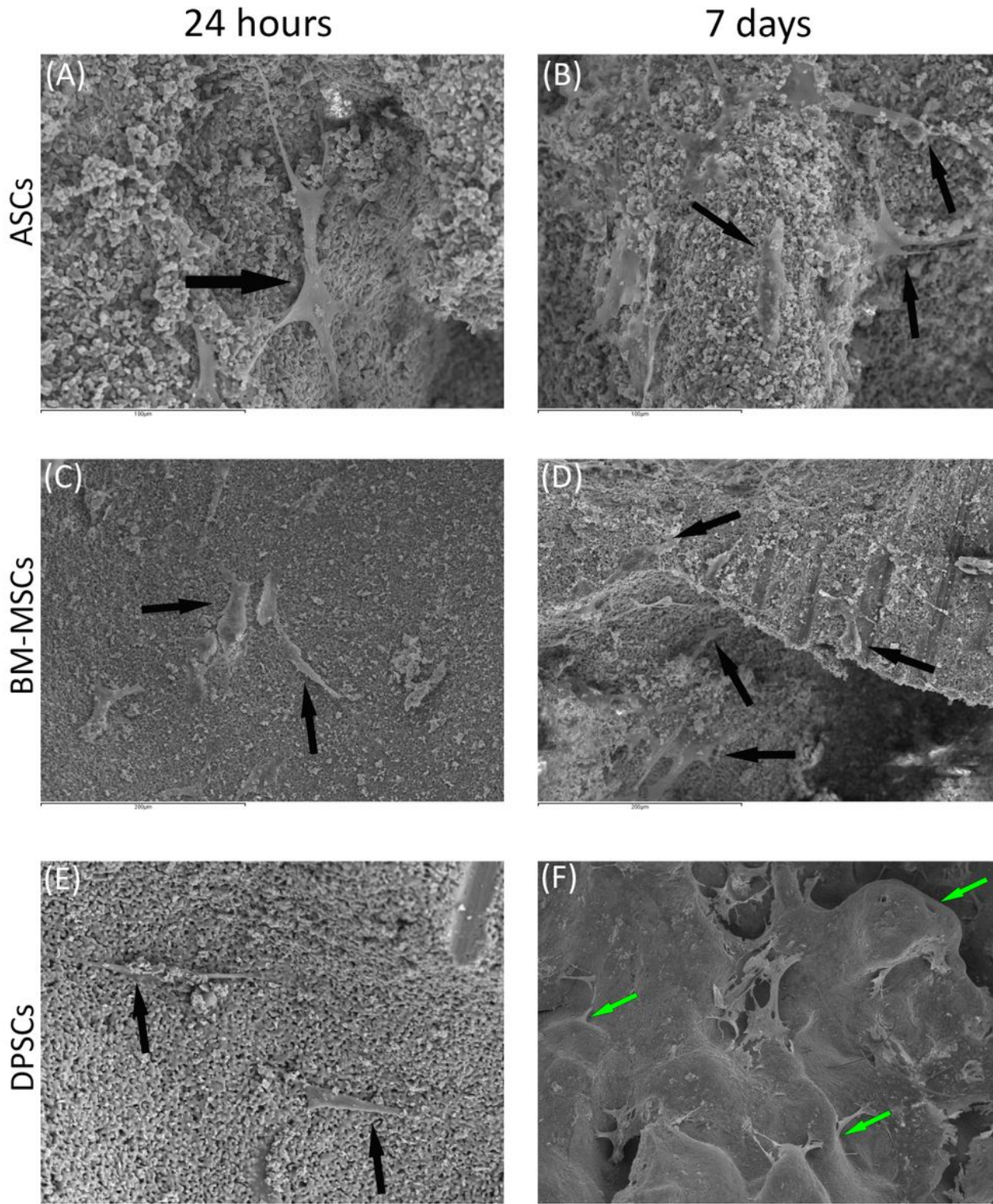


Figure 6

Behaviour of MSC seeded on HA scaffold at different time points. A) ASCs on HA scaffold after 24 hours (scale bar:100µm). B) ASCs forming cell layer on HA scaffold after 7 days (scale bar:100µm). C) BM-MSCs on HA scaffold after 24 hours (scale bar:200µm). D) BM-MSCs forming cell layer on HA scaffold after 7 days scale bar:200µm). E) DPSCs on HA scaffold at 24 hours (scale bar:100µm). F) DPSCs forming cell layer on HA scaffold after 7 days (scale bar:1mm). Black arrows point to unique cells. Green arrows point to cell layers.

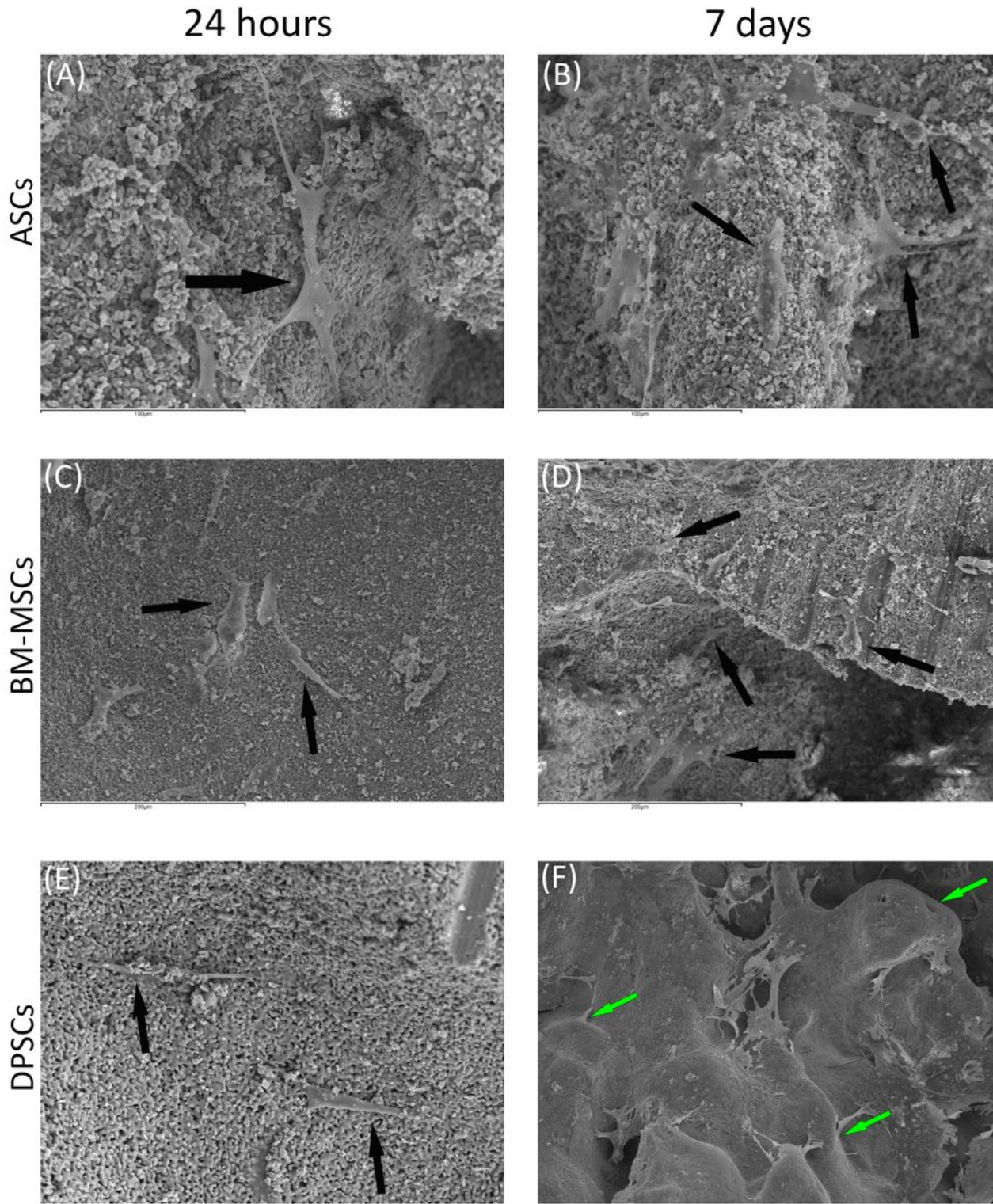


Figure 6

Behaviour of MSC seeded on HA scaffold at different time points. A) ASCs on HA scaffold after 24 hours (scale bar:100µm). B) ASCs forming cell layer on HA scaffold after 7 days (scale bar:100µm). C) BM-MSCs on HA scaffold after 24 hours (scale bar:200µm). D) BM-MSCs forming cell layer on HA scaffold after 7 days scale bar:200µm). E) DPSCs on HA scaffold at 24 hours (scale bar:100µm). F) DPSCs forming cell layer on HA scaffold after 7 days (scale bar:1mm). Black arrows point to unique cells. Green arrows point to cell layers.

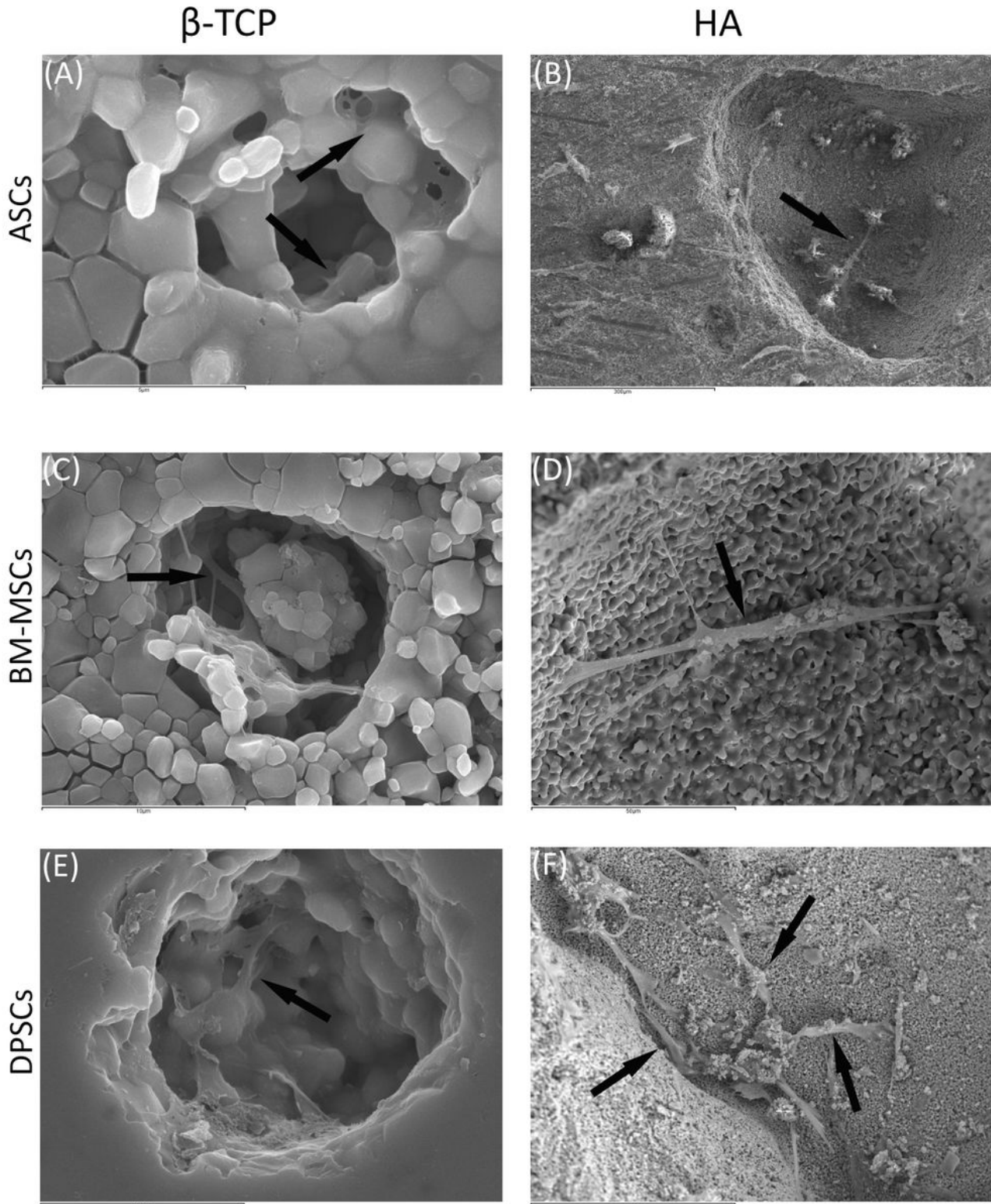


Figure 7

MSCs colonizing pores of both HA and β -TCP scaffolds after 24 hours. A) Existing pores in HA colonized by DPSCs (scale bar:5 μ m). B) Existing pores in HA colonized by BM-MSCs (scale bar:300 μ m). C) Existing pores in HA colonized by ASCs (scale bar:10 μ m). D) Existing pores in β -TCP colonized by DPSCs (scale bar:50 μ m). E) Existing pores in β -TCP colonized by BM-MSCs (scale bar:10 μ m). F) Existing pores in β -TCP colonized by ASCs (scale bar:200 μ m).

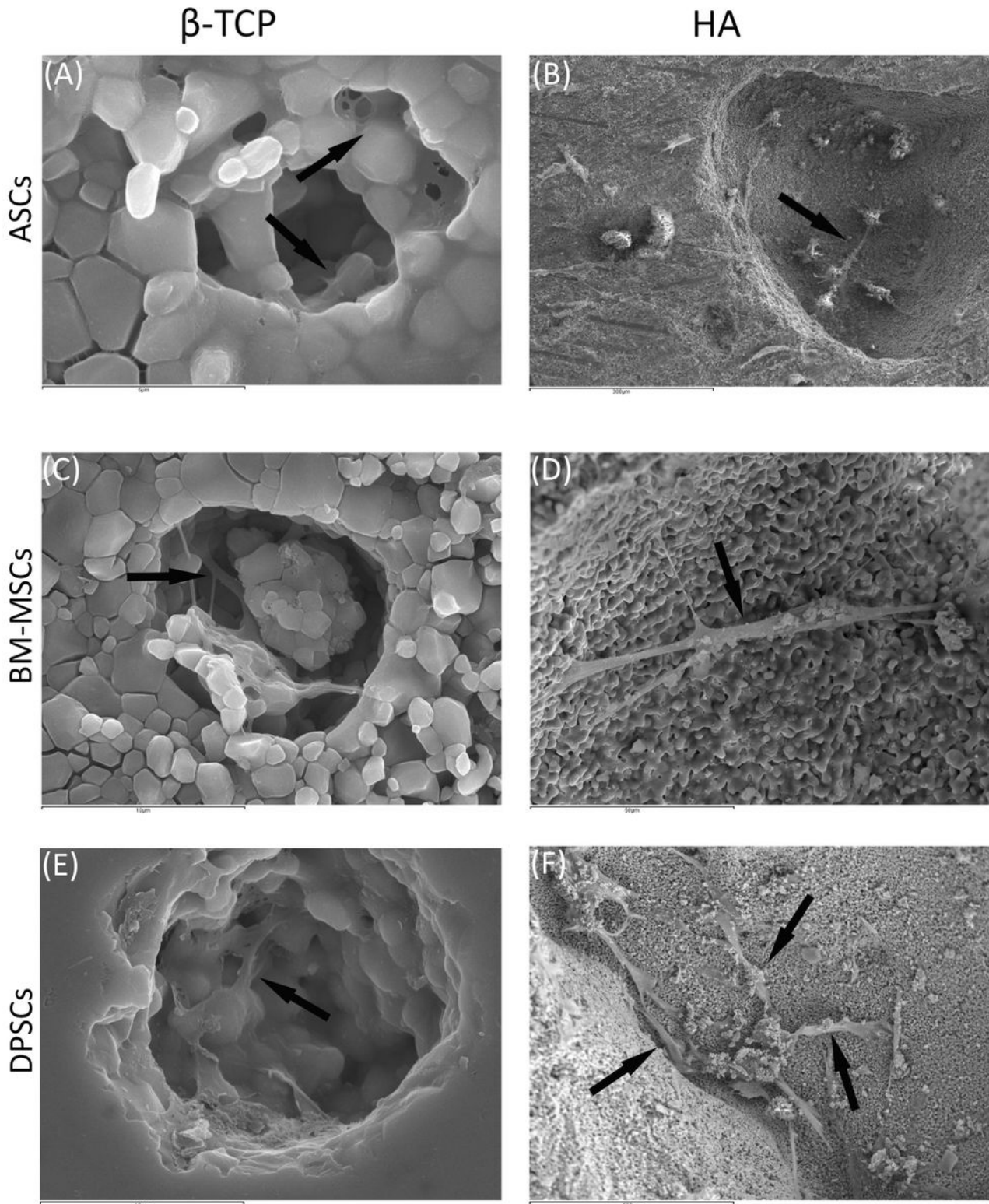


Figure 7

MSCs colonizing pores of both HA and β -TCP scaffolds after 24 hours. A) Existing pores in HA colonized by DPSCs (scale bar:5 μ m). B) Existing pores in HA colonized by BM-MSCs (scale bar:300 μ m). C) Existing pores in HA colonized by ASCs (scale bar:10 μ m). D) Existing pores in β -TCP colonized by DPSCs (scale bar:50 μ m). E) Existing pores in β -TCP colonized by BM-MSCs (scale bar:10 μ m). F) Existing pores in β -TCP colonized by ASCs (scale bar:200 μ m).

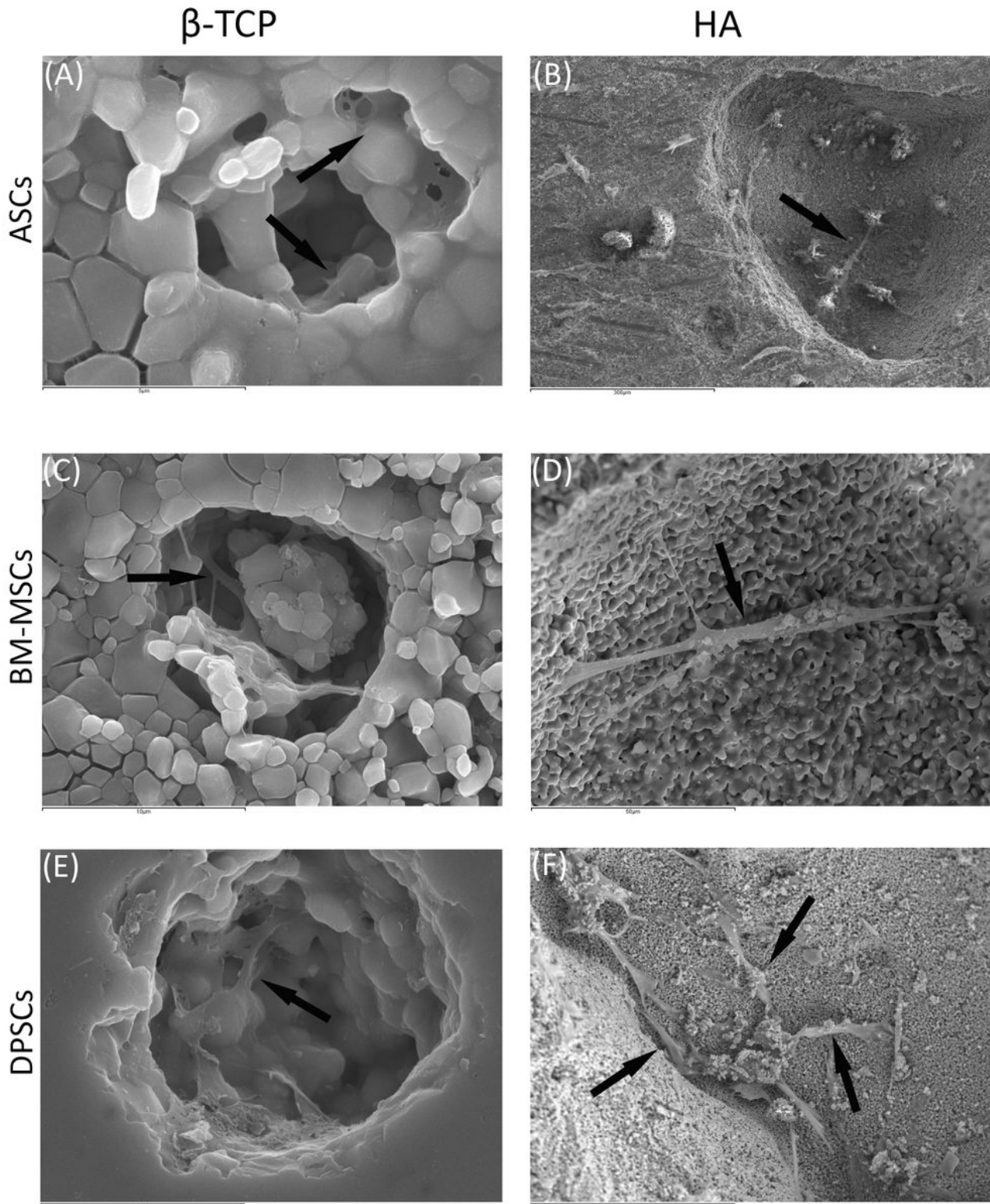


Figure 7

MSCs colonizing pores of both HA and β -TCP scaffolds after 24 hours. A) Existing pores in HA colonized by DPSCs (scale bar:5 μ m). B) Existing pores in HA colonized by BM-MSCs (scale bar:300 μ m). C) Existing pores in HA colonized by ASCs (scale bar:10 μ m). D) Existing pores in β -TCP colonized by DPSCs (scale bar:50 μ m). E) Existing pores in β -TCP colonized by BM-MSCs (scale bar:10 μ m). F) Existing pores in β -TCP colonized by ASCs (scale bar:200 μ m).

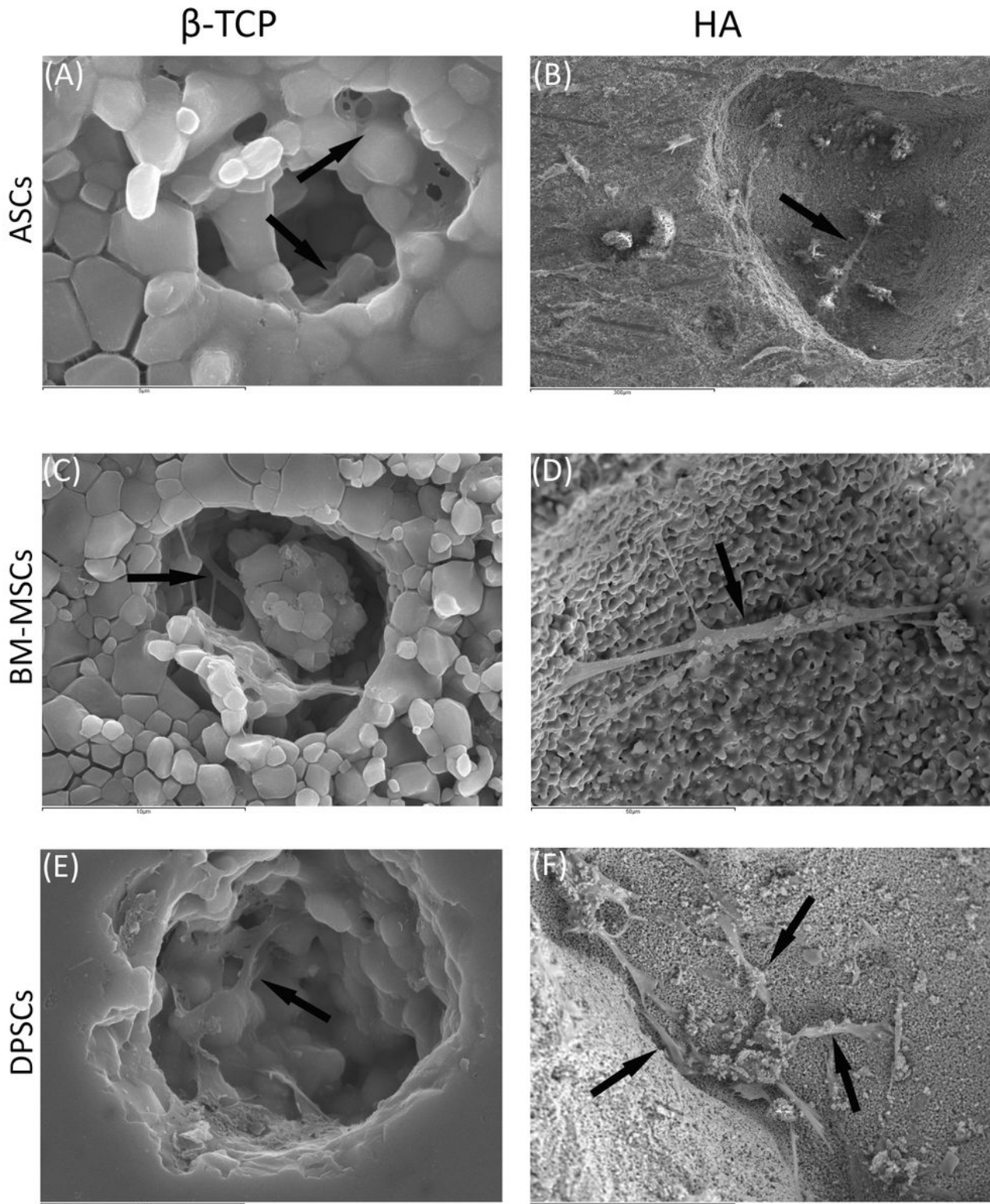


Figure 7

MSCs colonizing pores of both HA and β -TCP scaffolds after 24 hours. A) Existing pores in HA colonized by DPSCs (scale bar:5 μ m). B) Existing pores in HA colonized by BM-MSCs (scale bar:300 μ m). C) Existing pores in HA colonized by ASCs (scale bar:10 μ m). D) Existing pores in β -TCP colonized by DPSCs (scale bar:50 μ m). E) Existing pores in β -TCP colonized by BM-MSCs (scale bar:10 μ m). F) Existing pores in β -TCP colonized by ASCs (scale bar:200 μ m).

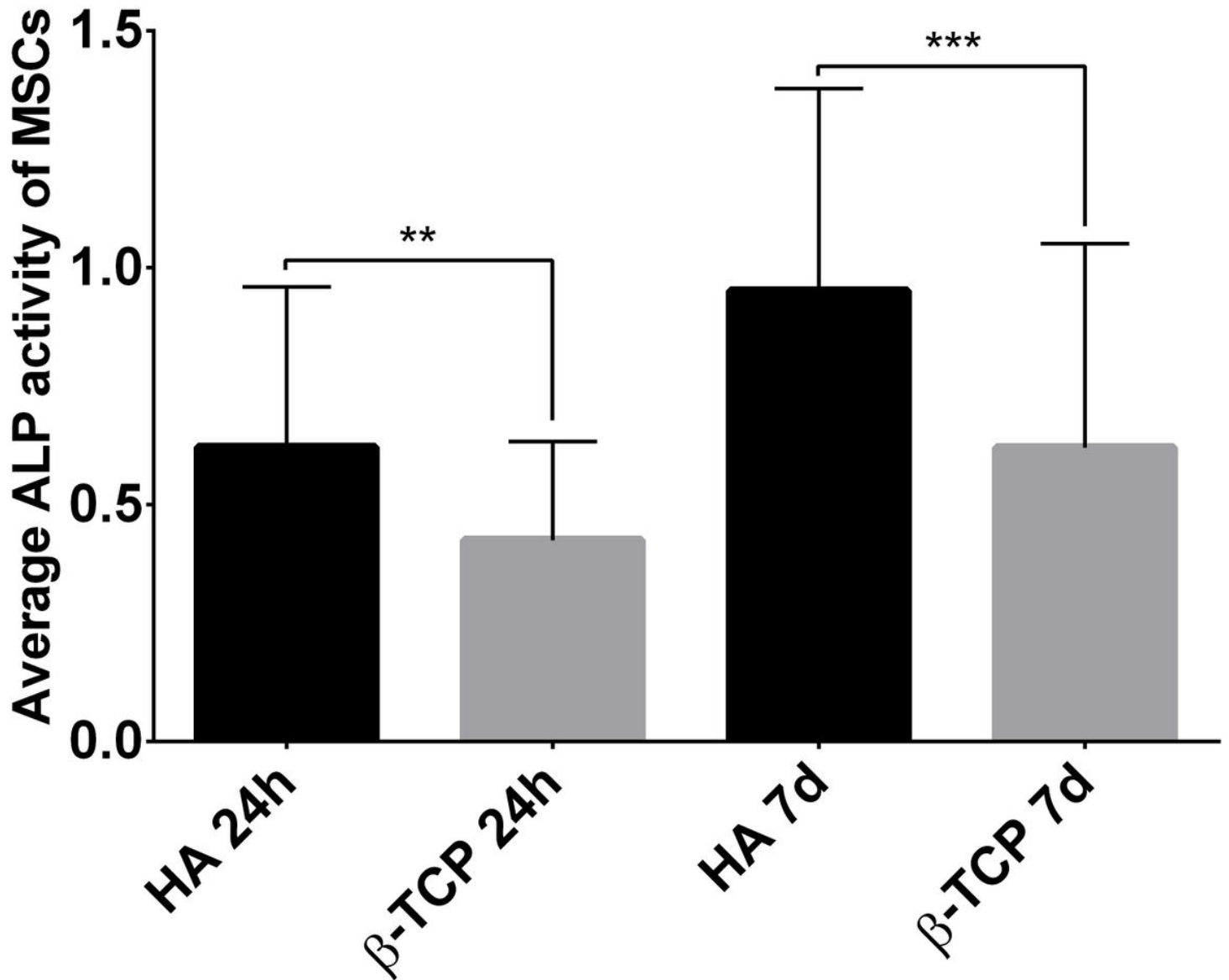


Figure 8

Average ALP activity showed by all MSCs on each CaP. Hydroxyapatite (HA) and β -tricalcium phosphate (β -TCP). All data are shown as mean \pm standard deviation. Significance level: ** \leq 0.01 *** \leq 0.001.

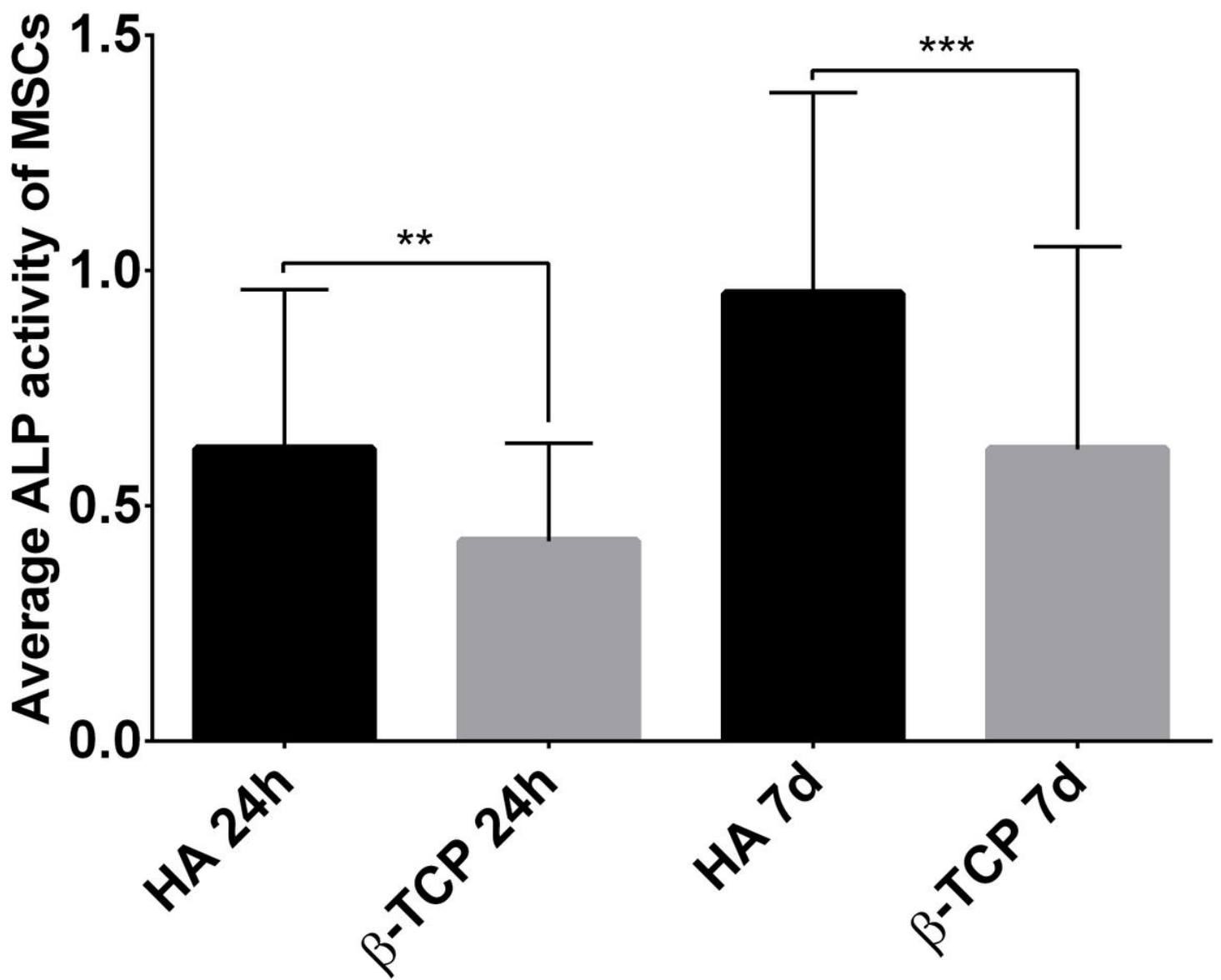


Figure 8

Average ALP activity showed by all MSCs on each CaP. Hydroxyapatite (HA) and β -tricalcium phosphate (β -TCP). All data are shown as mean \pm standard deviation. Significance level: ** \leq 0.01 *** \leq 0.001.

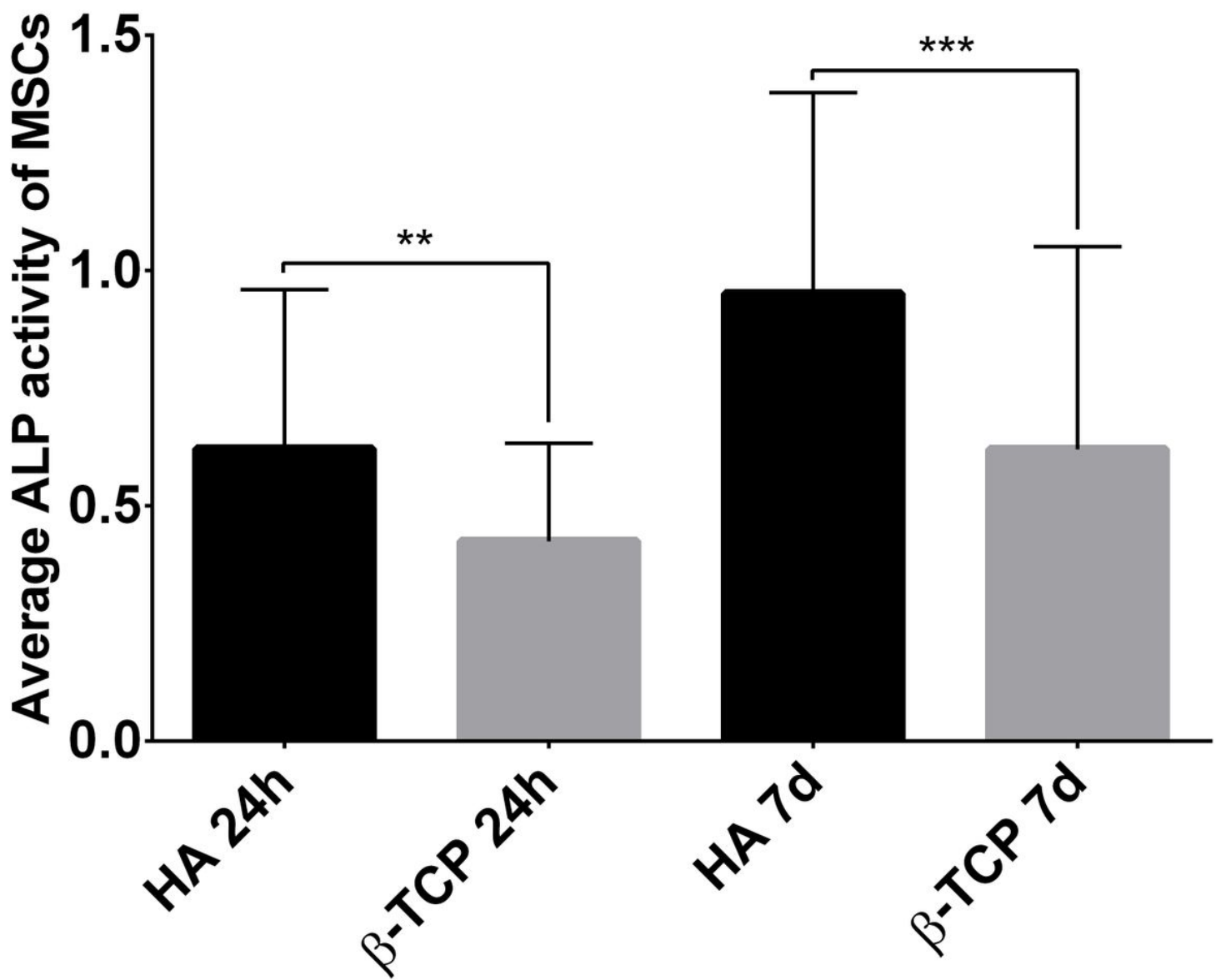


Figure 8

Average ALP activity showed by all MSCs on each CaP. Hydroxyapatite (HA) and β-tricalcium phosphate (β-TCP). All data are shown as mean ± standard deviation. Significance level: ** ≤ 0.01 *** ≤ 0.001.

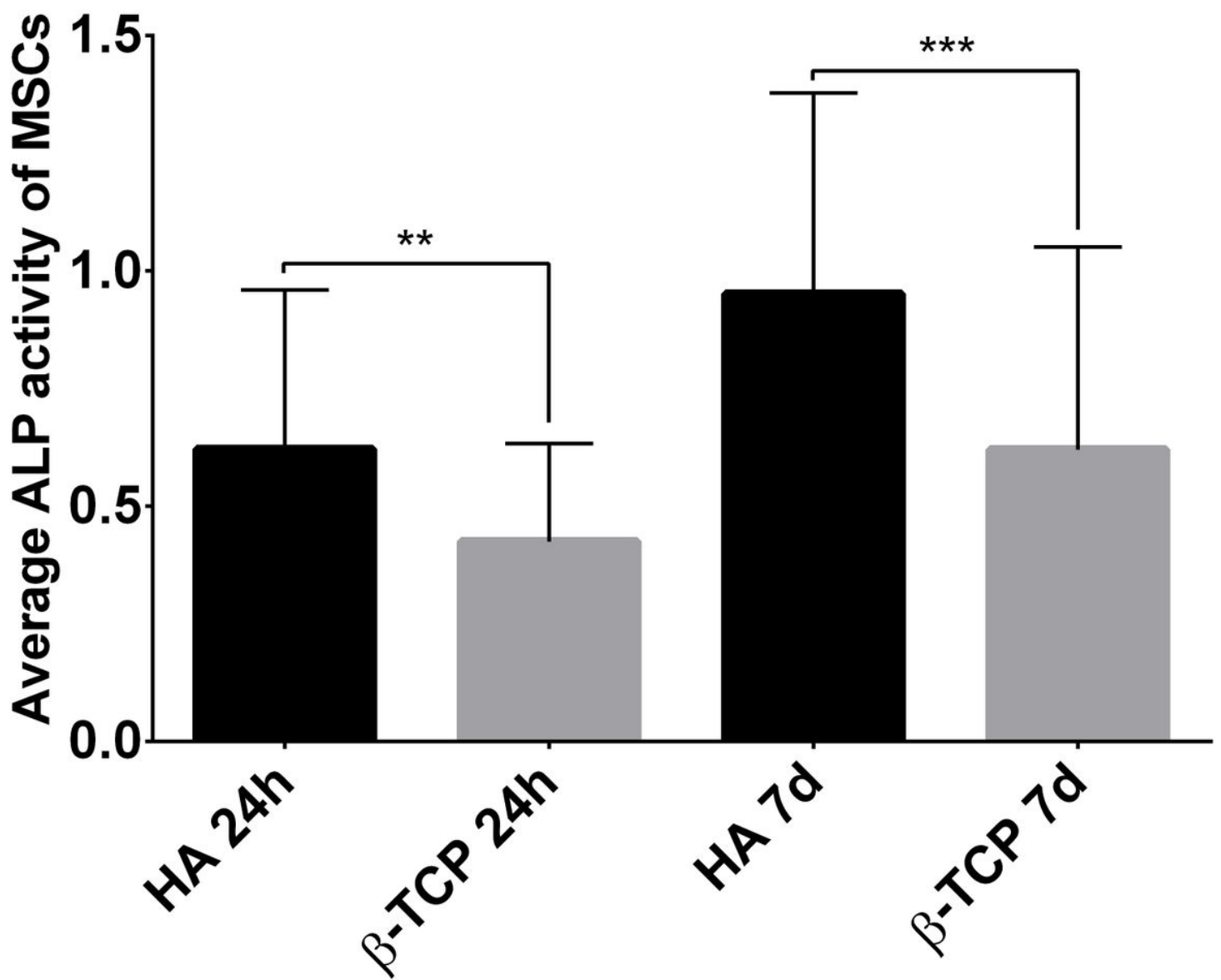


Figure 8

Average ALP activity showed by all MSCs on each CaP. Hydroxyapatite (HA) and β -tricalcium phosphate (β -TCP). All data are shown as mean \pm standard deviation. Significance level: ** \leq 0.01 *** \leq 0.001.

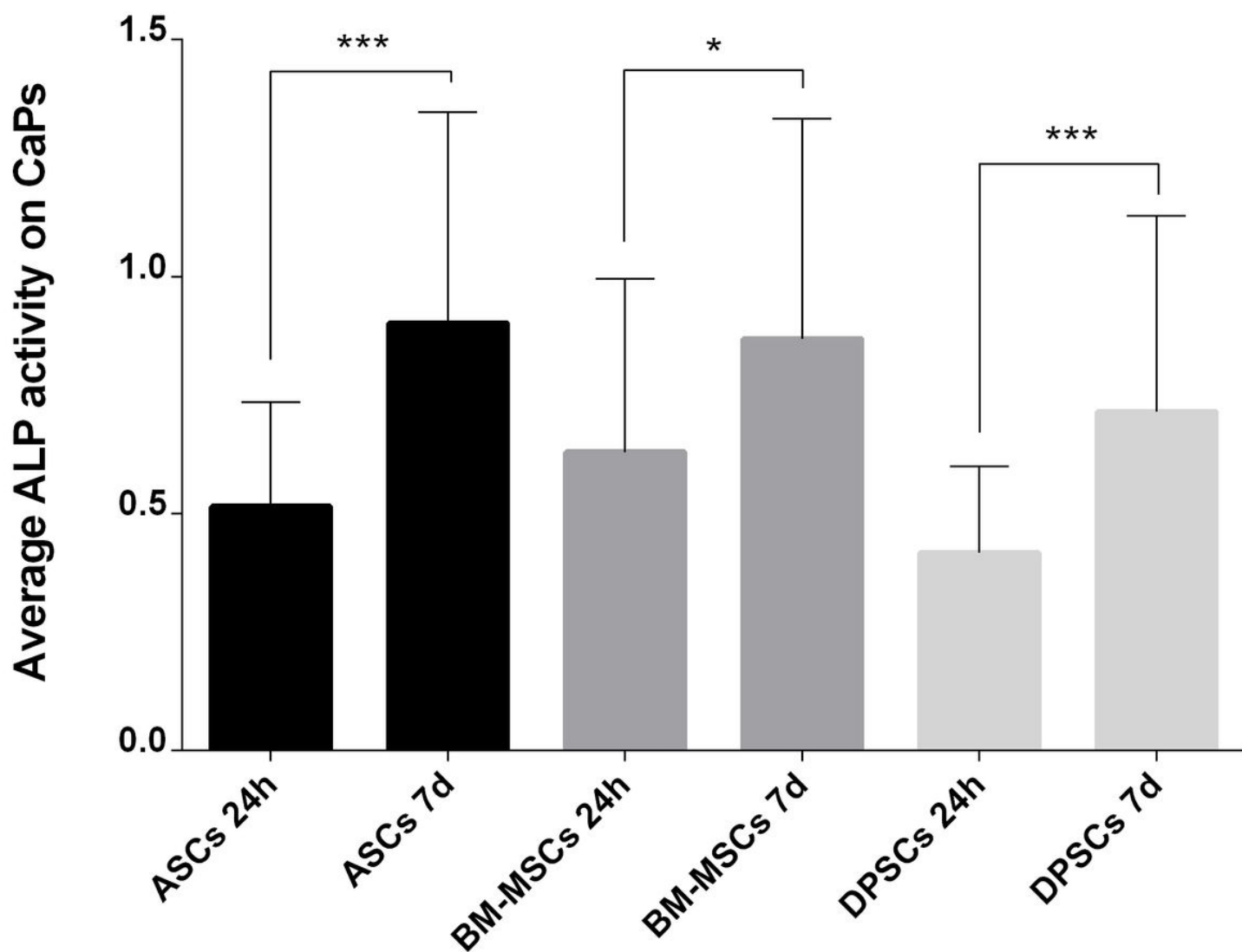


Figure 9

Average ALP activity showed by each MSC on both CaPs. Adipose tissue (ASCs), dental pulp (DPSCs) and bone marrow (BM-MSCs). All data are shown as mean \pm standard deviation. Significance level: * ≤ 0.05 *** ≤ 0.001 .

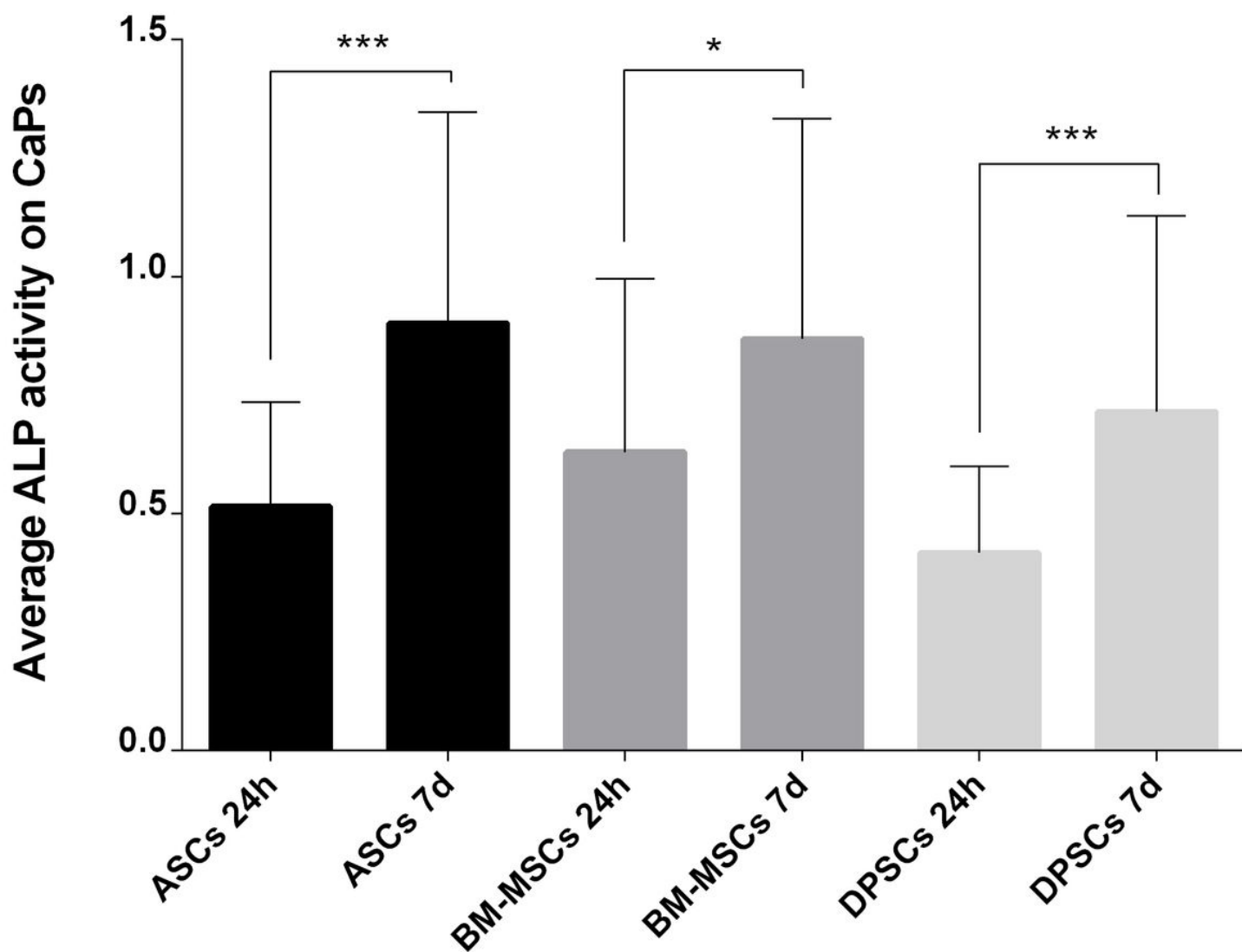


Figure 9

Average ALP activity showed by each MSC on both CaPs. Adipose tissue (ASCs), dental pulp (DPSCs) and bone marrow (BM-MSCs). All data are shown as mean \pm standard deviation. Significance level: * ≤ 0.05 *** ≤ 0.001 .

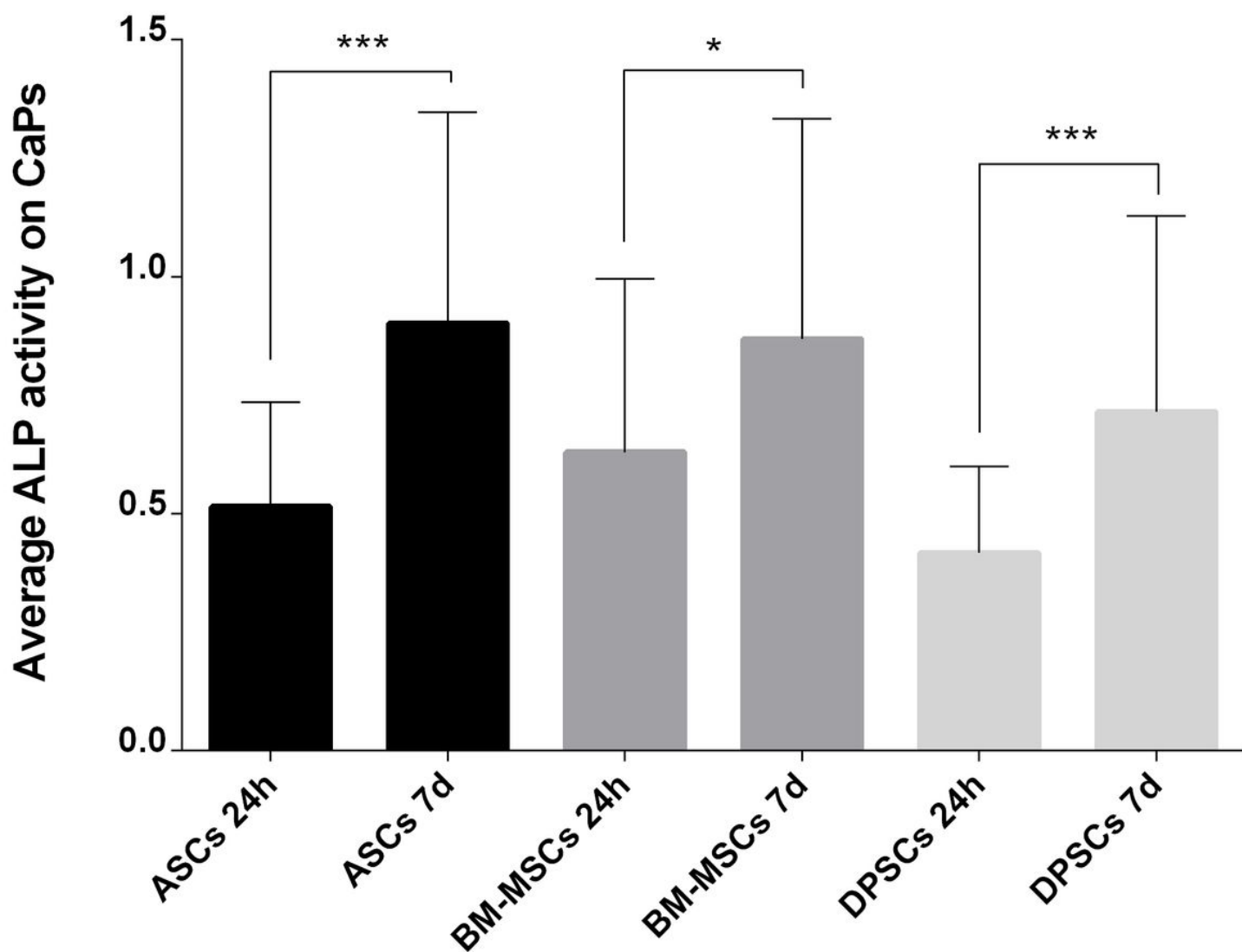


Figure 9

Average ALP activity showed by each MSC on both CaPs. Adipose tissue (ASCs), dental pulp (DPSCs) and bone marrow (BM-MSCs). All data are shown as mean \pm standard deviation. Significance level: * ≤ 0.05 *** ≤ 0.001 .

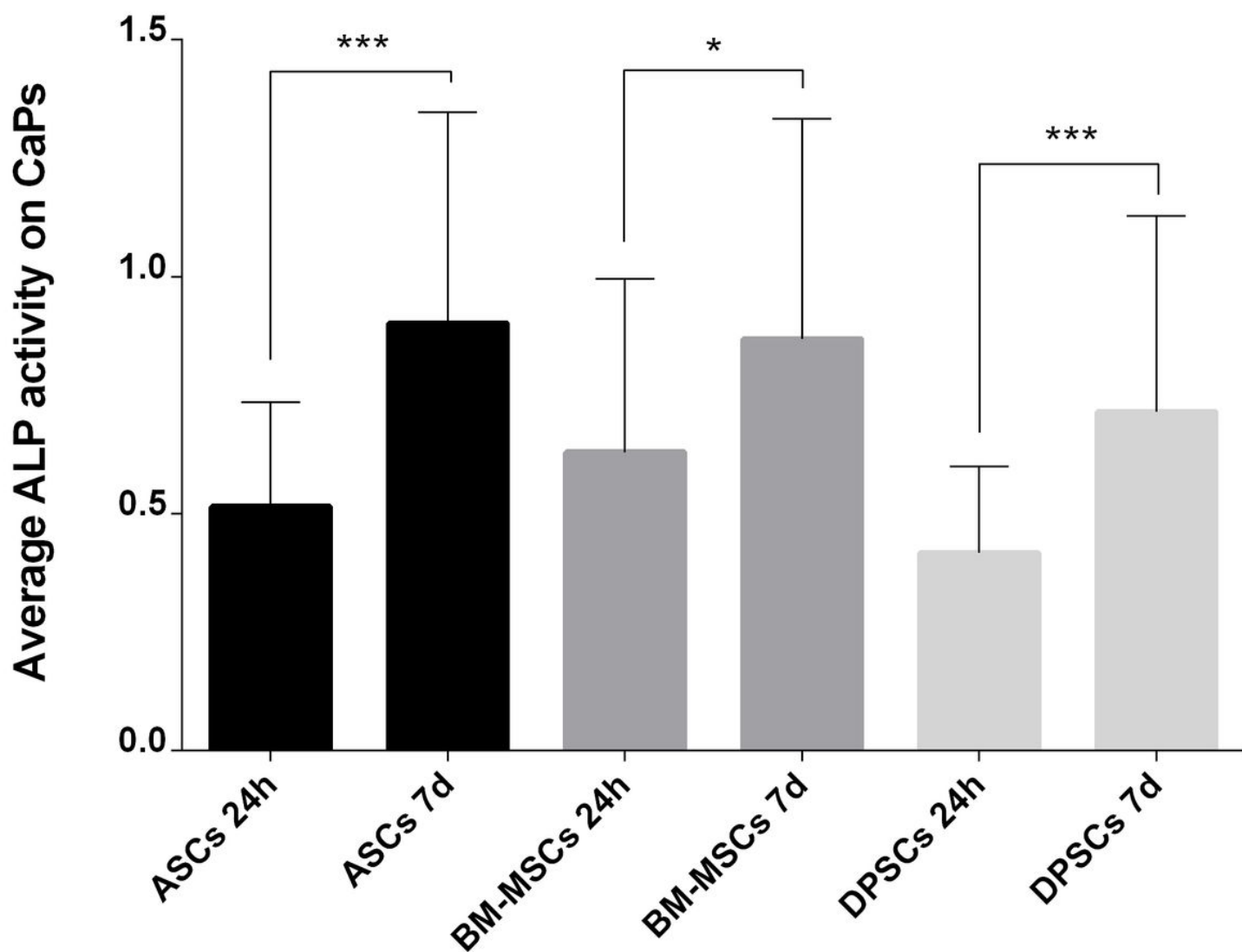


Figure 9

Average ALP activity showed by each MSC on both CaPs. Adipose tissue (ASCs), dental pulp (DPSCs) and bone marrow (BM-MSCs). All data are shown as mean \pm standard deviation. Significance level: * ≤ 0.05 *** ≤ 0.001 .

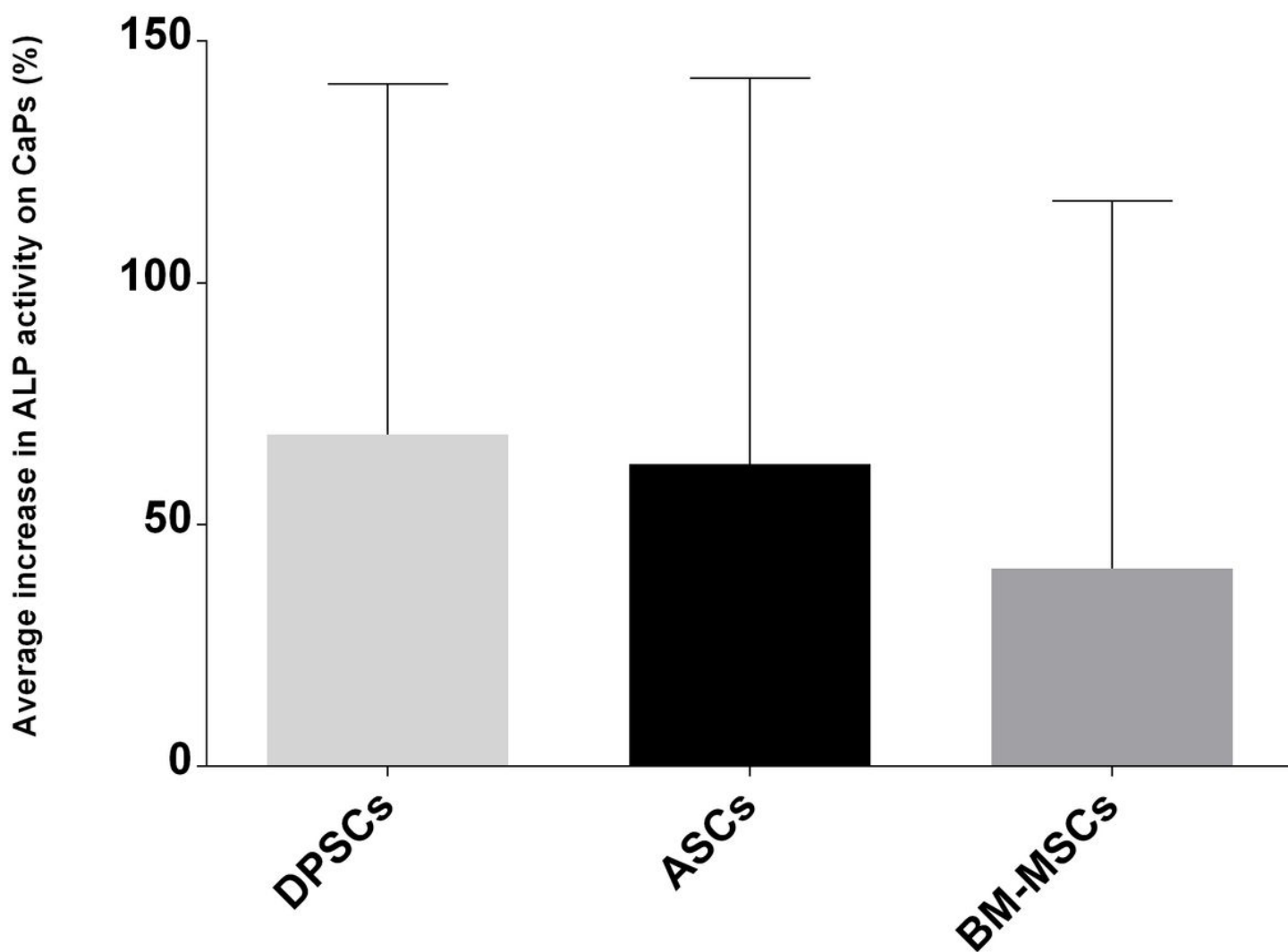


Figure 10

Average increase in ALP activity (in percentage) presented by each MSC on both CaPs. Adipose tissue (ASCs), dental pulp (DPSCs) and bone marrow (BM-MSCs). All data are shown as mean \pm standard deviation.

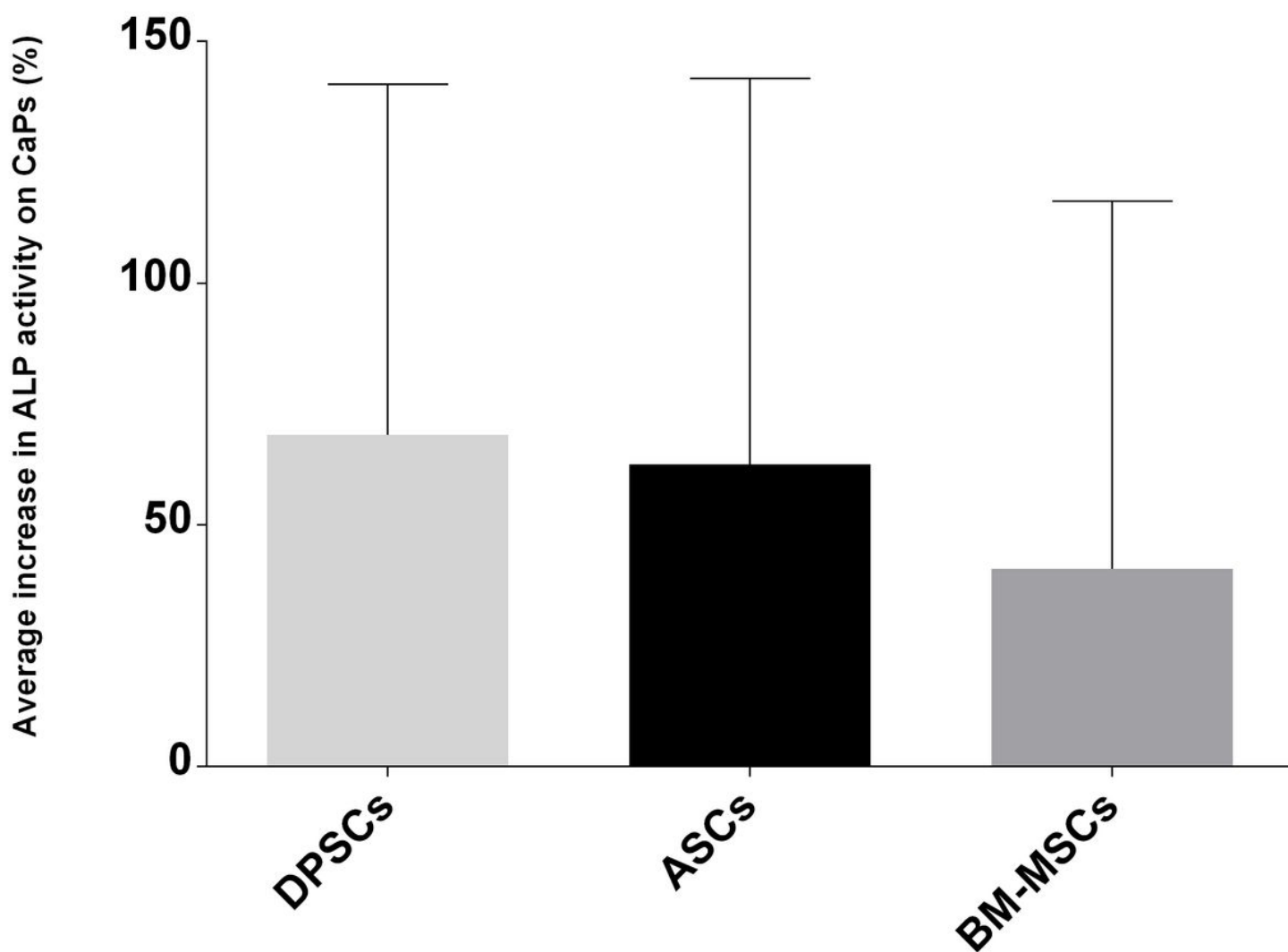


Figure 10

Average increase in ALP activity (in percentage) presented by each MSC on both CaPs. Adipose tissue (ASCs), dental pulp (DPSCs) and bone marrow (BM-MSCs). All data are shown as mean \pm standard deviation.

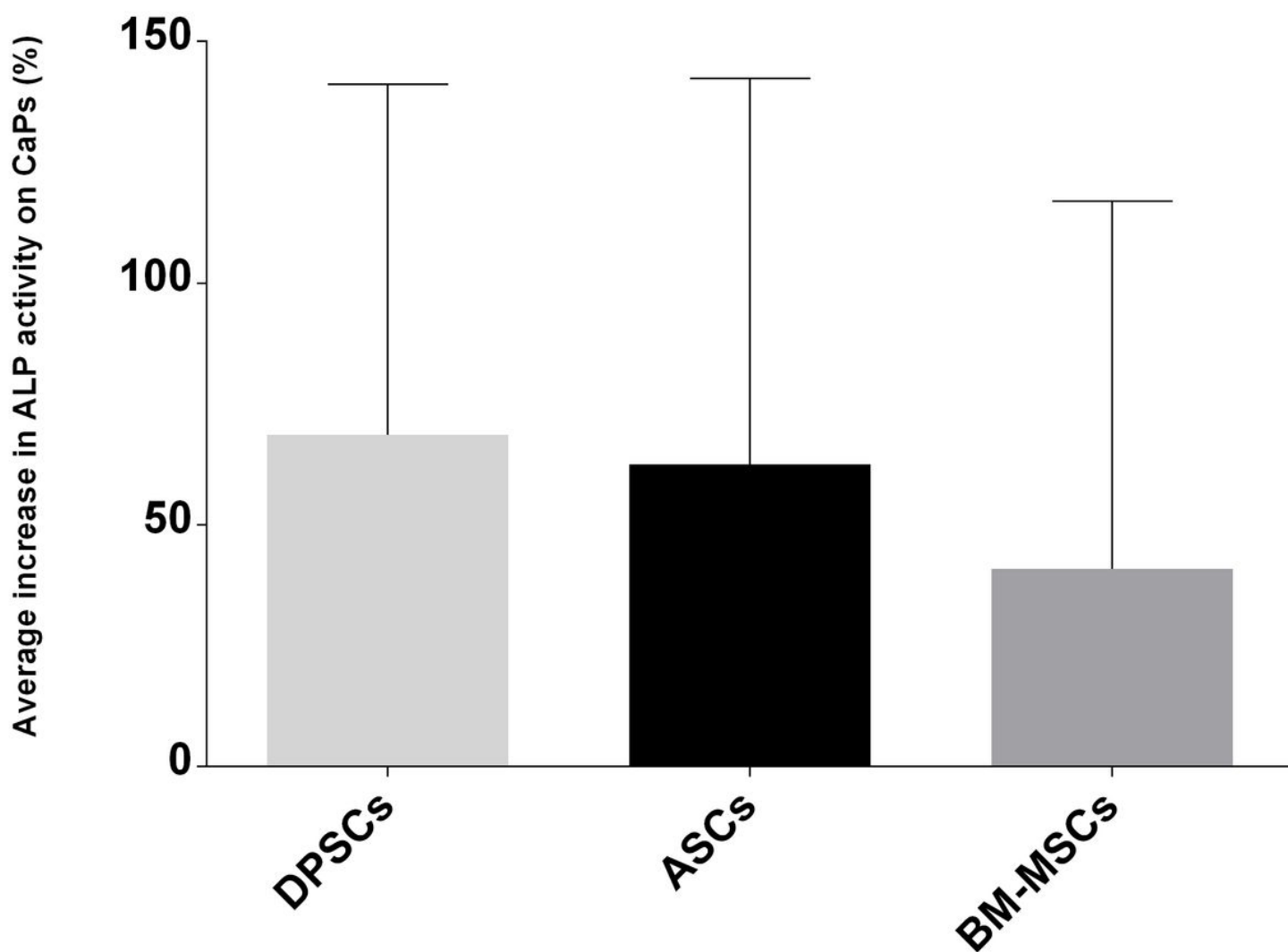


Figure 10

Average increase in ALP activity (in percentage) presented by each MSC on both CaPs. Adipose tissue (ASCs), dental pulp (DPSCs) and bone marrow (BM-MSCs). All data are shown as mean \pm standard deviation.

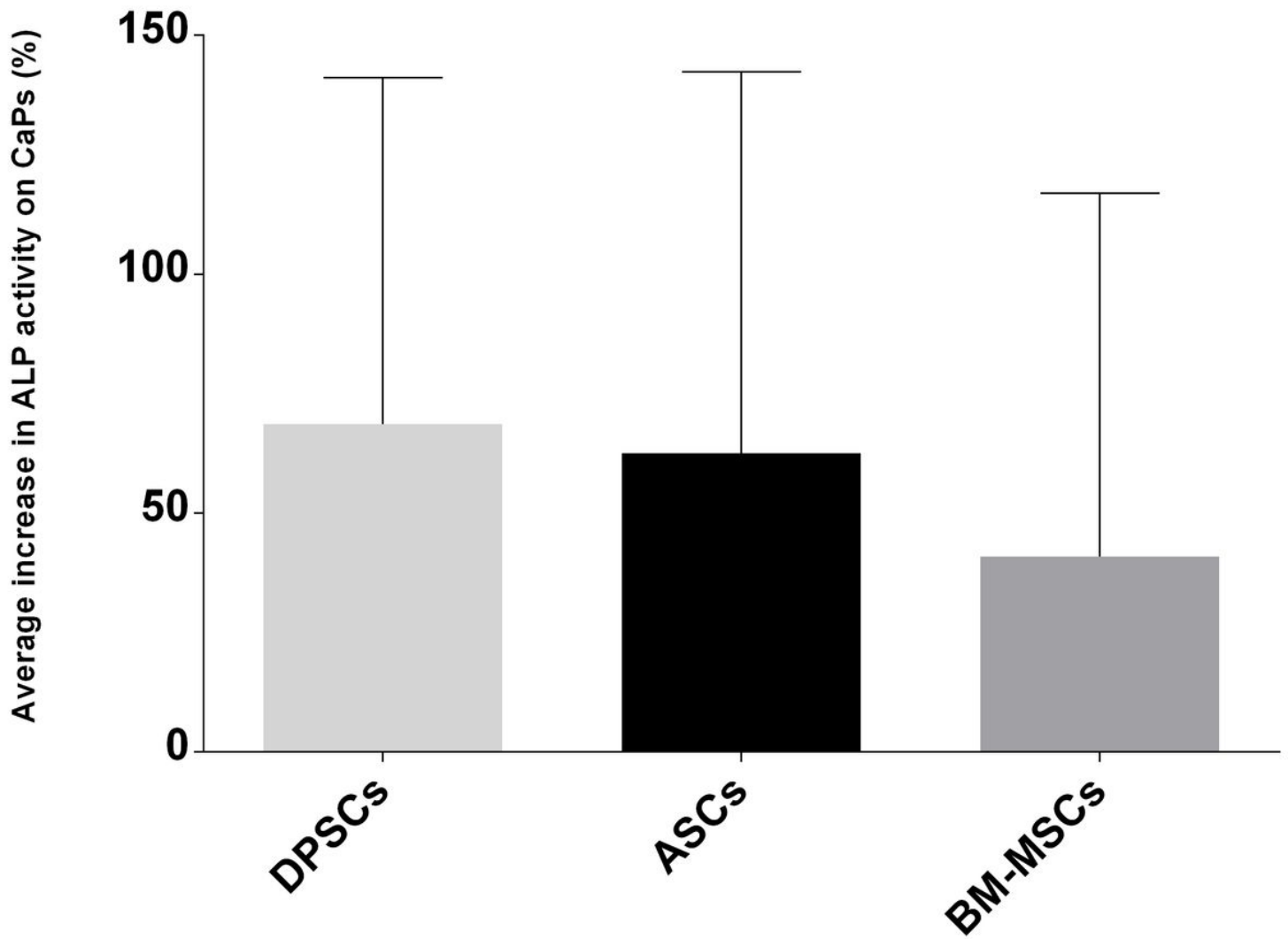


Figure 10

Average increase in ALP activity (in percentage) presented by each MSC on both CaPs. Adipose tissue (ASCs), dental pulp (DPSCs) and bone marrow (BM-MSCs). All data are shown as mean \pm standard deviation.

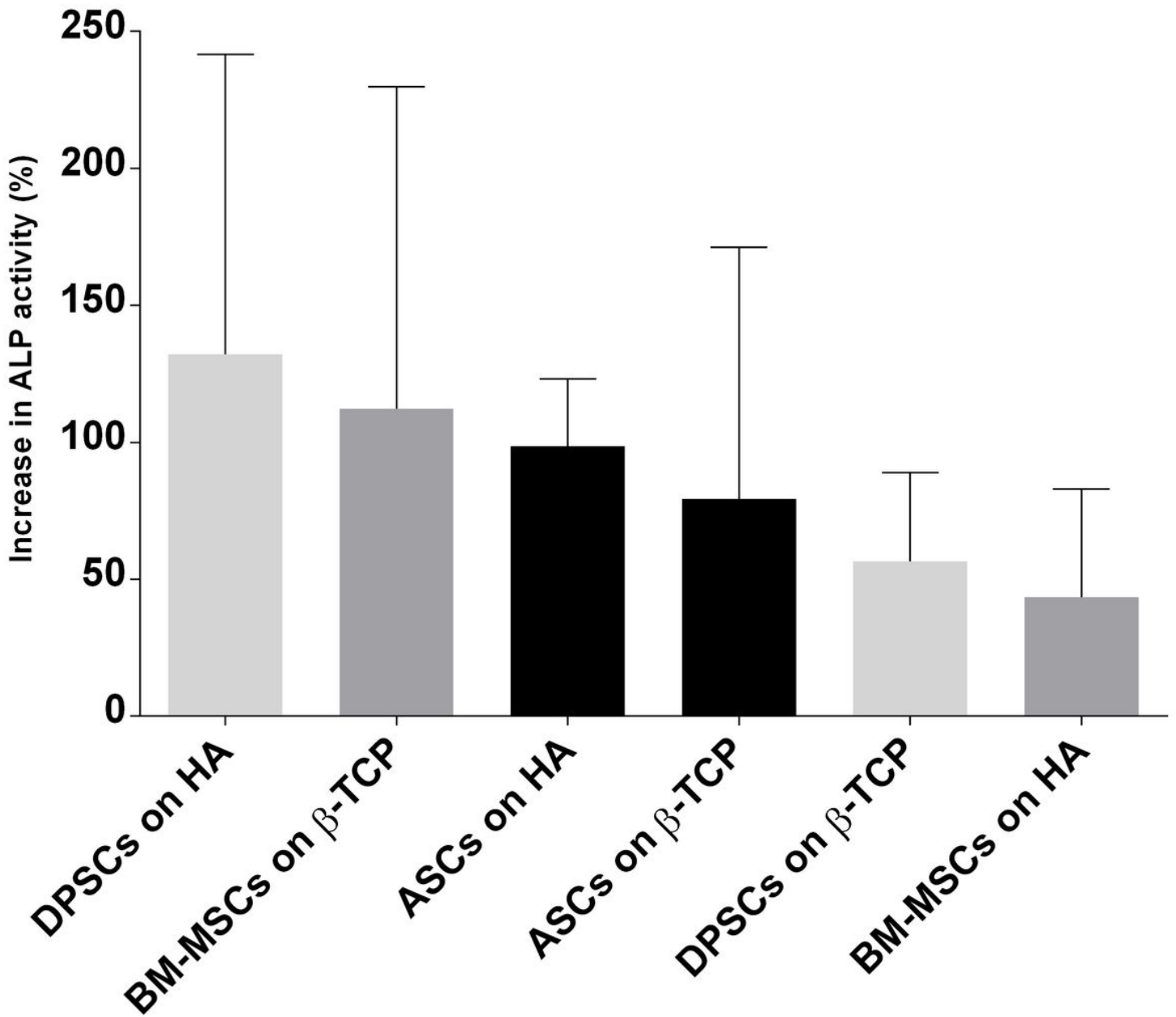


Figure 11

Increase in ALP activity (in percentage) presented by each construct. Hydroxyapatite (HA), β -tricalcium phosphate (β -TCP), adipose tissue (ASCs), dental pulp (DPSCs) and bone marrow (BM-MSCs). All data are shown as mean \pm standard deviation.

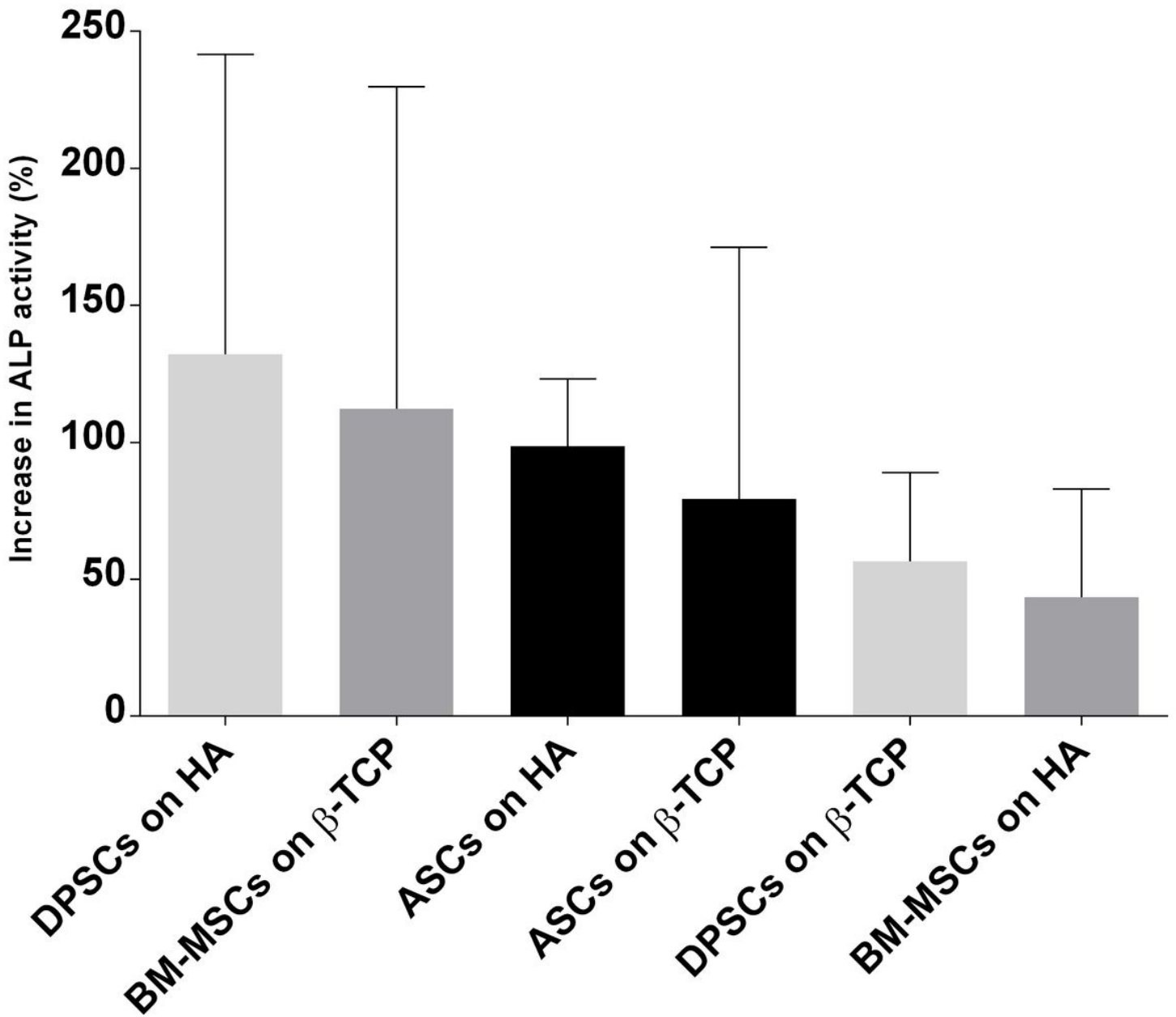


Figure 11

Increase in ALP activity (in percentage) presented by each construct. Hydroxyapatite (HA), β -tricalcium phosphate (β -TCP), adipose tissue (ASCs), dental pulp (DPSCs) and bone marrow (BM-MSCs). All data are shown as mean \pm standard deviation.

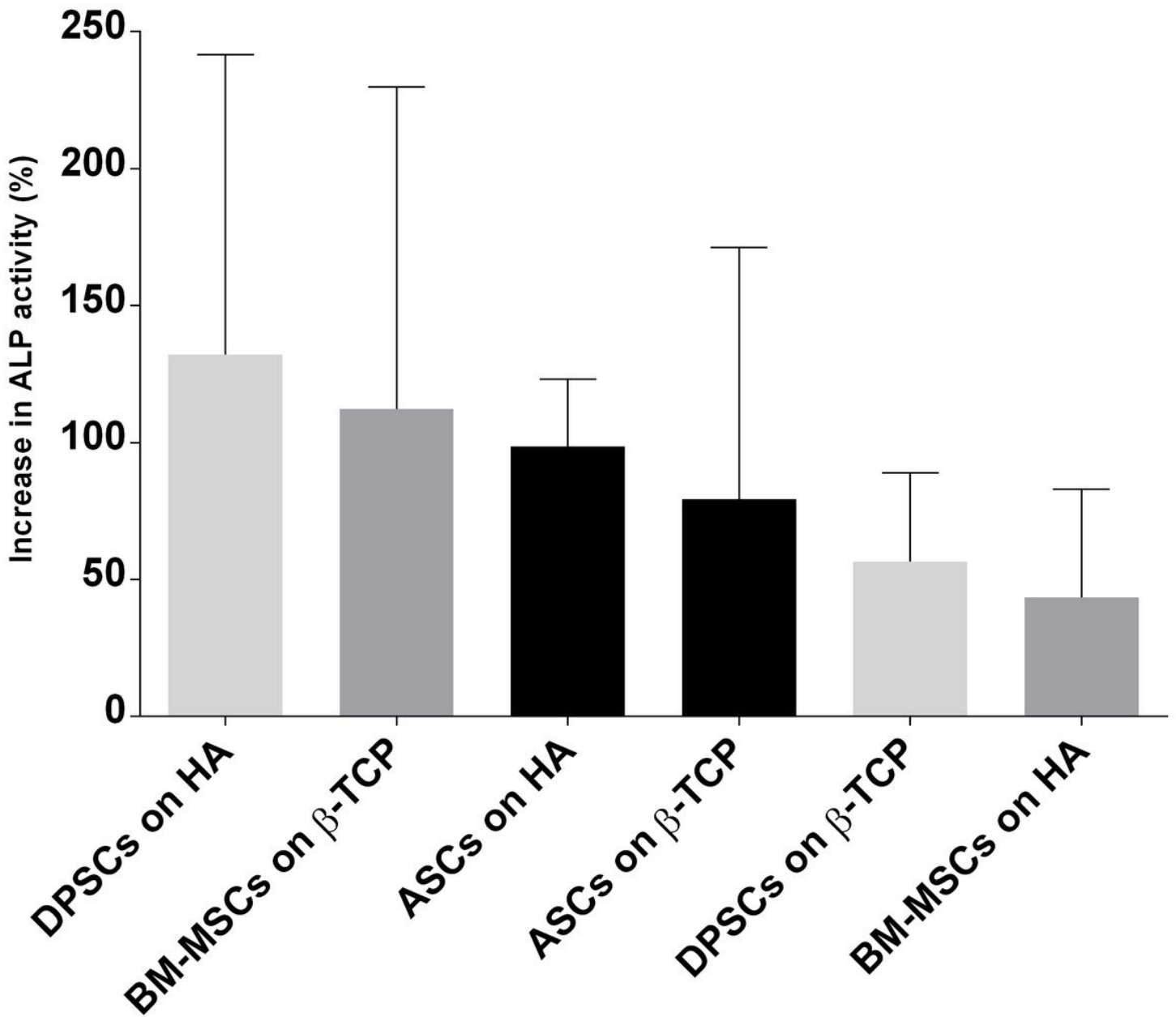


Figure 11

Increase in ALP activity (in percentage) presented by each construct. Hydroxyapatite (HA), β -tricalcium phosphate (β -TCP), adipose tissue (ASCs), dental pulp (DPSCs) and bone marrow (BM-MSCs). All data are shown as mean \pm standard deviation.

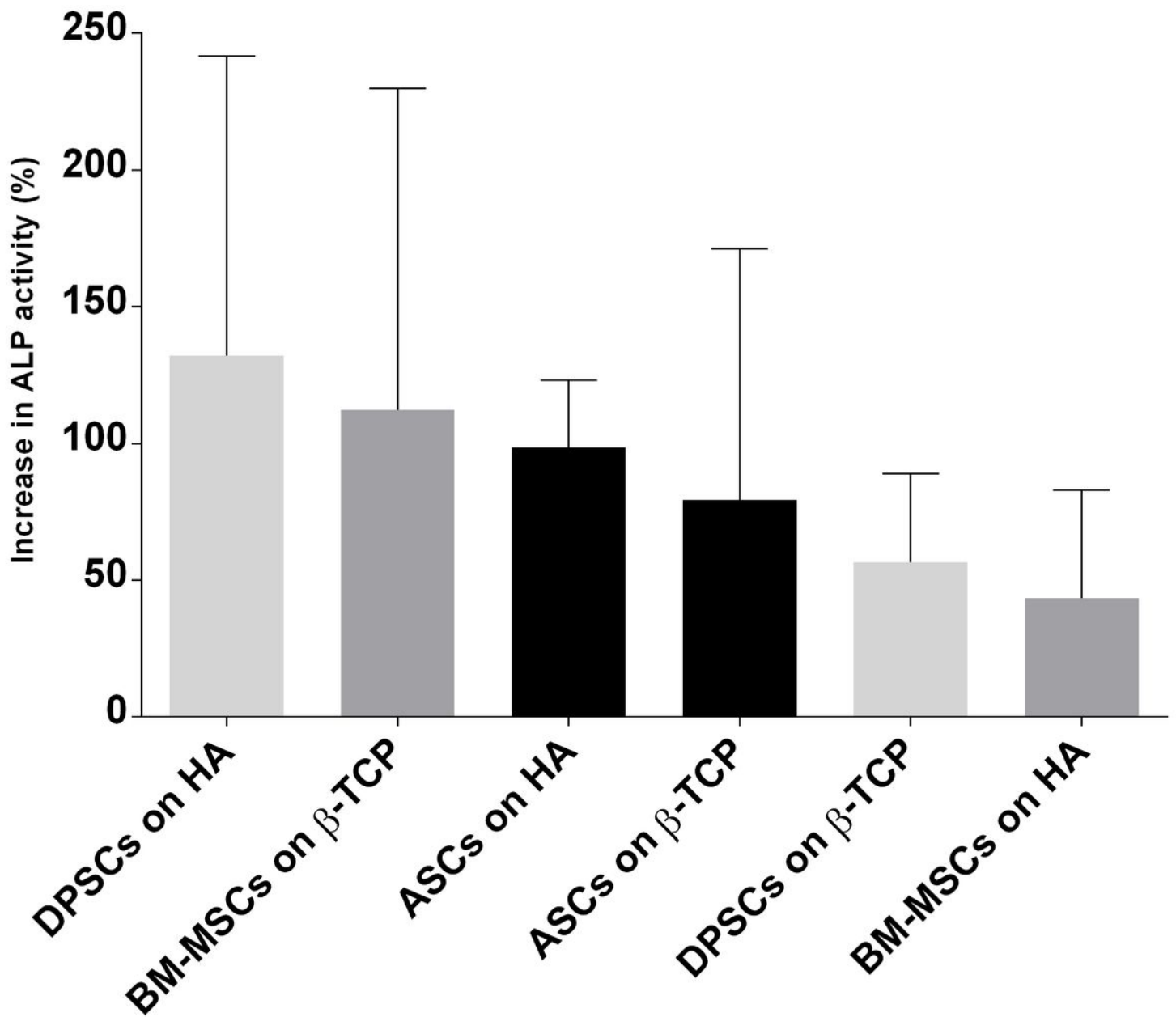


Figure 11

Increase in ALP activity (in percentage) presented by each construct. Hydroxyapatite (HA), β -tricalcium phosphate (β -TCP), adipose tissue (ASCs), dental pulp (DPSCs) and bone marrow (BM-MSCs). All data are shown as mean \pm standard deviation.

Supplementary Files

This is a list of supplementary files associated with this preprint. Click to download.

- [Additionalfile1.tif](#)

- Additionalfile1.tif
- Additionalfile1.tif
- Additionalfile1.tif
- Additionalfile2.jpg
- Additionalfile2.jpg
- Additionalfile2.jpg
- Additionalfile2.jpg